AD_____

Award Number: W81XWH-11-1-0495

TITLE: Adaptive Immune Responses Regulate the Pathophysiology of Lymphedema

PRINCIPAL INVESTIGATOR: Jamie Zampell, M.D.

CONTRACTING ORGANIZATION: Sloan-Kettering Institute for Cancer Research, New York, NY 10065

REPORT DATE: September 2012

TYPE OF REPORT: Annual Summary

PREPARED FOR: U.S. Army Medical Research and Materiel Command
Fort Detrick, Maryland 21702-5012

DISTRIBUTION STATEMENT: Approved for Public Release;
Distribution Unlimited

# REPORT DOCUMENTATION PAGE

*Form Approved*
*OMB No. 0704-0188*



| 1. REPORT DATE | 2. REPORT TYPE | 3. DATES COVERED |
|---|---|---|
| 01-09-2012 | Annual Summary | 01 September 2011 - 31 August 2012 |

**4. TITLE AND SUBTITLE**
Adaptive Immune Responses Regulate the Pathophysiology of Lymphedema

**5a. CONTRACT NUMBER**

**5b. GRANT NUMBER**
W81XWH-11-1-0495

**5c. PROGRAM ELEMENT NUMBER**

**6. AUTHOR(S)**
Jamie Zampell, Babak Mehrara, Evan Weitman, Sonia Elhadad, Alan Yan

E-Mail: jamie.zampell@nyumc.org, mehrarab@mskcc.org, weitmane@mskcc.org

**5d. PROJECT NUMBER**

**5e. TASK NUMBER**

**5f. WORK UNIT NUMBER**

**7. PERFORMING ORGANIZATION NAME(S) AND ADDRESS(ES)**
Sloan-Kettering Institute for Cancer Research, New York, NY 10065

**8. PERFORMING ORGANIZATION REPORT NUMBER**

**9. SPONSORING / MONITORING AGENCY NAME(S) AND ADDRESS(ES)**
U.S. Army Medical Research and Materiel Command
Fort Detrick, Maryland 21702-5012

**10. SPONSOR/MONITOR'S ACRONYM(S)**

**11. SPONSOR/MONITOR'S REPORT NUMBER(S)**

**12. DISTRIBUTION / AVAILABILITY STATEMENT**
Approved for Public Release; Distribution Unlimited

**13. SUPPLEMENTARY NOTES**

**14. ABSTRACT**

Lymphedema is a debilitating disorder affecting as many as 1 in 8 cancer survivors. Despite wide prevalence, limited understanding of disease pathogenesis has prevented development of effective treatment strategies. While inflammation, fibrosis, and lymphatic dysfunction are known clinical hallmarks, the mechanisms promoting these pathologic changes are unknown. The aim of this study therefore was to determine the cellular mechanisms regulating chronic lymphedema pathogenesis. Using a mouse models of lymphatic fluid stasis and chronic lymphedema, we show that sustained lymphatic fluid stasis leads to CD4+ T cell inflammation with a mixed T-helper cell type 1 (Th1)/T-helper cell type 2 (Th2) phenotype. Matched clinical specimens similarly demonstrate increased CD4+ T cell infiltrate and elevations in Th2-type cytokines. Furthermore, loss of CD4 prevents lymphedema development mouse models; more specifically, inhibition of Th2 differentiation through IL-4 and IL-13 blockade prevents both initiation of lymphedema development and progression of established lymphedema. Following Th2 abrogation, fibrosis is reduced, lymphatic function is improved, and lymphangiogenesis is augmented without a concomitant alteration in lymphangiogenic cytokines. The findings of this study demonstrate that lymphedema pathogenesis results from progressive lymphatic dysfunction resulting from chronic CD4+ inflammation, Th2 differentiation, and fibrosis. Blockade of Th2 responses prevents both initiation and progression of lymphedema without altering lymphangiogenic cytokines locally. Attenuation of Th2 inflammation therefore may be an effective strategy for blocking this pathologic sequence of events without altering metastatic risk in cancer survivors.

**15. SUBJECT TERMS**
Lymphedema, fibrosis, lymphangiogenesis, inflammation, T cell, T-helper type 2

| 16. SECURITY CLASSIFICATION OF: | | | 17. LIMITATION OF ABSTRACT | 18. NUMBER OF PAGES | 19a. NAME OF RESPONSIBLE PERSON |
|---|---|---|---|---|---|
| a. REPORT | b. ABSTRACT | c. THIS PAGE | | | USAMRMC |
| U | U | U | UU | 102 | 19b. TELEPHONE NUMBER *(include area code)* |

Table of Contents

## INTRODUCTION:

Lymphedema is a debilitating swelling of the extremity that occurs commonly after lymph node dissection for cancer operations and surgical staging. It is estimated that lymphedema affects 1 in 3 women following axillary lymph node dissection for cancer, 1 in 8 patients following lymph node dissection for other cancers, and 3-5 million Americans overall.[1,2] Lymphedema results in limb swelling and deformity, infection, debilitation, and reduced quality of life. There is an overall lack of knowledge regarding the pathogenesis of lymphedema. While current literature does support that inflammation, fibrosis, and lymphatic dysfunction are pathologic hallmarks of lymphedema, it is unclear which cellular and molecular events cause these changes, sometimes years to decades after surgical lymphatic disruption and lymph node removal. The purpose of this study was to determine the cellular and molecular events that lead to lymphedema. By understanding these pathologic events, we aim to suggest targeted preventive and therapeutic strategies.

## BODY:

The research accomplishments achieved by this grant are outlined below to address the work completed under each specific aim as outlined in the grant narrative and statement of work.

**Aim 1: Determine the roles of IL-4 and IL-13 in fibrosis and lymphatic dysfunction.** IL-4 and IL-13 are cytokines known to promote T helper type 2 immune responses and known to promote extracellular matrix remodeling, collagen deposition, and fibrosis in many fibroproliferative disorders.[3] As a result of work in this aim, we have shown that IL-4 and IL-13 contribute to the generation of T helper type 2 responses which contribute to progressive fibrosis and a specific inflammatory response that results in lymphatic dysfunction, worsened lymphatic fluid stasis, and lymphedema.

### 1.1 Determine the role of IL-13 in initiation and progression of fibrosis secondary to lymphedema.

To determine the role of IL-13 in the **initiation** of lymphedema, we used IL-13 monoclonal antibody to systemically block the effect of this cytokine following disruption of superficial and deep lymphatics in the mouse tail. These experiments were conducted using a well-described mouse tail model of lymphedema in which tail lymphatics are excised to generate progressive lymphedema, mimicking clinical lymphedema in patients.[4,5,6] Mice underwent tail lymphatic disruption, followed by systemic treatment with IL-13 monoclonal blocking antibody or isotype control. Alternate groups were treated with IL-4 monoclonal antibody or isotype control, since we have previously shown that this treatment largely prevents lymphedema initiation.

The results of these experiments have demonstrated that both IL-4 and IL-13 blockade prevent the initiation of edema, reduce abnormal fat deposition, reduce abnormal tissue inflammation, lessen abnormal fibrosis and scarring, and lead to improved lymphatic

function and better lymphatic flow. These results are fully described in the attached manuscript, currently in review at *Circulation*.[7] Specifically, we have shown that treatment with either IL-4mAb or IL-13mAb markedly decreases tail volumes as compared with controls (5-fold and 2.8-fold, respectively, $p<0.001$). Whereas control animals developed fixed tail contractures due to fibrosis ("J" configuration), the tails of IL-4mAb or IL-13mAb-treated animals remained pliable. Histologically, IL-4mAb or IL-13mAb-treated animals had significantly decreased subcutaneous edema/adipose deposition (1.3 and 1.5-fold, $p<0.001$), scar index (2.5 and 1.3-fold ($p<0.001$, $p<0.03$), and collagen deposition (1.7 and 1.3-fold,although the effect of IL-13mAb on collagen deposition was not statistically significant). IL-4 neutralization decreased tissue expression of CD45, CD4, IFN-gamma, IL-4, and IL-13 as well as peripheral blood concentrations of IL-4 and IL-13 (2.4 and 5.3-fold, respectively; $p<0.01$). These findings were corroborated by decreased numbers of Th1 and Th2 cells in tail tissues from IL4mAb-treated animals (2-fold, $p<0.001$). Decreased inflammation and fibrosis in IL-4mAb- or IL-13mAb-treated animals was associated with markedly improved lymphatic function (5-7-fold increased $^{99m}$Tc uptake, $p<0.01$; 3.5-30-fold increase in relative proximal fluorescence, $p<0.001$).

We hypothesize that inhibition of fibrosis is specific to Th2 differentiation rather than a generalized anti-inflammatory effect. In order to evaluate the isolated effects of IL-4 and IL-13 on fibrosis, selective inhibition of the JAK1/2 pathway (with inhibitor JAK1/2 (AZD1480)) was tested in our tail model against a vehicle control for 6 weeks.[8,9] The JAK1/2 pathway is an important regulator of acute/chronic inflammation, involved in signaling for a variety of inflammatory cytokines, including IL-6. As observed in two of our murine models (tail lymphatic ablation and axillary lymph node dissection) in addition to the findings of Karlson et al., IL-6 expression is increased in lymphedematous tissues (unpublished observations).[10] Inhibition of JAK1/2 spares the JAK3/STAT6 pathway, through which IL-4 and IL-13 signal, thus allowing for assessment of the fibrogenic effects of these cytokines independent from general inflammation. [11]

As expected, treatment with AZD1480 produced a near-complete blockade of STAT3 phosphorylation (pSTAT3) as evidenced by western blot analysis and decreased numbers of $pSTAT3^+$ cells (2.8-fold, $p<0.001$) in lymphedematous tissues. Mice treated with AZD1480 had no gross or measureable decrease in tail swelling and no difference in subcutaneous tissue thickness/interstitial edema compared with controls. Importantly, STAT3 inhibition did not decrease fibrosis or improve lymphatic function, suggesting that these outcomes are specific to Th2 cytokines as opposed to general inflammation.

To test the hypothesis that Th2 cytokines also regulate the **progression** of fibrosis and lymphatic dysfunction, we investigated 6-week post-tail lymphatic excision mice with well-established fibrosis (i.e. significantly increased tail volumes from baseline and fixed contracture deformity).[7] At this point, animals were randomized into groups and treated either with IL-4mAb or isotype control antibodies for 3 weeks, followed by a 3 week period

of treatment withdrawal. (We chose not to use IL-13mAb since our earlier experiments demonstrated that IL-4 was more efficacious in preventing initiation of fibrosis).

Animals treated with IL-4mAb demonstrated significant improvements in tail volumes (38% decrease; $p<0.01$) as compared with controls (15% decrease; p=na). Furthermore, IL-4mAb treatment markedly decreased tissue fibrosis with resolution of tail contracture; whereas, tail fibrosis persisted in control animals. These observations were confirmed by histologic analysis demonstrating significantly decreased subcutaneous tissue thickness, interstitial edema, and adipose deposition in IL-4mAb treated animals (1.4-fold; 40% reduction; $p<0.01$). No recurrence of fibrosis, increases in tail volumes or increases in subcutaneous tissue thickness were observed upon withdrawal of IL-4mAb. Control animals did display minor spontaneous improvements in these measures by 12 weeks; however, in contrast to our experimental group, these changes did not reach statistical significance.

IL-4 neutralization markedly decreased tail tissue inflammation (1.4-2.1-fold decreased CD45, CD4, IFN-γ, IL-4, and IL-13 expression by western blot), serum levels of IgE (2-fold, $p<0.01$), and serum levels of IL13 (6-fold; $p<0.01$). IL4mAb treatment did significantly decrease the number of Th1 (1.7-fold) and Th2 (2.1-fold) cells in lymphedematous tissues ($p<0.01$ for both). Interestingly, differences in serum IL-4 concentrations did not reach statistical significance.

IL-4 blockade in animals with established lymphedema significantly decreased tissue fibrosis (2-fold decreased scar index and type I collagen deposition, $p<0.01$ for both) and markedly improved lymphatic function (13-fold increased $^{99m}$Tc uptake, $p<0.01$; 3.1-fold increased proximal lymphatic fluorescence, $p<0.03$). Interestingly, these improvements persisted following treatment withdrawal (5-fold increased $^{99m}$Tc uptake, $p<0.01$; 2.9-fold increase proximal fluorescence, p=0.07).

### 1.2 Determine the effect of TGF-B1 on the progression of fibrosis and Th2 cytokine expression in lymphedema.

We have previously shown that blockade of TGF-B1, a molecule known to play a critical role in extracellular matrix remodeling which directly inhibits lymphangiogenesis decreases **initiation** of fibrosis and expression of Th2 cytokines in response to lymphedema.[6, 12, 13, 14] Therefore we hypothesized that inhibition of TGF-B1can also prevent **progression** of tissue fibrosis in established lymphedema. Using our tail model of lymphedema, we tested our hypothesis by treating 6-week post-op animals with a 3 week course of systemic TGF-B1 neutralizing antibody or isotype control. Contrary to our hypothesis, we observed no significant reduction in tail edema, subcutaneous tissue thickness, collagen deposition, scar index, lymphatic vessel number, or lymphatic function among groups. Experiments were repeated twice. These findings suggest that while TGF-B1 is critical for preventing the initiation of fibrosis associated with lymphatic fluid stasis, other molecules have a more significant role in promoting the progression of lymphedema and fibrosis. Importantly, due to the absence of significant differences among these treatment groups, experiments

investigating a potential synergistic effect of IL-4 and IL-13 blockade with TGFB-1, as proposed by the narrative, were not pursued. Furthermore, these findings support the concept that specific rather than generalized inflammatory responses promote the progression of lymphedema.

**Aim 2: Determine the effects of chronic lymphedema on Th2 inflammatory responses in patients with post-surgical lymphedema**. In this aim, we tested the hypothesis that patients with lymphedema develop a Th2-biased chronic inflammatory response. We demonstrated that lymphedema patients exhibit significant T-helper cell infiltrate within lymphedematous tissues as well as elevations in tissue expression of T-helper type 2 cytokines.

**2.1 Determine the effects of chronic lymphedema on Th2 inflammatory responses in patients with post-surgical lymphedema.**

To study the Th2 response in lymphedema patients, we worked in collaboration with Dr. Stanley Rockson at Stanford University. Previously, we collected serum and blood samples from 22 patients with varying degrees of post-surgical lymphedema as well as samples from 25 unaffected control patients who underwent a similar surgery. Tissue samples were also collected from the lymphedematous limb and a "matched" location on the unaffected limb from these 22 patients. Comparing lymphedema patients with normal controls, we analyzed serum markers of Th1 and Th2 differentiation by ELISA. This analysis included IFN-γ (Th1) and IL-4, IL-13, CD30, TGF-β and IgE (Th2). We observed a trend toward significance in CD30 and IgE; however, they were not significant. Analysis of RNA derived from fractions of peripherally isolated white blood cells showed no major differences in TGF-B ($p = 0.2773$). However, this may be due to the fact that cells were not activated prior to RNA harvest which may have led to inconclusive findings regarding cellular differentiation status.

IHC for IL-4, IL-13, IFNg, TGF-B1 as well as inflammatory cells including CD4, CD8, and CD11B was performed in matched specimen from lymphedematous and normal limbs. Compared to the normal controls, increases in the number of $IL4^+$ cells (1.5-fold, $p=0.018$), $IL13^+$ cells (2.3-fold, $p<0.001$), TGF-B1+ cells and infiltrating macrophages were observed in the lymphedematous limbs. Also noted in the experimental group, was an increase in the number of $CD4^+$ cells (2.6-fold; $p=0.01$) with a correlation between the severity of lymphedema and the degree of CD4+ cell inflammation ($r=0.6332$, $p<0.05$). No significant difference was observed in the number of CD8+ cells within the experimental model. We are continuing to perform studies on IFN-γ and Th1 markers in these tissues. Together these findings suggest that, locally, Th2 cytokines are upregulated in lymphedematous tissues in the setting of CD4+ infiltration. While the systemic effects are less clear, this local inflammatory response may govern the progression to lymphedema.

**2.2 Determine the effects of lymphedema treatment of chronic post-surgical**

**lymphedema on the Th2 inflammatory response.**

We are currently collecting samples from lymphedema patients at MD Anderson Cancer Center. The subjects for this study will be comprised of women with unilateral upper extremity lymphedema resulting from breast cancer surgery. Patients with Campisi stage II or III lymphedema will be identified by Dr. Chang and his team at MD Anderson Cancer Center and recruited to their ongoing IRB approved (MDACC Protocol ID #: 2011-0455) and funded clinical trial evaluating the efficacy of lymphaticovenous bypass surgery. 30 of these patients will be additionally consented to provide blood and tissue samples before and after surgery. Blood will be collected before and then 1, 3, and 6 months after bypass. Tissue biopsy will be performed before and 6 months after bypass. Similar to our colleagues at Stanford, all patients will be at least 1 year after their initial breast cancer surgery and will not have been treated with immunosuppressive or chemotherapy medications for at least 6 months prior to enrollment. Also similar to our efforts at Stanford, we will limit accrual to patients with Campisi grade II or III (International Society of Lymphology stage I or II). For our secondary analysis, arm volume measurements will be performed using perometry and subjective analysis will be performed using a validated questionnaire.

At present, we have matched samples from 5 patients. We hope that accrual will be completed in 9-10 months. Once we have received all of the specimens will run PCR on the samples for Th1/Th2 differentiation cytokines.

## KEY RESEARCH ACCOMPLISHMENTS:

1. Determination that sustained lymphatic fluid stasis results in CD4+ cell inflammation
2. Determination that inhibition of Th2 differentiation decreases initiation and progression of fibrosis and improves lymphatic function
3. Determination that fibrosis independently inhibits lymphatic function
4. Determination that patients with lymphedema demonstrate a local Th2-type response

## REPORTABLE OUTCOMES:

**Papers:**

1. Zampell JC, Avraham T, Yoder N, Fort N, Yan A, Weitman ES, and Mehrara BJ. Lymphatic function is regulated by coordinated expression of lymphangiogenic and anti-lymphangiogenic cytokines. *Amer J Physiol-Cell* 2011: 302(2):C392-404.
2. Zampell, JC, Avraham, TA, Yan, A, Elhadad, S, Weitman, ES, Rockson, SG, Bromberg, J, and Mehrara BJ. Mechanisms of fibrosis and lymphatic dysfunction in in post-surgical lymphedema. *Circulation* 2012 [Manuscript under review].

3. Zampell, JC, Yan, A, Elhadad, S, Avraham A, Weitman ES, Mehrara, BJ. CD4+ cells regulate fibrosis and lymphangiogenesis in response to lymphatic fluid stasis. PLOS One 2012 [Manuscript under review].

**Abstracts/ Presentations/Posters:**

1. **Zampell J,** Yan A, Avraham T, Yoder N, Fort N, and Mehrara BJ. T-cell deficiency is associated with accelerated lymphatic regeneration [Presentation]. In: Northeastern Society of Plastic Surgeons 28th Annual Meeting: 2011 October 20-23; Amelia Island, FL.

2. **Zampell JC**, Avraham T, Yan A, Malliaris S, and Mehrara BJ. Th2 cell-mediated inflammation mediates fibrosis and lymphatic dysfunction in chronic lymphedema. [Presentation]. In: Northeastern Society of Plastic Surgeons 28th Annual Meeting: 2011 October 20-23; Amelia Island, FL.

3. Weitman ES, **Zampell JC**, Avraham T, Yan A, Elhadad S, Rockson S, Mehrara BJ. The Role of IL-4 and IL-13 blockade in the Treatment of Lymphedema [Poster]. In: Gordon Research Conference: Molecular Mechanisms in Lymphatic Function and Disease: 2012 March 4-9; Ventura Beach, CA.

4. Mehrara, BJ, **Zampell JC**, Yan A, Avraham T, Elhadad S, Avraham T, and Weitman ES. Toll-like receptor signaling prevents fibrosis and lymphatic dysfunction following tissue injury and lymphatic disruption. [Poster]. In: Gordon Research Conference: Molecular Mechanisms in Lymphatic Function and Disease: 2012 March 4-9; Ventura Beach, CA.

5. Elhadad S, **Zampell JC**, Avraham T, Weitman ES, Yan A, and Mehrara BJ. T cell Deficiency is associated with accelerated lymphatic regeneration [Poster]. In: Gordon Research Conference: Molecular Mechanisms in Lymphatic Function and Disease: 2012 March 4-9; Ventura Beach, CA.

6. **Zampell JC**, Yan A, Avraham T, Weitman E, Del Vecchio S, and Mehrara BJ. IL-13 blockade reduces tissue fibrosis and improves lymphatic function in the progression of chronic lymphedema [Presentation]. In: Society of Surgical Oncology 65th Annual Cancer Symposium: 2012 March 20-23;

7. **Zampell, JC**, Yan, A, Malliaris, S, Avraham, T, Weitman ES, Elhadad, S, and Mehrara, BJ. Targeted Th2 immune modulation blocks chronic lymphedema progression. [Plenary Presentation]. In: Plastic Surgery Research Council 57$^{th}$ Annual Meeting: 2012 June 12-15; Ann Arbor, MI.

8. Weitman ES, **Zampell, JC**, Elhadad S, Aschen S, and Mehrara, BJ. Regulation of Adipogenesis in Lymphedema [Presentation]. In: Plastic Surgery Research Council 57$^{th}$ Annual Meeting: 2012 June 12-15; Ann Arbor, MI.

9. Elhadad, S, **Zampell JC**, Yan A, Weitman, E, Avraham, T, and Mehrara, BJ. CD4+ T cell infiltration is responsible for chronic inflammation in experimental lymphedema [Presentation]. In: Plastic Surgery Research Council 57th Annual Meeting: 2012 June 12-15; Ann Arbor, MI.

10. **Zampell, JC**, Yan A, Avraham T, Weitman ES, and Mehrara BJ. CD4+ Inflammation is Necessary for Pathologic Changes Associated with Sustained Lymphatic Fluid Stasis [Accepted Presentation]. In: American College of Surgeons 97th Clinical Congress: 2012.

## CONCLUSION:

Lymphedema is a debilitating disease that results in limb swelling and deformity, infection, and reduced quality of life commonly following lymph node dissection after cancer resection and surgical staging. Currently, there is no cure for lymphedema and therapeutic options are ineffective, providing little symptomatic relief. It is unclear which molecular and cellular mechanisms are responsible for the pathogenesis of lymphedema. Thus, the purpose of this study was to further elaborate these cellular and molecular events. Specifically, we aimed to determine the roles of IL-4 and IL-13 (cytokines known to play a role in other fibroproliferative disorders) in lymphatic dysfunction and the initiation and progression of fibrosis.

Interestingly, we found that IL-4 and IL-13 promote the generation of T helper type 2 responses resulting in lymphatic dysfunction, increased lymphatic fluid stasis, and lymphedema. Our experiments suggest that IL-4 and IL-13 play a role in both **initiation** and **progression** of fibrosis secondary to lymphedema. Blockade of both IL-4 and IL-13 prevent the **initiation** of edema, reduce abnormal fat deposition, reduce abnormal tissue inflammation, lessen abnormal fibrosis and scarring, and lead to improved lymphatic function and better lymphatic flow. Furthermore, through STAT3 inhibition we supported our hypothesis that fibrosis is specific to Th2 differentiation rather than generalized inflammation. Importantly, we found that Th2 cytokines regulate the **progression** of fibrosis and lymphatic dysfunction; animals treated with IL-4mAb demonstrated significant improvements of tail volumes as compared with controls, and IL-4mAb treatment markedly decreased tissue fibrosis with resolution of tail contracture.

Based on prior experiments that demonstrated the important role of TGF-B1 in the initiation of fibrosis, we aimed to investigate whether or not TGF-B1 would play a similar role in the progression of fibrosis and Th2 cytokine expression in lymphedema. However, our findings suggest that while TGF-B1 is critical for preventing the initiation of fibrosis associated with lymphatic fluid stasis, other molecules have a more significant role in promoting the progression of lymphedema and fibrosis.

Finally, we aimed to determine the effects of chronic lymphedema on Th2 inflammatory responses in patients with post-surgical lymphedema. Tissue samples from patients with lymphedematous limbs showed an increase in the numbers of $IL4^+$ cells, $IL13^+$ cells, TGF-B1+ cells and infiltrating macrophages when compared to controls. Also noted in the experimental group, was an increase in the number of $CD4^+$ cells with a correlation between the severity of lymphedema and the degree of CD4+ cell inflammation. These findings suggest that Th2 cytokines are upregulated in lymphedematous tissues

in the setting of CD4+ infiltration. While the systemic effects are less clear, this local inflammatory response may govern the progression to lymphedema.

Our results demonstrate that Th2 cytokines, specifically, IL-4 and IL-13, play a critical role in lymphatic dysfunction as well as the initiation and progression of fibrosis that contributes to the pathogenesis of lymphedema. By continuing to gain a better understanding of the molecular and cellular mechanisms responsible for lymphedema, it is our goal to identify putative targets for effective therapies in the prevention and treatment of lymphedema.

**REFERENCES:**


1. Szuba A, Achalu R, Rockson SG. Decongestive lymphatic therapy for patients with breast carcinoma-associated lymphedema: A randomized, prospective study of a role for adjunctive intermittent pneumatic compression. *Cancer*. 95:2260–2267 (2002).
2. Velanovich V, Szymanski W. Quality of life of breast cancer patients with lymphedema. *Am J Surg*.177:184–187; discussion 188. (1999).
3. Wynn TA. Fibrotic disease and the T(H)1/T(H)2 paradigm. *Nat Rev Immunol.* 4(8):583-94. (2004).
4. Rutkowski JM, Moya M, Johannes J, Goldman J, Swartz MA. Secondary lymphedema in the mouse tail: Lymphatic hyperplasia, VEGF-C upregulation, and the protective role of MMP-9. *Microvasc Res* 72: 161-171. (2006).
5. Clavin NW, Avraham T, Fernandez J, Daluvoy SV, Soares MA, Chaudhry A, Mehrara BJ. TGF-beta1 is a negative regulator of lymphatic regeneration during wound repair. *Am J Physiol Heart Circ Physiol*. 295(5):H2113-27. (2008).
6. Avraham T, Clavin NW, Daluvoy SV, Fernandez J, Soares MA, Cordeiro AP, Mehrara BJ. Fibrosis is a key inhibitor of lymphatic regeneration. *Plast Reconstr Surg.* 124(2):438-50. (2009).
7. Zampell, JC, Avraham, TA, Yan, A, Elhadad, S, Weitman, ES, Rockson, SG, Bromberg, J, and Mehrara BJ. Mechanisms of fibrosis and lymphatic dysfunction in in post-surgical lymphedema. *Circulation* (2012). [Manuscript under review].
8. Liu W, Cai Z, Wang D, Wu X, Cui L, Shang Q, Qian Y, Cao Y. Blocking transforming growth factor-beta receptor signaling down-regulate transforming growth factor-beta1 autoproduction in keloid fibroblasts. *Chin J Traumatol* 5: 77–81 (2002).
9. Leask A, Abraham DJ. TGF-beta signaling and the fibrotic response. *FASEB J* 18: 816–827. (2004).
10. Karlsen TV, Karkkainen MJ, Alitalo K, Wiig H. Transcapillary fluid balance consequences of missing initial lymphatics studied in a mouse model of primary lymphedema. *J Physiol.* Jul 15;574(Pt 2):583-96. (2006).
11. Neurath MF, Finotto S. IL-6 signaling in autoimmunity, chronic inflammation and inflammation-associated cancer. *Cytokine Growth Factor Rev.* 22(2):83-9. (2011).
12. Shi Y, Massague J. Mechanisms of TGF-beta signaling from cell membrane to the nucleus. *Cell.* 13;113(6):685-700. (2003).
13. Avraham T, Daluvoy S, Zampell J, Yan A, Haviv YS, Rockson SG, Mehrara BJ. Blockade of transforming growth factor-beta1 accelerates lymphatic regeneration during wound repair. *Am J Pathol.*;177(6):3202-14. (2010).
14. Kataru RP, Kim H, Jang C, Choi DK, Koh BI, Kim M, Gollamudi S, Kim YK, Lee SH, Koh GY. T lymphocytes negatively regulate lymph node lymphatic vessel formation. *Immunity.* 28;34(1):96-107. (2011).

**Appendices**: *None*

**Manuscripts/Reprints, Abstracts**: *attached*

# Mechanisms of fibrosis and lymphatic dysfunction in post-surgical lymphedema

Key words: Lymphedema, fibrosis, IL-4, IL-13, Th2

Running Head: Lymphedema and fibrosis

**Tomer Avraham, MD[1,**], Jamie C. Zampell, MD[1,**], Alan Yan, MD[1], Sonia Elhadad, PhD[1], Evan Weitman, MD[1], Stanley G. Rockson, MD[2], Jacqueline Bromberg, MD[3], and Babak J. Mehrara, MD[1]**

1. Division of Plastic and Reconstructive Surgery, Department of Surgery, Memorial Sloan-Kettering Cancer Center, New York, NY 10065
2. Division of Cardiology, Department of Medicine, Stanford University Medical Center, Stanford, CA 94305-2200
3. Department of Medicine, Memorial Sloan-Kettering Cancer Center, New York, NY 10065

** These authors contributed equally to this manuscript

Correspondence:

Babak J. Mehrara, MD FACS
1275 York Avenue
Room MRI 1005
New York, NY 10065
mehrarab@mskcc.org
212-639-8639
212-717-3677 Fax

Disclosures

None of the authors have any commercial associations or financial relationships that would create a conflict of interest with the work presented in this article.

# Abstract

Lymphedema is a debilitating disorder affecting as many as 1 in 8 cancer survivors. Despite wide prevalence, limited understanding of disease pathogenesis has prevented development of effective treatment strategies. While inflammation, fibrosis, and lymphatic dysfunction are known clinical hallmarks, the mechanisms promoting these pathologic changes are unknown. The aim of this study therefore was to determine the cellular mechanisms regulating chronic lymphedema pathogenesis. Using a mouse axillary lymph node dissection model of lymphatic fluid stasis and a mouse tail model of chronic lymphedema, we show that sustained lymphatic fluid stasis leads to CD4+ T cell inflammation with a mixed T-helper cell type 1 (Th1)/T-helper cell type 2 (Th2) phenotype. Matched clinical specimens similarly demonstrate increased CD4+ T cell infiltrate and elevations in Th2-type cytokines. Furthermore, loss of T cells or knockout of CD4 prevents lymphedema development in the tail model. More specifically, inhibition of Th2 differentiation through IL4 and IL13 blockade prevents both initiation of lymphedema development and progression of established lymphedema. Following Th2 abrogation, fibrosis is reduced, lymphatic function is improved, and, importantly, lymphangiogenesis is augmented without a concomitant alteration in lymphangiogenic cytokines. The findings of this study demonstrate that lymphedema pathogenesis results from progressive lymphatic dysfunction resulting from chronic CD4+ inflammation, Th2 differentiation, and fibrosis. Blockade of Th2 responses prevents both initiation and progression of lymphedema without altering lymphangiogenic cytokines locally. Attenuation of Th2 inflammation therefore may be an effective strategy for blocking this pathologic sequence of events without altering metastatic risk in cancer survivors.

# Introduction

Lymphedema is chronic tissue swelling that occurs when lymphatic transport capacity is exceeded. In the US, lymphedema occurs most commonly as a complication of lymph node dissection for cancer treatment and affects 3-5 million patients resulting in significant medical expenditures, decreased quality of life, and severe soft tissue infections.[1-3]

Although numerous studies have shown that lymphedema is characterized histologically by chronic inflammation and fibrosis,[4-9] the etiology of this disorder remains unknown.[10] It is unclear, for instance, why an identical operation leads to lymphedema in some patients and not others. Perhaps the most perplexing aspect of lymphedema is the fact that progressive swelling, in most cases, occurs in a delayed fashion 1-5 years after surgery.[11] These clinical features suggest that injury and resultant lymphatic stasis are only the initiating events and that other pathologic steps are required for lymphedema development.

Based on the clinical features of lymphedema, we hypothesized that lymphatic stasis initiates a cycle of inflammation→progressive tissue fibrosis→worsening lymphatic function.[12] This cycle, over time, leads to end organ failure of the lymphatic system and clinically apparent lymphedema. This hypothesis is supported by the fact that fibrosis is a common mode of organ failure and, similar to lymphedema, fibrotic disorders are characterized by inflammation, replacement of parenchyma with scar, and progressive organ dysfunction.[13] In addition, our hypothesis explains the delayed development of lymphedema after injury since the progressive fibrosis necessary to cause end organ failure of the lymphatics takes time to develop. Fibrosis also provides a mechanism for the known risk factors of lymphedema such as radiation, obesity, and infection, since these predisposing conditions contribute either directly or indirectly to fibrosis.[14,15]

The purpose of this study was to identify the cellular mechanisms that regulate fibrosis and lymphatic dysfunction in response to lymphatic stasis. We show that lymphatic stasis results in chronic T cell inflammation and a mixed T-helper-1/T-helper-2 (Th1/Th2) response. In addition, we show that inhibition of T cell inflammation or Th2 differentiation significantly attenuates the initiation and progression of fibrosis, improves lymphatic function, and markedly decreases pathologic tissue changes, suggesting that this approach can serve as a novel treatment modality for lymphedema.

# Results

## Sustained lymphatic stasis results in CD4$^+$ cell inflammation

To determine how lymph stasis regulates inflammation, we compared the effects of temporary and sustained lymphatic stasis using a mouse tail model in which the superficial/deep lymphatics are excised, and the wound is either covered with collagen gel to accelerate repair (control) or left open to delay lymphatic regeneration (lymphedema, **Figure 1A-I**).[12,16,17]

Six weeks following surgery, sustained lymphatic stasis resulted in significantly increased tail edema, decreased lymphatic function (2.7-fold decreased uptake of $^{99m}$Tc), and increased CD45$^+$ cell inflammation distal to the zone of lymphatic ligation (4.3-fold increase) as compared with temporary stasis (all $p<0.01$; **Figure 1A-B, Supplemental Figure 1A**). Gradients of lymphatic stasis comparing distal to proximal regions of the tail within the lymphedema group also demonstrated markedly increased infiltration by CD45$^+$ (7.5-fold; $p<0.001$) and CD4+ cells (4-fold; $p<0.001$; **Figure 1C-D**). In fact, 70% of the CD45$^+$ leukocytes were also CD4$^+$ (**Supplemental Figure 1B**). These findings were confirmed with flow cytometry analysis comparing proximal/distal regions of the tail (7.5- and 38-fold increase in %TCR$\beta^+$ CD4$^+$ cells 3- and 6-weeks post-operatively, respectively; $p<0.001$; **Figure 1 E-F**).

Localization of Th1 (IFN-$\gamma^+$/CD4$^+$) and Th2 (IL13$^+$/CD4$^+$, IL4$^+$, or GATA-3$^+$) cells demonstrated a mixed Th1/Th2 inflammatory response to sustained stasis (3.1-fold increased Th1, 3.9-fold increased Th2; $p<0.001$; **Figure 1G-H, Supplemental Figure 1C-E**). These findings were supported by western blot analysis demonstrating increased Th1 and Th2 cytokine expression in tissues exposed to sustained lymphatic stasis peaking 6 weeks after surgery (**Figure 1I, Supplemental Figure 1F**).

## Lymph node dissection results in $CD4^+$ cell inflammation

In support of our tail model findings, we found an 11- and 30-fold increase in mature $CD4^+$ cells 3 and 6 weeks post-operatively, respectively, when we compared mice that had undergone axillary lymph node dissection (ALND) with those treated with axillary incision alone ($p<0.001$; **Figure 2A-B**). Similarly, both Th1 and Th2 cytokines were upregulated (1.4-1.6x) compared with controls (**Figure 2C**).

We confirmed these findings in patients with upper extremity lymphedema by comparing matched specimens taken from lymphedematous and normal arms. In this analysis, lymphedema was associated with an increased number of $CD4^+$ cells (2.6-fold; $p=0.01$), the degree of $CD4^+$ cell inflammation correlated with the severity of lymphedema ($r=0.6332$, $p<0.05$; **Figure 2D-E**), and there were increased numbers of $IL4^+$ (1.5-fold, $p=0.018$) and $IL13^+$ cells (2.3-fold, $p<0.001$; **Figure 2F-G**).

## $CD4^+$ cells are necessary for fibrosis and lymphatic dysfunction

Using our tail model in nude, CD4 knockout (CD4KO), and wild type mice, we found that loss of T cell (nudes) or $CD4^+$ cell inflammation decreased tail edema (3-4 fold; $p<0.01$), subcutaneous tissue thickness (1.9-fold nudes; 1.4-fold CD4KO; $p<0.01$), and $CD45^+$ cell infiltrate ($p<0.001$; **Figure 3A-D)**. Nude and CD4KO mice also had less tissue fibrosis (2-fold decreased scar index, 6-fold decreased type I collagen deposition; $p<0.01$) and markedly improved lymphatic function (3-fold increased $^{99m}Tc$ uptake, $p<0.01$; **Figure 3E-G**). Using microlymphangiography, we detected capillary lymphatic flow traversing the site of lymphatic incision resulting in a >4-fold increase in proximal tail fluorescence in CD4KO mice compared to controls ($p<0.001$; **Figure 3H**).

## Inhibition of Th2 differentiation decreases initiation and progression of fibrosis & improves lymphatic function

To test the hypothesis that Th2 differentiation regulates initiation of fibrosis in response to lymphatic stasis, we treated wild type mice with isotype control or monoclonal neutralizing antibodies against IL4 or IL13 (IL4mAb or IL13mAb) beginning immediately after tail skin/lymphatic excision. As expected, neutralization of IL4 decreased IgE production, confirming that our treatment prevented Th2 differentiation since class switching to IgE is IL4 dependent ($p<0.02$; **Supplemental Figure 2**).[18] Treatment with either IL4mAb or IL13mAb markedly decreased tail volumes as compared with controls (5-fold and 2.8-fold, respectively, $p<0.001$; **Figure 4A-B**). Whereas control animals developed fixed tail contractures due to fibrosis ("J" configuration), the tails of IL4mAb or IL13mAb-treated animals remained pliable. Histologically, IL4mAb or IL13mAb-treated animals had significantly decreased subcutaneous edema/adipose deposition (1.3 and 1.5-fold, $p<0.001$ for both), scar index (2.5 and 1.3-fold ($p<0.001$, $p<0.03$), and collagen deposition (1.7 and 1.3-fold) although the effect of IL13mAb on collagen deposition was not statistically significant (**Figure 4C-E**). IL4 neutralization decreased tissue expression of CD45, CD4, IFN-γ, IL4, and IL13 as well as peripheral blood concentrations of IL4 and IL13 (2.4 and 5.3-fold, respectively; $p<0.01$; **Figure 4F-G**). These findings were corroborated by decreased numbers of Th1 and Th2 cells in tail tissues from IL4mAb-treated animals (2-fold, $p<0.001$; **Figure 4H**). Decreased inflammation and fibrosis in IL4mAb- or IL13mAb-treated animals was associated with markedly improved lymphatic function (5-7-fold increased $^{99m}$Tc uptake, $p<0.01$; 3.5-30-fold increase in relative proximal fluorescence, $p<0.001$; **Figure 4I-J**).

To test the hypothesis that Th2 cytokines also regulate the progression of fibrosis and lymphatic dysfunction once established, we performed tail skin/lymphatic excisions in wild type mice and waited 6 weeks for fibrosis to become established (i.e. significantly increased tail volumes from baseline and fixed contracture deformity; **Figure 5A-B**). At this point, animals were randomized into groups and treated either with IL4mAb or isotype control antibodies for 3 weeks, followed by a 3 week period of treatment withdrawal. We chose not to use IL13mAb since our earlier experiments demonstrated that IL4 was more efficacious in preventing initiation of fibrosis.

Measurement of tail volumes demonstrated significant improvements in animals treated with IL4mAb (38% decrease; $p<0.01$) as compared with controls (15% decrease; p=ns; **Figure 5A-B**). IL4mAb treatment also markedly decreased tissue fibrosis with resolution of tail contracture; whereas, control animals had persistent tail fibrosis. These observations were confirmed by histological analysis demonstrating significantly decreased subcutaneous tissue thickness, interstitial edema, and adipose deposition in IL4mAb treated animals (1.4-fold; 40% reduction; $p<0.01$; **Figure 5C**). Withdrawal of IL4mAb did not result in recurrent fibrosis, increased tail volumes, or increased subcutaneous tissue thickness; although, this analysis was somewhat weakened by the fact that control animals also had minor, though non-significant, spontaneous improvements in these measures by 12 weeks post-operatively.

IL4 neutralization markedly decreased tail tissue inflammation (1.4-2.1-fold decreased CD45, CD4, IFN-γ, IL4, and IL13 expression by western blot) and serum levels of IgE (2-fold, $p<0.01$) and IL13 (6-fold; $p<0.01$; **Figure 5D-E, Supplemental Figure 2**). Differences in serum IL4 concentrations did not quite reach statistical significance. IL4mAb treatment also significantly decreased the number of Th1 (1.7-fold) and Th2 (2.1-fold) cells in lymphedematous tissues ($p<0.01$ for both; **Figure 5F**).

IL4 blockade in animals with established lymphedema significantly decreased tissue fibrosis (2-fold decreased scar index and type I collagen deposition, $p<0.01$ for both) and markedly improved lymphatic function (13-fold increased $^{99m}$Tc uptake, $p<0.01$; 3.1-fold increased proximal lymphatic fluorescence, $p<0.03$; **Figure 6A-D**). These improvements persisted even after treatment withdrawal (5-fold increased $^{99m}$Tc uptake, $p<0.01$; 2.9-fold increase proximal fluorescence, $p=0.07$).

We have previously observed that fibrosis in the mouse tail either due to radiation or skin/lymphatic excision results in the expression of α-sma by *capillary* lymphatic vessels (an abnormal finding since capillary lymphatics lack pericyte coverage).[16,17,19] Consistent with these observations, we found that IL4 neutralization for 6 weeks decreased the number of α-sma$^+$ capillary lymphatics compared with controls; however, this difference did not reach statistical significance (**Figure 6E, Supplemental Figure 3A**). In contrast, animals treated with IL4mAb for 3 weeks after development of established lymphedema had significantly fewer α-sma$^+$/LYVE-1$^+$ capillary lymphatics (3.3-fold; $p<0.001$). This finding correlated with our observation that IL4mAb treatment resulted in decreased type I collagen deposition around capillary lymphatic vessels (**Supplemental Figure 3B**).

## Inhibition of JAK1/2 does not prevent fibrosis or preserve lymphatic function

To test the hypothesis that inhibition of fibrosis is specific to Th2 differentiation rather than a generalized anti-inflammatory effect, we performed tail skin/lymphatic excision on wild type mice followed by treatment with either with an inhibitor of JAK1/2 (AZD1480)[20,21] or vehicle control for 6 weeks. We chose to block this pathway since IL4/IL13 signal through JAK3/STAT6 rather than JAK1/2/STAT3 and because JAK1/2 signaling by a variety of inflammatory cytokines, including IL6, is an important regulator of acute/chronic

inflammation.[22] This is relevant to lymphatic stasis-induced inflammation since we have noted that IL6 expression is increased in our tail and ALND models (unpublished observations), and Karlsen *et al* have shown that IL6 expression is significantly increased in lymphedematous tissues of mice with congenital lymphatic abnormalities.[23]

As expected, treatment with AZD1480 virtually completely blocked STAT3 phosphorylation (pSTAT3) by western blot analysis and decreased the number of $pSTAT3^+$ cells (2.8-fold, $p<0.001$) in lymphedematous tissues (**Figure 7A, B**). Mice treated with AZD1480 had no gross or measureable decrease in tail swelling and no difference in subcutaneous tissue thickness/interstitial edema compared with controls (**Figure 7C-E**). Importantly, STAT3 inhibition did not decrease fibrosis or improve lymphatic function, suggesting that these outcomes are specific to Th2 cytokines (**Figures 7F-H**).

## Fibrosis independently inhibits lymphatic function

We have previously reported that inhibition of radiation-induced fibrosis significantly improves lymphatic transport, suggesting that fibrosis is an independent regulator of lymphatic function.[19] To further test this hypothesis, we injected bleomycin intradermally into tails of wild type mice to induce fibrosis without skin/lymphatic excision.[24] Bleomycin injection resulted in skin and soft tissue fibrosis (2.2-fold increased scar index; 1.4-fold increased collagen deposition; $p<0.01$), increased subcutaneous tissue thickness/interstitial edema, and most importantly, severely impaired lymphatic function (12-fold decreased $^{99m}Tc$; $p<0.001$; **Figure 7I-K, Supplemental Figure 4A-B**). Inhibition of bleomycin-induced fibrosis with IL4mAb increased $^{99m}Tc$ uptake 5-fold; although, this difference did not quite reach statistical significance. However, we did note significantly improved lymphatic function using microlymphangiography (3-fold increase in fluorescence; $p<0.03$) and increased numbers of

functional lymphatics as assessed by FITC-conjugated lectin uptake by lymphatic endothelial cells[25] (1.5-fold increase in lectin+/LYVE-1+ lymphatics, $p<0.01$; **Figure 7K-L; Supplemental Figure 4C**). Using whole mount staining with FITC-conjugated lectin, we found that IL4mAb-treated animals had normal appearing, thin-walled lymphatics with interconnections (**Figure 7M**). In contrast, control animals displayed distal pooling of injected lectin and markedly atrophic superficial lymphatic vessels lacking interconnections.

## IL4 blockade does not increase VEGF-A or VEGF-C expression

We have previously shown that lymphatic stasis regulates lymphatic function by regulating the ratio of pro- and anti-lymphangiogenic cytokine expression and that this effect is dependent on T cell inflammation.[26] Further, we and others have shown that inhibition of anti-lymphangiogenic cytokines, such as IFN-γ or TGF-β1, can increase lymphatic function independent of significant changes in lymphangiogenesis or VEGF-A/C expression.[12,17,26,27] Consistent with these observations, we found that treatment with IL4mAb was not associated with significant changes in the number of lymphatic vessels or expression of lymphatic markers (LYVE-1 or PROX1) in the regions of the tail immediately distal to the wound; however, IL4mAb-treated animals more commonly exhibited lymphatic vessels traversing the wound (**Figure 8A-D, Supplemental Figure 5**). In fact, we noted a paradoxical slight increase in LYVE-1 and PROX1 expression in control animals treated with IL4mAb after lymphedema was established.

Consistent with the lack of difference in lymphatic vessel counts, we found that protein expression of lymphangiogenic growth factors was little changed (VEGF-A, VEGF-C) or paradoxically *decreased* (hepatocyte growth factor, HGF) by IL4mAb treatment regardless of the

time of treatment initiation (**Figure 8E-F**). In contrast, the expression of anti-lymphangiogenic cytokines such as IFN-γ or TGF-β1 was markedly decreased in IL4mAb treated animals.

Using an inflammatory lymph node lymphangiogenesis model to avoid potential confounding effects of wound healing, we found that, in contrast to our tail model, IL4 neutralization significantly increased lymph node lymphatic vessel density 2 weeks after CFA/OVA injection in the paw ($p<0.001$; **Figure 8G**). However, consistent with our tail model, IL4mAb treatment did not increase VEGF-A or VEGF-C protein expression (**Figure 8H**).

# Discussion

Our findings support the hypothesis that the pathophysiology of lymphedema is related to progressive lymphatic dysfunction occurring as a consequence of a $CD4^+$ inflammation, Th2 differentiation, and fibrosis. The importance of T cell inflammation in this sequence is highlighted by the observation that $CD4^+$ inflammatory responses are a key difference between temporary and sustained lymphatic stasis, as well as the fact that loss of T cells or $CD4^+$ cells markedly decreased inflammation, decreased fibrosis, and improved lymphatic function. The conclusion that lymphatic stasis initiates pathologic changes by inducing inflammation is also consistent with previous studies demonstrating that: **1.)** Lymphatic stasis potently induces the expression of endogenous danger signals[28] and upregulates the expression of inflammation and fibrosis regulatory genes both clinically and in the mouse tail model;[29] **2.)** Lymphedema is clinically associated with mononuclear cell tissue inflammation[5] and increased numbers of T lymphocytes in the lymphatic fluid;[30] and **3.)** Lymphedema-associated inflammation is markedly decreased by decongestive therapy and resultant decreased limb swelling.[31]

Our study also suggests that fibrosis is a critical step in the pathologic sequence of lymphedema and that this response is dependent on Th2 differentiation. This hypothesis is supported by our observation that: **1.)** Inhibition of T cell inflammation or Th2 differentiation but not generalized inflammation (JAK1/2/STAT3 inhibitor) markedly decreases initiation/progression of fibrosis and improves lymphatic function; **2.)** Bleomycin-induced fibrosis independently impairs lymphatic function and this effect is partially mitigated by IL4mAb; and **3.)** Sustained lymphatic stasis is associated with fibrosis of lymphatic capillaries. The fibrosis hypothesis is also supported by our previous studies demonstrating that inhibition of fibrosis (resulting from lymphatic vessel ligation or radiation) using therapies aimed at the pro-fibrotic growth factor TGF-β1 markedly improves lymphatic function, decreases T cell

inflammation, and markedly down-regulates IL4/IL13 expression, suggesting that TGF-β1 and Th2 responses have independent and interactive roles in this process.[12,16,17,19] Our results are also consistent with the fact that bleomycin-induced lung fibrosis is attenuated in nude mice[32] or mice depleted of CD4+ T cells.[33] The finding that the composition of the extracellular matrix (ECM) can directly regulate interstitial fluid flow by altering the hydraulic conductivity of the skin,[34] possibly as a consequence of changes in the compliance of lymphatic vessels[35] and their connection to the ECM by anchoring filaments,[36] also supports the concept that fibrosis or mechanical changes in the ECM can regulate lymphatic function. This hypothesis is further directly supported by clinical anatomic studies demonstrating encasement of lymphatics in fibrotic shells in patients with chronic lymphedema.[5,6] Based on these findings, we hypothesize that lymphedema develops in a subset of patients as a consequence of cumulative loss of lymphatic function resulting from lymphatic injury in combination with progressive fibrosis-induced lymphatic dysfunction (**Figure 8I**). In other patients, lymphedema does not develop due to spontaneous resolution of lymphatic stasis (i.e. regeneration or lymphatic by-pass channels)[37] or inhibition of fibrosis resulting from other variables.

The finding that targeted blockade of the Th2 response can prevent initiation/progression of fibrosis and improve lymphatic function is important and clinically relevant since it suggests for the first time that inhibiting tissue changes that occur in response to stagnating lymphatic fluid can be a means of preventing or treating lymphedema. These findings are consistent with other fibrotic disorders involving the lung, liver, skin, and radiation-induced fibrosis demonstrating that inhibition of Th2 cytokines can decrease ECM deposition and preserve functional tissue parenchyma. The fact that targeting Th2 inflammation can markedly improve lymphatic function is important since broad spectrum

anti-inflammatory treatments (e.g. corticosteroids) are not clinically applicable, as these interventions have significant deleterious effects on wound healing and other biologic processes. In fact, Rockson *et al* have shown that targeted inhibition of TNF-α, a cytokine with critical roles in acute inflammatory reactions, paradoxically results in increased inflammation and worsening lymphedema in the mouse tail, suggesting that some inflammation is necessary for wound healing and lymphangiogenesis to occur.[39]

Although it is clear that VEGF-C is *necessary* for lymphatic regeneration in most settings, it is also clear that this stimulus is not *sufficient* to restore lymphatic function in the context of lymphatic stasis, suggesting that other stimuli actively or passively inhibit this process.[40,41] These findings are consistent with previous reports from our lab and others demonstrating that inhibition of anti-lymphangiogenic cytokines can augment lymphatic function even in the context of normal or decreased VEGF-C expression.[12,17,26,27,42] Similarly, in the current study, we noted that IL4 neutralization improved lymphatic function in the mouse tail and increased lymph node lymphangiogenesis without significantly changing the expression of lymphangiogenic cytokines. This is critical since previous experimental strategies for treating lymphedema have focused on *repairing* surgically damaged lymphatics using lymphangiogenic cytokines (e.g. VEGF-C);[25] however, these approaches are contraindicated in most cancer patients since these molecules also potently promote tumor growth/metastasis.[43-46] Therefore, the use of targeted anti-fibrotic strategies may enable treatment of cancer survivors without increasing oncologic risks.

# Materials and Methods

## Animal models

We used a well-described mouse tail model [12,16,17,28,47,48] in 10-14week old female mice (C57BL/6J, Nude (B6.Cg-Foxn1nu), CD4KO (CBY.129S2(B6)-Cd4$^{tm1mak/J}$), or IL4-GFP; Jackson Labs, Bar Harbor, ME) to study the effects of lymphatic stasis on inflammation and tissue fibrosis. Briefly, lymphatic stasis in the tail was induced by excising a 2mm circumferential segment of skin and deep lymphatics 20 mm from the base of the tail.[17] The wound was then covered with or without 0.1% rat tail collagen (Sigma-Aldrich, St. Louis, MO) and sterile dressings for 5 days. We have previously shown that collagen in this model accelerates lymphatic regeneration resulting in temporary lymphatic stasis. In contrast, wounds treated without collagen have delayed lymphatic repair and sustained lymphatic stasis.[12,16,17,49] Axillary lymph node dissection (ALND) was performed in adult female C57BL/6J mice as previously described.[28,49] Control mice underwent axillary skin incision without lymph node removal.

Bleomycin-induced skin fibrosis was performed using a modification of a previously reported model.[50] Briefly, 10 µl bleomycin (0.5 U/ml, Sigma-Aldrich) was intradermally injected on the superior and inferior aspect of the tail 20 mm distal to the base twice weekly for 14 days; control animals were injected with phosphate buffered saline (PBS). All animal studies were approved by the Resource Animal Research Center IACUC at Memorial Sloan-Kettering Cancer Center.

## Antibodies and Inhibitors

We used well-described monoclonal antibodies against mouse IL4 (clone 11B11; 5 µg/g/dose; Bio-X-cell, West Lebanon, NH) or rat monoclonal antibody against mouse IL13 (clone 38213; 5 µg/g; R&D Systems, Minneapolis, MN) administered intraperitoneally.[51,52] Controls were treated with similar doses of isotype control antibodies (Bio-X-cell). To determine the role of IL4 in the initiation of fibrosis, C57BL/6J mice were treated with IL4mAb, IL13mAb, or isotype control antibodies 24 hours prior to, then weekly (IL4mAb) or every 4 days (IL13mAb) for 6 weeks following tail skin/lymphatic excision. To determine the role of IL4 in progression of established fibrosis, wild type mice underwent tail skin/lymphatic excision and were allowed to recover for 6 weeks. Animals were then randomized to receive either IL4mAb or isotype control antibody weekly for 3 weeks. A subset of this group was sacrificed at this time point, while other animals were followed for an additional 3 weeks after completion of treatment. A minimum of 6-8 animals was evaluated in each group.

We used our previously described inflammatory lymph node lymphangiogenesis model to determine the role of IL4 in this process.[26,28,49] Briefly, a mixture of 2% ovalbumin/complete freund's adjuvant (OVA/CFA) was injected in the hind paw of adult female C57BL/6J mice. Animals were then immediately treated with IL4mAb (5 µg/g weekly) or isotype control followed by weekly treatments for 2 weeks after which time popliteal lymph nodes were harvested and analyzed.

To determine the effects of non-specific inflammation in the regulation of fibrosis, we used a well-described small molecule inhibitor of the JAK1/2 signaling (AZD1480, Astra-Zeneca Wilmington, DE).[20,21] C57BL/6Jmice were administered 60 mg/kg AZD1480 (in 0.5% HPMC/0.1% Tween80) or vehicle control daily by oral gavage for 6 weeks beginning immediately after tail skin/lymphatic excision.

## Evaluation of lymphatic function

Tail volumes were determined from tail circumference measurements made by blinded reviewers at 10 mm intervals using the truncated cone formula as previously reported.[17] Subcutaneous tissue thickness was measured from the basal layer of epidermis to the underlying fascia of histological cross-sections 10 mm distal to the surgical site by blinded reviewers at 2X magnification in a minimum of 4 areas/animal (Mirax Imaging Software, Carl Zeiss, Munich, Germany).

Microlymphangiography was performed to evaluate gross structure and function of capillary lymphatics by injection of fluorescein isothiocyanate (FITC)-conjugated dextran (2,000 kDa, 10 mg/ml, Invitrogen) using our previous methods.[12,26,47,49] FITC-dextran was visualized 15 minutes following injection at 10 mm intervals along the tail using the Lumar Stereoscope (Carl Zeiss Inc, Peabody, MA) and Metamorph imaging software (Molecular Devices, Sunnyvale CA), keeping exposure, gain, and magnification constant. Uptake of FITC-Dextran in the proximal region of the tail was calculated using Metamorph and expressed as the ratio of average pixel intensity of regions proximal and distal to the surgical site 15 minutes after injection.

Lymphoscintigraphy was performed to quantify lymphatic flow by injecting 50µl of technetium Tc 99m ($^{99m}$Tc ) sulfur colloid in the distal tail as previously described.[12] Peak lymph node uptake was calculated using X-SPECT camera (Gamma Medica, Northridge, CA) and region-of-interest analysis performed to derive decay-adjusted activity using ASIPro software (CTI Molecular Imaging, Knoxville, TN). Functional lymphatic vessel staining was performed by injecting tomato lectin (1 mg/ml, Sigma) 20mm to the distal tip of the tail followed by sacrifice 45 minutes later as previously described.[25]

## Immunohistochemistry

Tissues were fixed in 4% paraformaldehyde, decalcified in Immunocal (Decal Chemical Corporation, Tallman, NY), and embedded in paraffin or OCT (Sigma-Aldrich).

Immunohistochemical staining was performed using our previous methods.[12,17] Lymphatic vessels were identified using podoplanin or LYVE-1 antibodies (Abcam, Cambridge, MA). Inflammatory cells were identified using antibodies against CD45 (R&D Systems, Minneapolis, MN), CD4 (Abcam), CD8 (Abcam), IL4 (Abcam), IL13 (R&D), IFN-γ (Abcam), and pSTAT3 (Abcam). Appropriate horseradish-peroxidase-conjugated secondary antibody (Vector, Burlingame, CA) was applied and sections were developed with diaminobenzamine (DAB; Vector). Negative control sections were incubated with isotype control antibody or secondary antibody alone. Bright-field images were obtained using a Leica TCS microscope and imaged with a Mirax slide scanner (Carl Zeiss).

Confocal microscopy for antigen co-localization (LYVE-1 and α-smooth muscle actin (SMA; Abcam), or CD4 and IFN-γ or IL13) was performed as previously described and was visualized using Nuance Multispectral imaging System (LOT Oriel Group, Daimstadt, Germany).[12,17] Specificity was confirmed using single-stained sections and negative controls. Images were captured using an Axioskope (Carl Zeiss).[12,17] Lymph node lymphatic vessel density was determined using Metamorph™ Offline software and expressed relative to node area (vessels/$mm^2$) as previously described.[28]

Fibrosis was assessed using our previously published methods to quantify Sirius Red staining and type I collagen immunohistochemistry.[12,16,17] Sirius red (Sigma) scar index was calculated using polarized light microscopy to calculate the ratio of orange/red to yellow/green birefringence and analyzed using Metamorph™ Offline software. Type I collagen immunohistochemistry was performed using an antibody to mouse type I collagen (Abcam)

and quantified as a ratio of the area of positively-stained dermis and subcutaneous tissue within a fixed threshold to total tissue area/HPF.

## Human Lymphedema Samples

Thirteen patients with post-surgical upper extremity lymphedema (grade I-III) were identified at the Stanford Center for Lymphatic and Venous Disorders. Full-thickness 5 mm skin punch biopsies were obtained from identical locations of the lymphedematous and contralateral normal limb. Immunohistochemistry using antibody against human CD4, IL4, and IL13 (all from Abcam) was conducted on all specimens and correlation made to lymphedema grade. The number of positive cells was calculated in a minimum of 3 high-powered fields (HPF)/patient/limb by 2 blinded reviewers using a Leica TCS microscope. Results are expressed as the number of positive cells/$mm^2$ or per HPF. The Institutional Review Boards of Stanford University and Memorial Sloan-Kettering Cancer Center approved all studies.

## Flow cytometry

One centimeter skin/subcutaneous sections were harvested from regions located 15mm proximal or distal to the wound in the tail or axilla of mice 3 or 6 weeks following surgery and digested with Collagenase P (n=3-5 animals/group/time point). Cell suspensions were stained with fluorophore-conjugated antibodies to CD4 and TCRβ (Biolegend, San Diego, CA) and analyzed using a FACSCalibur flow-cytometer (BD Biosciences, San Jose, CA). Results were analyzed using Flowjo software (Tree Star, Ashland, OR) to calculate the percentage of $CD4^+$ and $CD4^+/TCR\beta^+$ lymphocytes by gating on lymphocyte populations.

## Western Blot Analysis, ELISA

Skin/subcutaneous tissues were isolated from the tail or upper extremity 15mm distal to the wound margin, lysed in buffer (Thermofisher, Waltham, MA), and quantified using the Bradford method (Biorad, Hercules, CA). Western blots were performed using our previous methods to quantify expression of CD45, CD4, IL4, IFN-γ, IL13, and TGF-β1, VEGF-C, VEGF-A, LYVE-1, PROX1 and hepatocyte growth factor (HGF; all from Abcam).[49] Equal loading was confirmed with Actin (Abcam) and relative changes in band density was determined as a ratio of mean band density and normalized to actin using ImageJ software (http://rsbweb.nih.gov/ij/). All experiments were performed in triplicate. For ELISA, serum was isolated from peripheral blood (n=3-5 animals/group) and analyzed to quantify IgE, IL4, and IL13 according to the manufacturer's directions (eBioscience, San Diego, CA).

## Statistical analysis

The Student's T-test was used to compare differences between 2 groups. Multi-group comparisons were performed using analysis of variance (ANOVA) with the Tukey-Kramer post-hoc test. Analysis of clinical lymphedema samples was performed using the Wilcoxon matched pair T-test. Correlation between lymphedema grade and CD4+ infiltrate was evaluated by Spearman correlation. Data are presented as mean ± standard deviation unless otherwise noted with $p<0.05$ considered significant.

## Acknowledgments

The authors thank Dr. Ronald DeMatteo for his helpful advice regarding planning and execution of the experiments.

## Funding

This work was funded in part by the Plastic Surgery Educational Foundation and The Society of Memorial Sloan-Kettering Cancer Center grants to BJM. TA was funded in part by a fellowship grant from the Plastic Surgery Educational Foundation. TA and JZ were also supported by T32 Surgical Oncology Training Grant NIH T32 CA 009501. JZ was also partially supported from a grant (BC103691) from the Department of Defense.

Technical services provided by the MSKCC Small-Animal Imaging Core Facility, supported in part by NIH Small-Animal Imaging Research Program (SAIRP) Grant No R24 CA83084 and NIH Center Grant No P30 CA08748, are gratefully acknowledged.

# References


1. Pyszel A, Malyszczak K, Pyszel K, Andrzejak R, Szuba A (2006) Disability, psychological distress and quality of life in breast cancer survivors with arm lymphedema. Lymphology 39: 185-192.
2. Rockson SG, Rivera KK (2008) Estimating the population burden of lymphedema. Ann N Y Acad Sci 1131: 147-154.
3. Shih YC, Xu Y, Cormier JN, Giordano S, Ridner SH, et al. (2009) Incidence, treatment costs, and complications of lymphedema after breast cancer among women of working age: a 2-year follow-up study. J Clin Oncol 27: 2007-2014.
4. Crockett D (1965) Lymphatic anatomy and lymphoedema. Br J Plast Surg 18: 12.
5. Olszewski WL, Jamal S, Manokaran G, Lukomska B, Kubicka U (1993) Skin changes in filarial and non-filarial lymphoedema of the lower extremities. Trop Med Parasitol 44: 40-44.
6. Suami H, Pan WR, Taylor GI (2007) Changes in the lymph structure of the upper limb after axillary dissection: radiographic and anatomical study in a human cadaver. Plast Reconstr Surg 120: 982-991.
7. Allegra C, Sarcinella R, Bartolo M, Jr. (2002) Morphologic and functional changes of the microlymphatic network in patients with advancing stages of primary lymphedema. Lymphology 35: 114-120.
8. Manduch M, Oliveira AM, Nascimento AG, Folpe AL (2009) Massive localised lymphoedema: a clinicopathological study of 22 cases and review of the literature. J Clin Pathol 62: 808-811.
9. Tassenoy A, De Mey J, Stadnik T, De Ridder F, Peeters E, et al. (2009) Histological findings compared with magnetic resonance and ultrasonographic imaging in irreversible postmastectomy lymphedema: a case study. Lymphat Res Biol 7: 145-151.
10. Petrek JA, Senie RT, Peters M, Rosen PP (2001) Lymphedema in a cohort of breast carcinoma survivors 20 years after diagnosis. Cancer 92: 1368-1377.
11. Petrek JA, Heelan MC (1998) Incidence of breast carcinoma-related lymphedema. Cancer 83: 2776-2781.
12. Avraham T, Daluvoy S, Zampell J, Yan A, Haviv YS, et al. (2010) Blockade of Transforming Growth Factor-{beta}1 Accelerates Lymphatic Regeneration during Wound Repair. Am J Pathol 177: 3202-3214.
13. Wynn T (2008) Cellular and molecular mechanisms of fibrosis. J Pathol 214: 199-210.
14. Hinrichs CS, Watroba NL, Rezaishiraz H, Giese W, Hurd T, et al. (2004) Lymphedema secondary to postmastectomy radiation: incidence and risk factors. Ann Surg Oncol 11: 573-580.
15. Beesley V, Janda M, Eakin E, Obermair A, Battistutta D (2007) Lymphedema after gynecological cancer treatment : prevalence, correlates, and supportive care needs. Cancer 109: 2607-2614.
16. Avraham T, Clavin NW, Daluvoy SV, Fernandez J, Soares MA, et al. (2009) Fibrosis is a key inhibitor of lymphatic regeneration. Plast Reconstr Surg 124: 438-450.
17. Clavin NW, Avraham T, Fernandez J, Daluvoy SV, Soares MA, et al. (2008) TGF-beta1 is a negative regulator of lymphatic regeneration during wound repair. Am J Physiol Heart Circ Physiol 295: H2113-2127.
18. Poulsen LK, Hummelshoj L (2007) Triggers of IgE class switching and allergy development. Ann Med 39: 440-456.

19. Avraham T, Yan A, Zampell JC, Daluvoy SV, Haimovitz-Friedman A, et al. (2010) Radiation therapy causes loss of dermal lymphatic vessels and interferes with lymphatic function by TGF-beta1-mediated tissue fibrosis. Am J Physiol Cell Physiol 299: C589-605.
20. Scuto A, Krejci P, Popplewell L, Wu J, Wang Y, et al. (2011) The novel JAK inhibitor AZD1480 blocks STAT3 and FGFR3 signaling, resulting in suppression of human myeloma cell growth and survival. Leukemia 25: 538-550.
21. Mankan AK, Greten FR (2011) Inhibiting signal transducer and activator of transcription 3: rationality and rationale design of inhibitors. Expert Opin Investig Drugs 20: 1263-1275.
22. Neurath MF, Finotto S (2011) IL-6 signaling in autoimmunity, chronic inflammation and inflammation-associated cancer. Cytokine Growth Factor Rev 22: 83-89.
23. Karlsen TV, Karkkainen MJ, Alitalo K, Wiig H (2006) Transcapillary fluid balance consequences of missing initial lymphatics studied in a mouse model of primary lymphoedema. J Physiol 574: 583-596.
24. Yoshizaki A, Iwata Y, Komura K, Ogawa F, Hara T, et al. (2008) CD19 regulates skin and lung fibrosis via Toll-like receptor signaling in a model of bleomycin-induced scleroderma. Am J Pathol 172: 1650-1663.
25. Tammela T, Saaristo A, Holopainen T, Lyytikka J, Kotronen A, et al. (2007) Therapeutic differentiation and maturation of lymphatic vessels after lymph node dissection and transplantation. Nat Med 13: 1458-1466.
26. Zampell JC, Avraham T, Yoder N, Fort N, Yan A, et al. (2012) Lymphatic function is regulated by a coordinated expression of lymphangiogenic and anti-lymphangiogenic cytokines. Am J Physiol Cell Physiol 302: C392-404.
27. Kataru RP, Kim H, Jang C, Choi DK, Koh BI, et al. (2011) T lymphocytes negatively regulate lymph node lymphatic vessel formation. Immunity 34: 96-107.
28. Zampell JC, Yan A, Avraham T, Andrade V, Malliaris S, et al. (2011) Temporal and spatial patterns of endogenous danger signal expression after wound healing and in response to lymphedema. Am J Physiol Cell Physiol 300: C1107-1121.
29. Tabibiazar R, Cheung L, Han J, Swanson J, Beilhack A, et al. (2006) Inflammatory manifestations of experimental lymphatic insufficiency. PLoS Med 3: e254.
30. Galkowska H, Olszewski WL (1986) Cellular composition of lymph in experimental lymphedema. Lymphology 19: 139-145.
31. Foldi E, Sauerwald A, Hennig B (2000) Effect of complex decongestive physiotherapy on gene expression for the inflammatory response in peripheral lymphedema. Lymphology 33: 19-23.
32. Schrier DJ, Phan SH, McGarry BM (1983) The effects of the nude (nu/nu) mutation on bleomycin-induced pulmonary fibrosis. A biochemical evaluation. Am Rev Respir Dis 127: 614-617.
33. Xu J, Mora AL, LaVoy J, Brigham KL, Rojas M (2006) Increased bleomycin-induced lung injury in mice deficient in the transcription factor T-bet. Am J Physiol Lung Cell Mol Physiol 291: L658-667.
34. Bennuru S, Maldarelli G, Kumaraswami V, Klion AD, Nutman TB (2010) Elevated levels of plasma angiogenic factors are associated with human lymphatic filarial infections. Am J Trop Med Hyg 83: 884-890.
35. Rutkowski JM, Markhus CE, Gyenge CC, Alitalo K, Wiig H, et al. (2010) Dermal collagen and lipid deposition correlate with tissue swelling and hydraulic conductivity in murine primary lymphedema. Am J Pathol 176: 1122-1129.

36. Rossi A, Weber E, Sacchi G, Maestrini D, Di Cintio F, et al. (2007) Mechanotransduction in lymphatic endothelial cells. Lymphology 40: 102-113.
37. Aboul-Enein A, Eshmawy I, Arafa S, Abboud A (1984) The role of lymphovenous communication in the development of post mastectomy lymphedema. Surgery 95: 562.
38. Wynn TA (2008) Cellular and molecular mechanisms of fibrosis. J Pathol 214: 199-210.
39. Nakamura K, Radhakrishnan K, Wong YM, Rockson SG (2009) Anti-inflammatory pharmacotherapy with ketoprofen ameliorates experimental lymphatic vascular insufficiency in mice. PLoS One 4: e8380.
40. Goldman j, Rutkowski J, Shields J, Pasquier M, Cui Y, et al. (2007) Cooperative and redundant roles of VEGFR-2 and VEGFR-3 signaling in adult lymphangiogenesis. FASEB J 21: 1003-1012.
41. Rutkowski JM, Moya M, Johannes J, Goldman J, Swartz MA (2006) Secondary lymphedema in the mouse tail: Lymphatic hyperplasia, VEGF-C upregulation, and the protective role of MMP-9. Microvasc Res 72: 161-171.
42. Oka M, Iwata C, Suzuki HI, Kiyono K, Morishita Y, et al. (2008) Inhibition of endogenous TGF-{beta} signaling enhances lymphangiogenesis. Blood.
43. Feng Y, Wang W, Hu J, Ma J, Zhang Y, et al. (2010) Expression of VEGF-C and VEGF-D as significant markers for assessment of lymphangiogenesis and lymph node metastasis in non-small cell lung cancer. Anat Rec (Hoboken) 293: 802-812.
44. Gu Y, Qi X, Guo S (2008) Lymphangiogenesis induced by VEGF-C and VEGF-D promotes metastasis and a poor outcome in breast carcinoma: a retrospective study of 61 cases. Clin Exp Metastasis 25: 717-725.
45. Hirakawa S, Brown LF, Kodama S, Paavonen K, Alitalo K, et al. (2007) VEGF-C-induced lymphangiogenesis in sentinel lymph nodes promotes tumor metastasis to distant sites. Blood 109: 1010-1017.
46. Kazama S, Watanabe T, Kanazawa T, Hatano K, Nagawa H (2007) Vascular endothelial growth factor-C (VEGF-C) is a more specific risk factor for lymph node metastasis than VEGF-D in submucosal colorectal cancer. Hepatogastroenterology 54: 71-76.
47. Zampell J, Elhadad S, Avraham T, Weitman E, Aschen S, et al. (2011) Toll-Like Receptor Deficiency Worsens Inflammation and Lymphedema after Lymphatic Injury. Am J Physiol Cell Physiol.
48. Goldman J, Le TX, Skobe M, Swartz MA (2005) Overexpression of VEGF-C causes transient lymphatic hyperplasia but not increased lymphangiogenesis in regenerating skin. Circ Res 96: 1193-1199.
49. Zampell JC, Yan A, Avraham T, Daluvoy S, Weitman ES, et al. (2011) HIF-1alpha coordinates lymphangiogenesis during wound healing and in response to inflammation. FASEB J.
50. Castelino FV, Seiders J, Bain G, Brooks SF, King CD, et al. (2011) Amelioration of dermal fibrosis by genetic deletion or pharmacologic antagonism of lysophosphatidic acid receptor 1 in a mouse model of scleroderma. Arthritis Rheum 63: 1405-1415.
51. Romani L, Mencacci A, Grohmann U, Mocci S, Mosci P, et al. (1992) Neutralizing antibody to interleukin 4 induces systemic protection and T helper type 1-associated immunity in murine candidiasis. J Exp Med 176: 19-25.
52. Yang G, Volk A, Petley T, Emmell E, Giles-Komar J, et al. (2004) Anti-IL-13 monoclonal antibody inhibits airway hyperresponsiveness, inflammation and airway remodeling. Cytokine 28: 224-232.

# Figure Legends

**Figure 1. Sustained lymphatic stasis results in CD4$^+$ cell inflammation.**

**A.** Photograph 6 weeks post-operatively comparing temporary (control) and sustained lymphatic stasis (lymphedema).

**B.** Heat maps (above) and peak lymph node uptake of $^{99m}$Tc by sacral lymph nodes (arrows) after distal injection.

**C.** CD4+ cell counts proximal/distal to the wound.

**D.** Representative 2x (upper) and 40x (magnification of boxed area; lower) longitudinal sections demonstrating CD4$^+$ staining in an excision animal (wound=brackets).

**E,F.** Representative flow cytometry analysis (**E**) and quantification of triplicate experiments demonstrating mature T-helper cells (TCR$\beta^+$/CD4$^+$) in proximal/distal tail regions tail 3/6 weeks post-operatively.

**G,H.** Cell counts of Th1 (**G;** IFN-$\gamma^+$/CD4$^+$) and Th2 (**H;** IL13$^+$/CD4$^+$) in proximal/distal tail regions tail 6 weeks after surgery.

**I.** Representative western blot of protein from tissues harvested 6 weeks post-operatively 15 mm distal (dashed line) to the wound (arrow). Relative fold-increase comparing lymphedema groups to controls is shown.

**Figure 2. Lymph node dissection results in CD4+ cell inflammation.**

**A,B.** Representative flow cytometry analysis (**A**) and quantification of triplicate experiments (**B**) demonstrating mature T-helper cells in tissues harvested from upper extremities of mice following ALND or axillary incision (sham) 3/6 weeks post-operatively.

**C.** Representative western blot of protein harvested from the upper extremity 6 weeks post-operatively with relative fold-increase comparing ALND to sham.

**D.** Number of $CD4^+$ cells in normal and lymphedematous upper extremities of lymphedema patients.

**E.** Correlation of the number of $CD4^+$ cells in the lymphedematous limb with severity of lymphedema.

**F,G.** Number of $IL4^+$ cells/$mm^2$ (**F**) and $IL13^+$ cells/$mm^2$ (**G**) in normal and lymphedematous upper extremities of patients with lymphedema.

**Figure 3. CD4+ cells are necessary for fibrosis and lymphatic dysfunction.**

**A.** Representative photographs of nude, CD4KO, and wild type mouse tails 6 weeks after tail skin/lymphatic excision. Note fixed contracture of wild type tail.

**B.** Tail volume changes (% change from pre-operative) 6 weeks after surgery.

**C.** Subcutaneous tissue thickness and representative cross-sectional histology 6 weeks after surgery. Gross photograph is shown for orientation and site of tissue harvest (dashed line). Note markedly decreased subcutaneous adipose deposition and edema (brackets) in nude and CD4KO mice.

**D.** CD45 cell counts and representative photomicrographs (40X) in distal tail tissues of CD4KO and wild type mice 6 weeks post-operatively.

**E.** Scar index and representative histology (40X) of distal tail tissues 6 weeks post-operatively.

**F.** Collagen deposition and representative histology (20X) of distal tail tissues 6 weeks post-operatively.

**G.** Peak nodal uptake of $^{99m}Tc$ injected in the distal tail 6 weeks after surgery.

**H.** Proximal tail fluorescence (% of proximal fluorescence as a function of distal fluorescence) 6 weeks after surgery comparing CD4KO and wild type mice.

**Figure 4. Inhibition of Th2 differentiation prevents initiation of fibrosis and improves lymphatic function.**

**A.** Representative photographs of tails from animals treated with IL4mAb, IL13mAb, or isotype control antibodies (control) for 6 weeks beginning immediately after tail skin/lymphatic excision. Note lack of fibrotic contracture in the tails of IL4/IL13mAb treated mice as compared to fixed contracture of controls.

**B.** Tail volume changes (% change from pre-operative) 6 weeks after surgery.

**C.** Subcutaneous tissue thickness and representative cross-sectional histology 6 weeks after surgery. Note marked decreased adipose deposition and edema in IL4mAb/IL13mAb treated mice (brackets).

**D.** Scar index and representative histology (40X) of distal tail tissues 6 weeks post-operatively.

**E.** Collagen deposition and representative histology (20X) of distal tail tissues 6 weeks post-operatively.

**F.** Western blot analysis of distal tail tissues harvested 15mm distal to the wound (wound=arrow in photograph; harvest site=dotted line) comparing IL4mAb and control animals 6 weeks after surgery. Fold decrease in expression in IL4mAb animals relative to controls is shown.

**G.** Serum IL4 and IL13 levels in animals treated with IL4mAb or isotype control antibody 6 weeks after surgery.

**H.** Number of Th1 (IFN-$\gamma^+$/$CD4^+$) and Th2 ($IL13^+$/$CD4^+$) cells in distal tail tissues of IL4mAb and control antibody-treated animals 6 weeks post-operatively.

**I.** Representative heat maps (above) and peak nodal uptake of $^{99m}Tc$ in sacral lymph nodes (white arrows) following distal tail injection 6 weeks after surgery.

**J.** Representative microlymphangiography and calculation of proximal tail fluorescence (%of proximal fluorescence as a function of distal fluorescence) 6 weeks after surgery.

**Figure 5. Inhibition of Th2 differentiation decreases established lymphedema.**

**A-C.** Representative photographs (**A**), tail volumes (**B**), and subcutaneous tissue thickness (**C**) of tails from animals 6 weeks after skin excision/lymphatic disruption (pre-tx), following 3 week treatment with IL4/control antibodies (post-tx) beginning 6 weeks after surgery, and following an additional 3 week treatment withdrawal (post-tx withdrawal).

**D.** Western blot of distal tail tissues from animals following 3 week treatment course with IL4/control antibodies beginning 6 weeks post-operatively (fold-decrease=normalized expression from IL4mAb-treated animals relative to controls).

**E.** Serum IL4 and IL13 levels in animals post-treatment with IL4/control antibodies for 3 weeks.

**F.** Number of Th1/Th2 cells in distal tail tissues post-treatment with IL4/control antibodies.

**Figure 6. Inhibition of Th2 differentiation decreases established fibrosis and improves lymphatic function.**

**A,B.** Scar index (**A;** representative 40x views) and collagen staining (**B;** representative 20x views) of distal tail tissues post-treatment with IL-4/control antibodies.

**C.** Representative heat maps (above) and peak nodal uptake of $^{99m}$Tc in sacral lymph nodes following distal tail injection post-treatment (Ab Tx) and following treatment withdrawal (Tx withdrawal).

**D.** Representative microlymphangiography and proximal tail fluorescence post-treatment (Ab Tx) and following treatment withdrawal (Tx withdrawal) with IL4/control antibodies.

**E.** Number of $\alpha$-sma$^+$ capillary lymphatic vessels/hpf.

**Figure 7. Inhibition of JAK1/2 does not prevent fibrosis or preserve lymphatic function.**

**A,B.** pSTAT3 cell counts (**A**) and representative western blot of pSTAT3 and total STAT3 (**B**) in distal tail tissues of JAK1/2 inhibitor- or control-treated animals.

**C**. Representative photographs of JAK1/2 inhibitor or control-treated mouse tails 6 weeks post-operatively.

**D,E.** Change in tail volume (**D**) and subcutaneous tissue thickness (**E**) in JAK1/2 inhibitor or control treated mice 6 weeks postoperatively.

**F,G.** Scar index (**F;** representative 40x views) and collagen staining (**G;** representative 20x views) of distal tail tissues following treatment with JAK1/2 inhibitor or control 6 weeks post-operatively.

**H.** Peak nodal uptake of $^{99m}$Tc in JAK1/2 inhibitor or control-treated animals 6 weeks post-operatively.

**I.** Subcutaneous tissue thickness of animals treated with bleomycin or phosphate-buffered saline (PBS).

**J**,**K**. Peak nodal uptake of $^{99m}$Tc by sacral lymph nodes (**J**) and microlymphangiography/proximal fluorescence (**K**) in animals treated with bleomycin, bleomycin and IL-4mAb, or PBS control.

**L**,**M.** Quantification of lectin$^+$ capillary lymphatics (**L;** % of total lymphatics) and representative whole mount lectin stain (**M**) in bleomycin/IL4mAb and bleomycin/control antibody-treated animals. White arrows are capillary lymphatics; dotted circles represent pooled areas of lectin in interstitial space.

## Figure 8. IL4 blockade does not increase VEGF-A or VEGF-C expression

**A, B.** LYVE-1$^+$ (**A**) and Podoplanin$^+$ (**B**) vessel counts in IL4/control antibody-treated animals beginning immediately after surgery and continued for 6 weeks (initiation) or beginning 6 weeks after surgery and continued for 3 weeks (progression).

**C.** Representative western blots (of triplicate experiments) for LYVE-1 and PROX1 expression in distal tail protein of animals treated with IL4mAb/control antibody for 6 weeks beginning immediately after surgery (left) or after treatment with IL4mAb/control antibodies for 3 weeks beginning 6 weeks post-operatively (right). Normalized fold-increase in expression relative to controls is shown.

**D.** Representative 40x photomicrograph of wound area following treatment with IL4mAb/control antibody for 6 weeks beginning immediately after surgery. Arrow shows lymphatic vessel crossing the wound.

**E, F.** Representative western blots (of triplicate experiments) from distal tail protein isolated from animals treated with IL4mAb/control antibody for 2 or 6 weeks beginning

immediately after surgery (**D;** Initiation of fibrosis) or after treatment with IL-4/control antibodies for 3 weeks beginning 6 weeks after surgery (**E;** Progression of fibrosis). Normalized fold-increase in expression relative to controls is shown.

**G.** LYVE-1$^+$ lymphatic vessel density and representative photomicrographs of popliteal lymph nodes harvested from animals treated with IL4mAb/control antibodies 2 weeks post-CFA/OVA injection into hind paw.

**H.** Expression of VEGF-A/C (by ELISA) in popliteal lymph nodes harvested from animals treated with IL4mAb/control antibodies 2 weeks post-CFA/OVA injection into the hind paw.

**I.** Schema depicting proposed mechanism of lymphedema development in response to lymphatic fluid stasis.

**Supplemental Figure 1.**

**A.** Number of CD45$^+$ cells/hpf in proximal and distal tail tissues of control and lymphedema groups 6 weeks after surgery.

**B.** Number of CD4$^+$/CD45$^+$ and CD4$^-$/CD45$^+$ cells and percentage of total number in distal tail tissues of control and lymphedema groups.

**C.** Representative fluorescent photomicrographs of Th1 (CD4$^+$/IFN-γ$^+$) and Th2 (CD4$^+$/IL13$^+$) cells in distal tail tissues of control and lymphedema groups 6 weeks after surgery (60x magnification).

**D.** Cell counts of IL4$^+$ cells/hpf in proximal and distal tail sections of mice 6 weeks after tail skin and lymphatic excision. Representative 40x figures are shown above.

**E.** Cell counts of GATA-3$^+$ cells in distal tail tissues of control and lymphedema groups 6 weeks after surgery.

**F.** Western blot analysis of temporal protein expression in the distal tail (protein harvested at the region of the dotted line in photograph). Fold-change represents ratio of expression between 1 and 6 weeks post-operatively.

**Supplemental Figure 2.** IgE concentration in the peripheral serum of animals treated with IL4mab or control antibody for 6 weeks beginning immediately after tail skin/lymphatic excision.

**Supplemental Figure 3.**

**A.** Representative photomicrographs in tail tissues from animals treated with antibodies beginning either immediately after surgery (initiation) or for 3 weeks after lymphedema was established (progression).

**B.** Type I collagen staining (green) surrounding capillary lymphatics (red=LYVE-1) from tail tissues of animals treated with IL4/control antibodies for 3 weeks beginning 6 weeks after surgery.

**Supplemental Figure 4.**

**A,B.** Scar index (**A;** representative 40x views) and collagen staining (**B;** representative 20x views) of distal tail tissues in animals treated with Bleomycin or PBS for 3 weeks.

**C.** Representative figure (100x) demonstrating lectin$^{+}$ (functional) and lectin$^{-}$ (non-functional) lymphatic vessels in proximal tail tissues. Lectin is stained green; LYVE-1 is red.

**Supplemental Figure 5.**

**A,B.** Representative figure (40x views) demonstrating LYVE-1 staining in IL4mAb and control animals with treatment initiated immediately after surgery for 6 weeks (**A**, initiation) or beginning 6 weeks after surgery for 3 weeks (**B,** progression). Arrows show LYVE-1-positive capillary lymphatics.

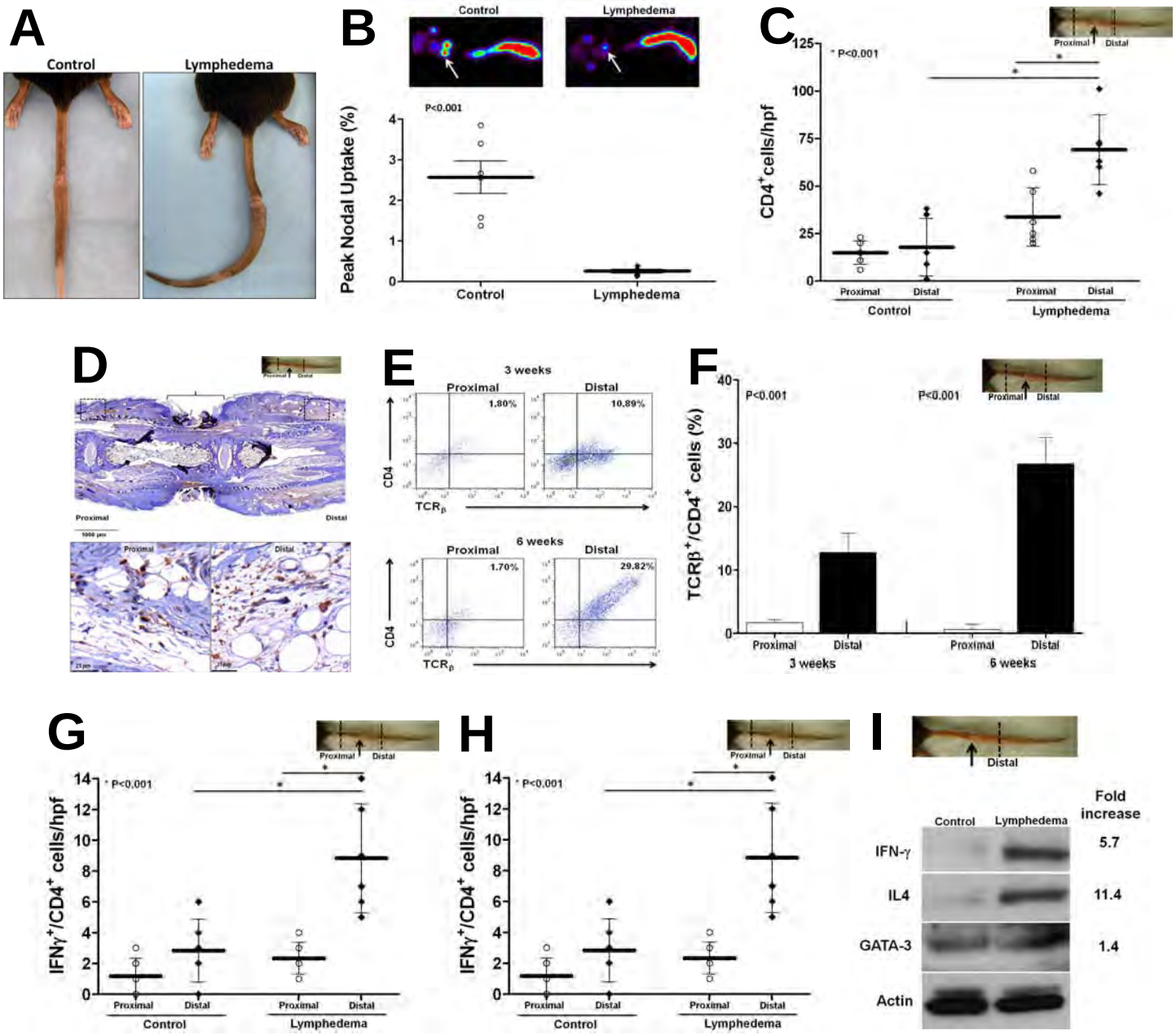


**Figure 1. Sustained lymphatic stasis results in CD4⁺ cell inflammation.**

- **A.** Photograph 6 weeks post-operatively comparing temporary (control) and sustained lymphatic stasis (lymphedema).
- **B.** Heat maps (above) and peak lymph node uptake of $^{99m}$Tc by sacral lymph nodes (arrows) after distal injection.
- **C.** CD4+ cell counts proximal/distal to the wound.
- **D.** Representative 2x (upper) and 40x (magnification of boxed area; lower) longitudinal sections demonstrating CD4⁺ staining in an excision animal (wound=brackets).
- **E,F.** Representative flow cytometry analysis (**E**) and quantification of triplicate experiments demonstrating mature T-helper cells (TCRβ⁺/CD4⁺) in proximal/distal tail regions tail 3/6 weeks post-operatively.
- **G,H.** Cell counts of Th1 (**G;** IFN-γ⁺/CD4⁺) and Th2 (**H;** IL13⁺/CD4⁺) in proximal/distal tail regions tail 6 weeks after surgery.
- **I.** Representative western blot of protein from tissues harvested 6 weeks post-operatively 15 mm distal (dashed line) to the wound (arrow). Relative fold-increase comparing lymphedema groups to controls is shown.

**Figure 1**

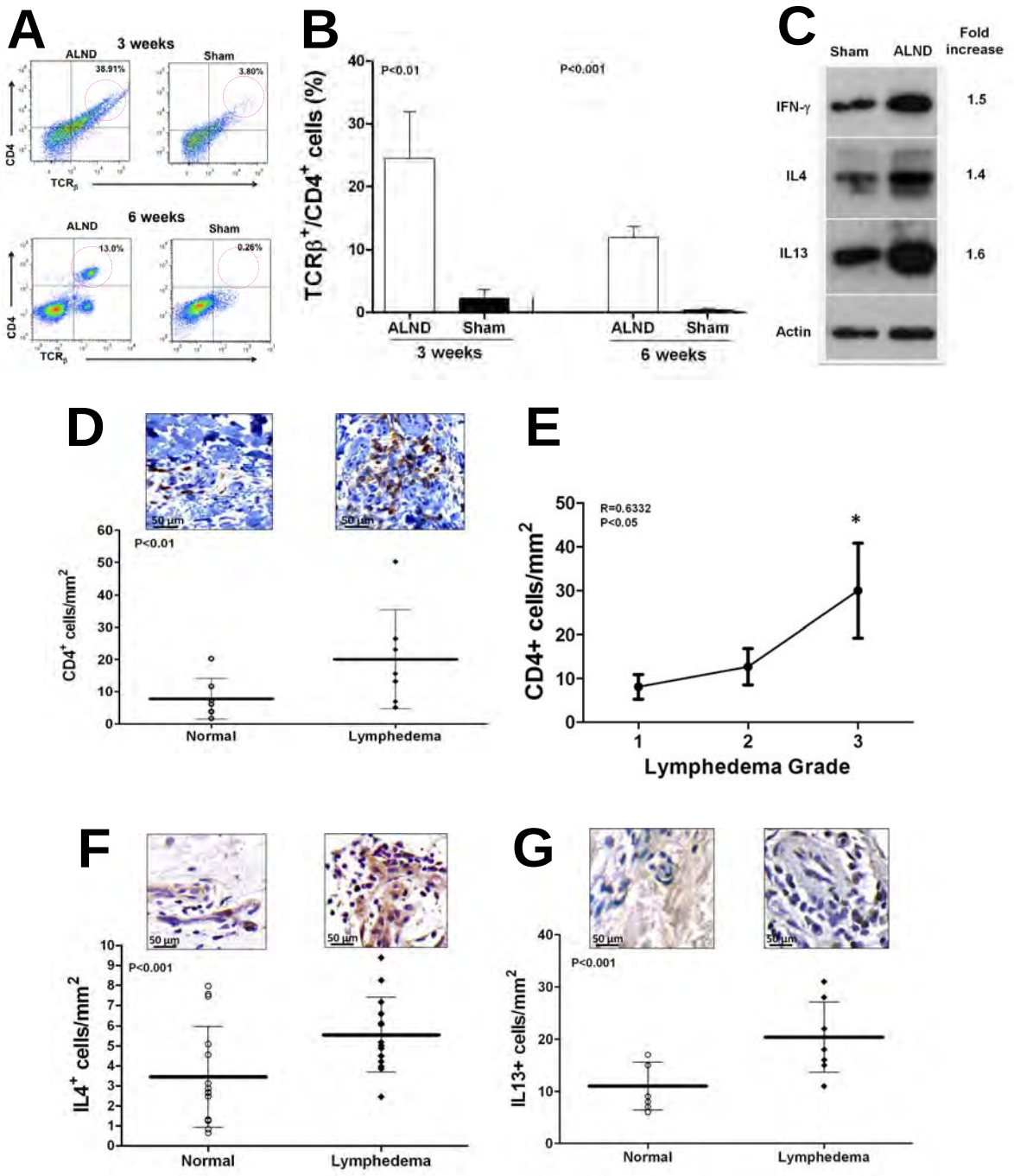


**Figure 2. Lymph node dissection results in CD4+ cell inflammation.**

**A,B.** Representative flow cytometry analysis (**A**) and quantification of triplicate experiments (**B**) demonstrating mature T-helper cells in tissues harvested from upper extremities of mice following ALND or axillary incision (sham) 3/6 weeks post-operatively.

**C.** Representative western blot of protein harvested from the upper extremity 6 weeks post-operatively with relative fold-increase comparing ALND to sham.

**D.** Number of $CD4^+$ cells in normal and lymphedematous upper extremities of lymphedema patients.

**E.** Correlation of the number of $CD4^+$ cells in the lymphedematous limb with severity of lymphedema.

**F,G.** Number of $IL4^+$ cells/$mm^2$ (**F**) and $IL13^+$ cells/$mm^2$ (**G**) in normal and lymphedematous upper extremities of patients with lymphedema.

**Figure 2**

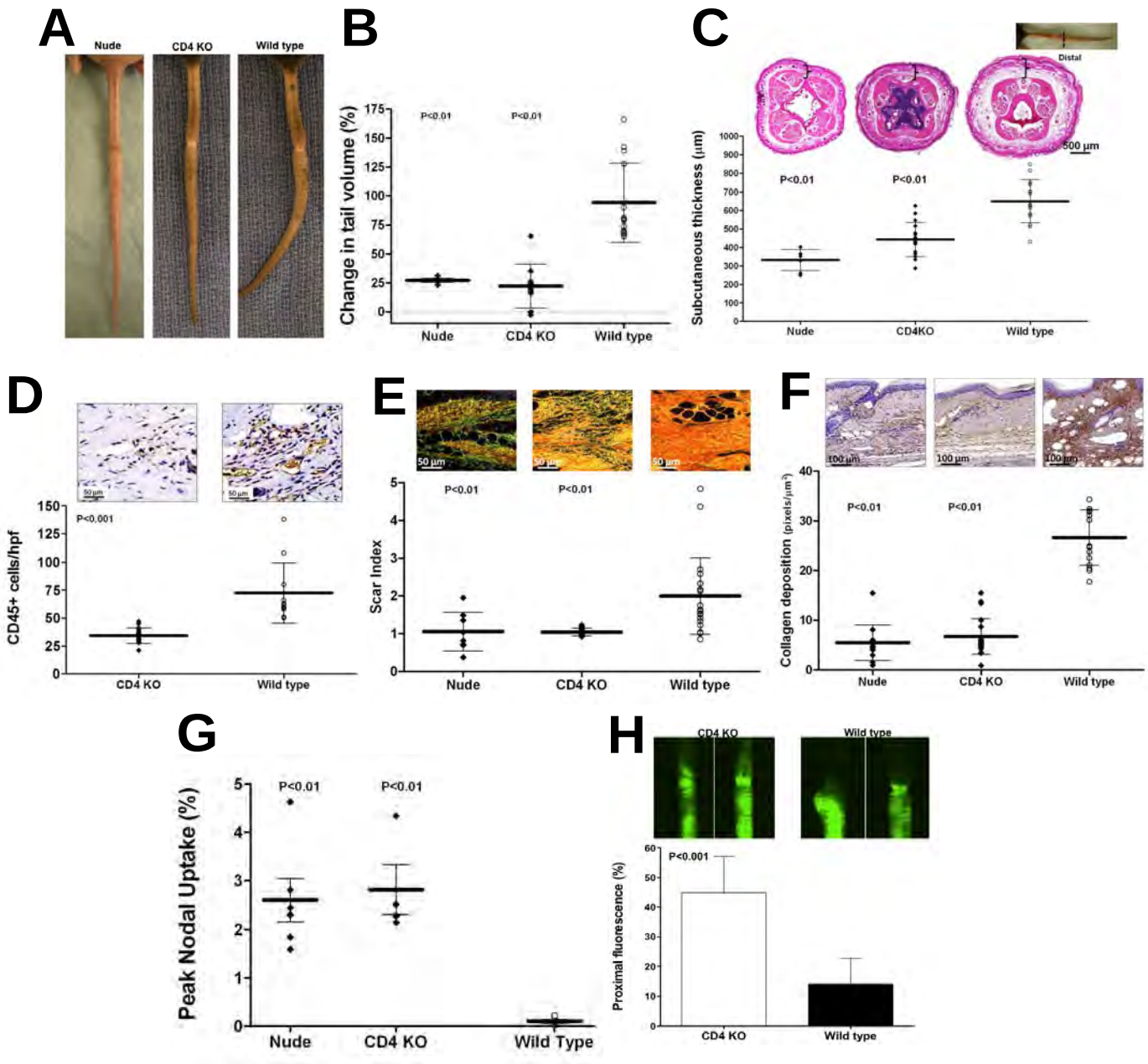


**Figure 3. CD4+ cells are necessary for fibrosis and lymphatic dysfunction.**

- **A.** Representative photographs of nude, CD4KO, and wild type mouse tails 6 weeks after tail skin/lymphatic excision. Note fixed contracture of wild type tail.
- **B.** Tail volume changes (% change from pre-operative) 6 weeks after surgery.
- **C.** Subcutaneous tissue thickness and representative cross-sectional histology 6 weeks after surgery. Gross photograph is shown for orientation and site of tissue harvest (dashed line). Note markedly decreased subcutaneous adipose deposition and edema (brackets) in nude and CD4KO mice.
- **D.** CD45 cell counts and representative photomicrographs (40X) in distal tail tissues of CD4KO and wild type mice 6 weeks post-operatively.
- **E.** Scar index and representative histology (40X) of distal tail tissues 6 weeks post-operatively.
- **F.** Collagen deposition and representative histology (20X) of distal tail tissues 6 weeks post-operatively.
- **G.** Peak nodal uptake of $^{99m}$Tc injected in the distal tail 6 weeks after surgery.
- **H.** Proximal tail fluorescence (% of proximal fluorescence as a function of distal fluorescence) 6 weeks after surgery comparing CD4KO and wild type mice.

**Figure 3**

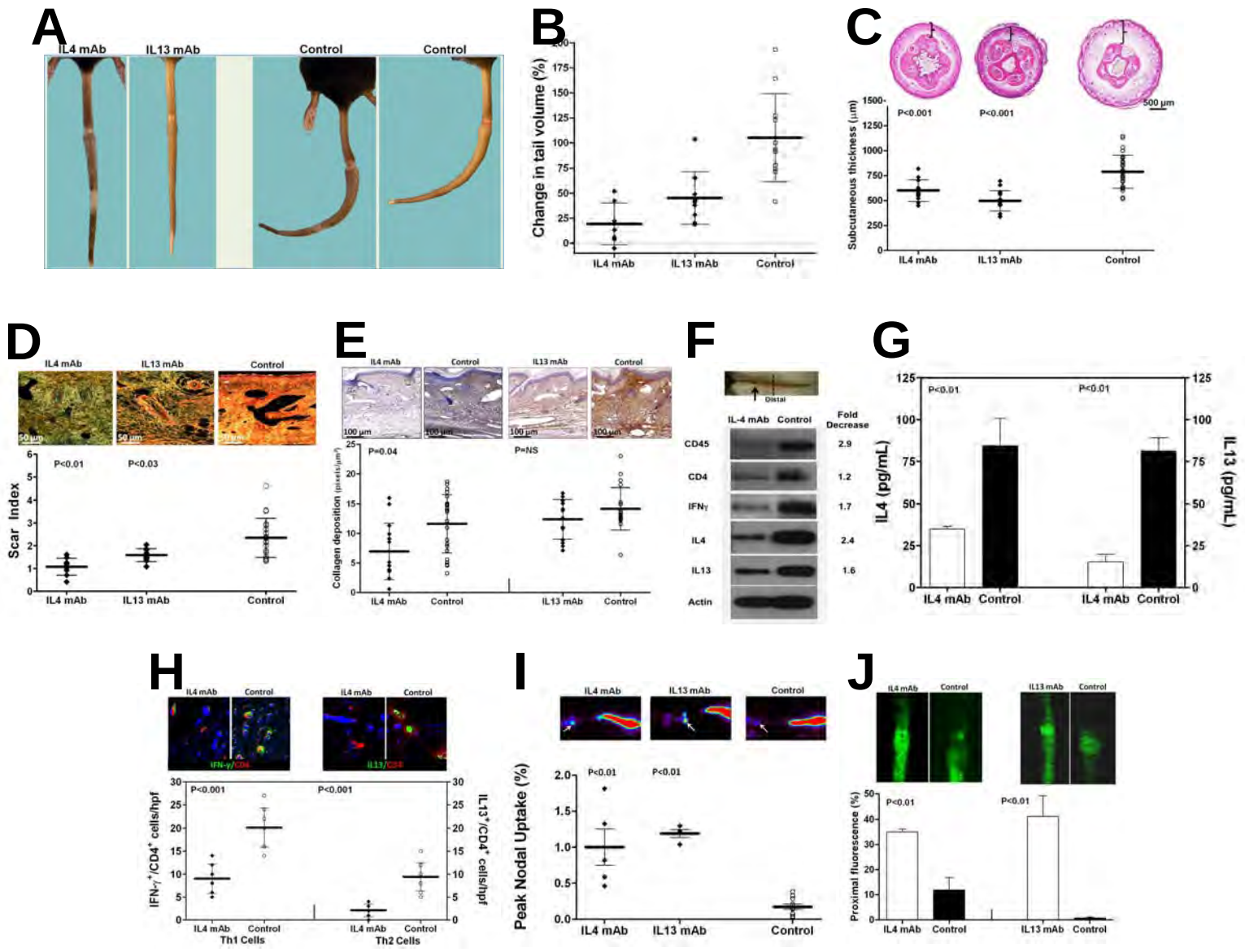


**Figure 4. Inhibition of Th2 differentiation prevents initiation of fibrosis and improves lymphatic function.**

- **A.** Representative photographs of tails from animals treated with IL4mAb, IL13mAb, or isotype control antibodies (control) for 6 weeks beginning immediately after tail skin/lymphatic excision. Note lack of fibrotic contracture in the tails of IL4/IL13mAb treated mice as compared to fixed contracture of controls.
- **B.** Tail volume changes (% change from pre-operative) 6 weeks after surgery.
- **C.** Subcutaneous tissue thickness and representative cross-sectional histology 6 weeks after surgery. Note marked decreased adipose deposition and edema in IL4mAb/IL13mAb treated mice (brackets).
- **D.** Scar index and representative histology (40X) of distal tail tissues 6 weeks post-operatively.
- **E.** Collagen deposition and representative histology (20X) of distal tail tissues 6 weeks post-operatively.
- **F.** Western blot analysis of distal tail tissues harvested 15mm distal to the wound (wound=arrow in photograph; harvest site=dotted line) comparing IL4mAb and control animals 6 weeks after surgery. Fold decrease in expression in IL4mAb animals relative to controls is shown.
- **G.** Serum IL4 and IL13 levels in animals treated with IL4mAb or isotype control antibody 6 weeks after surgery.
- **H.** Number of Th1 (IFN-$\gamma^+$/CD4$^+$) and Th2 (IL13$^+$/CD4$^+$) cells in distal tail tissues of IL4mAb and control antibody-treated animals 6 weeks post-operatively.
- **I.** Representative heat maps (above) and peak nodal uptake of $^{99m}$Tc in sacral lymph nodes (white arrows) following distal tail injection 6 weeks after surgery.
- **J.** Representative microlymphangiography and calculation of proximal tail fluorescence (%of proximal fluorescence as a function of distal fluorescence) 6 weeks after surgery.

**Figure 4**

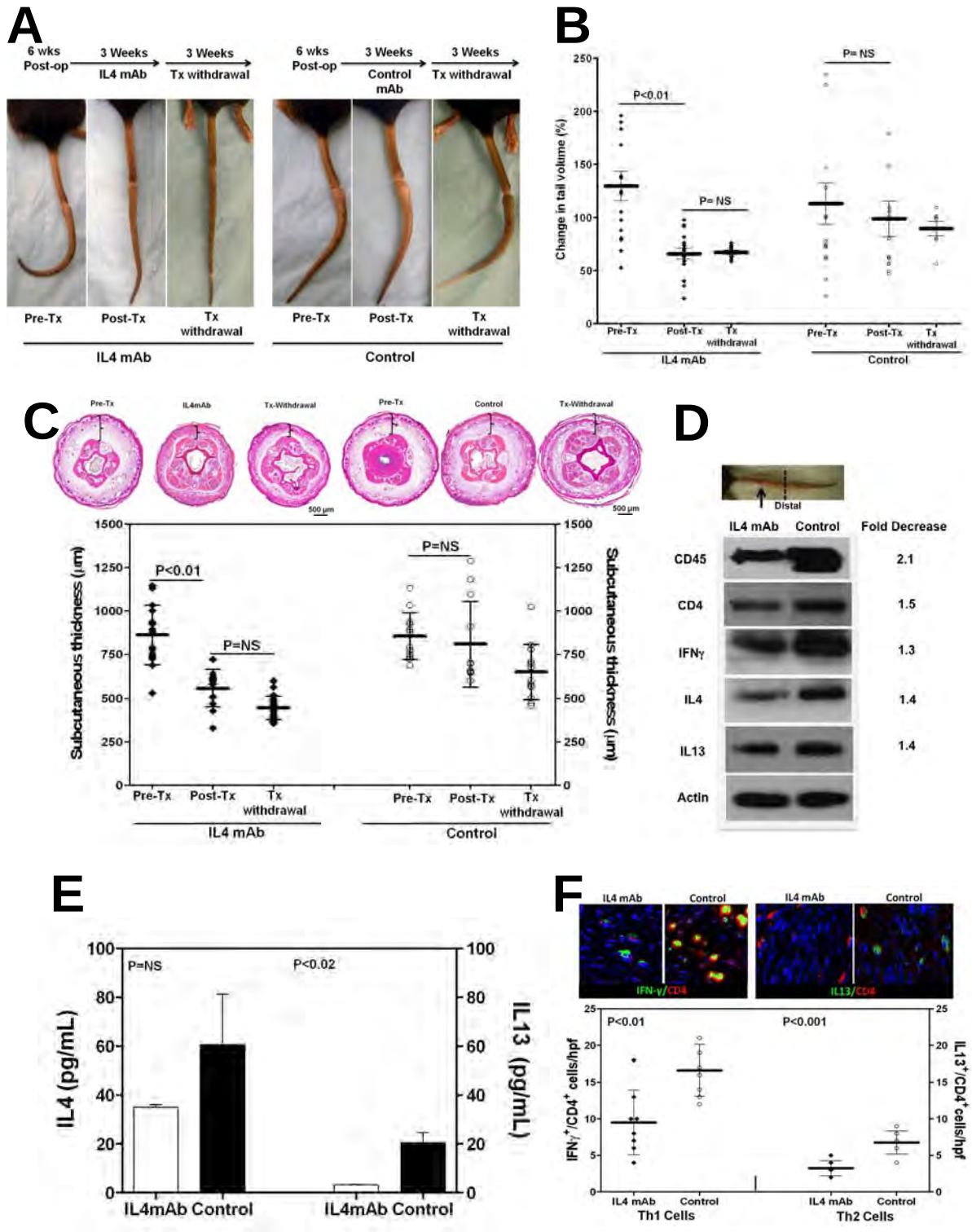


**Figure 5. Inhibition of Th2 differentiation decreases established lymphedema.**

**A-C.** Representative photographs (**A**), tail volumes (**B**), and subcutaneous tissue thickness (**C**) of tails from animals 6 weeks after skin excision/lymphatic disruption (pre-tx), following 3 week treatment with IL4/control antibodies (post-tx) beginning 6 weeks after surgery, and following an additional 3 week treatment withdrawal (post-tx withdrawal).

**D.** Western blot of distal tail tissues from animals following 3 week treatment course with IL4/control antibodies beginning 6 weeks post-operatively (fold-decrease=normalized expression from IL4mAb-treated animals relative to controls).

**E.** Serum IL4 and IL13 levels in animals post-treatment with IL4/control antibodies for 3 weeks.

**F.** Number of Th1/Th2 cells in distal tail tissues post-treatment with IL4/control antibodies.

**Figure 5**

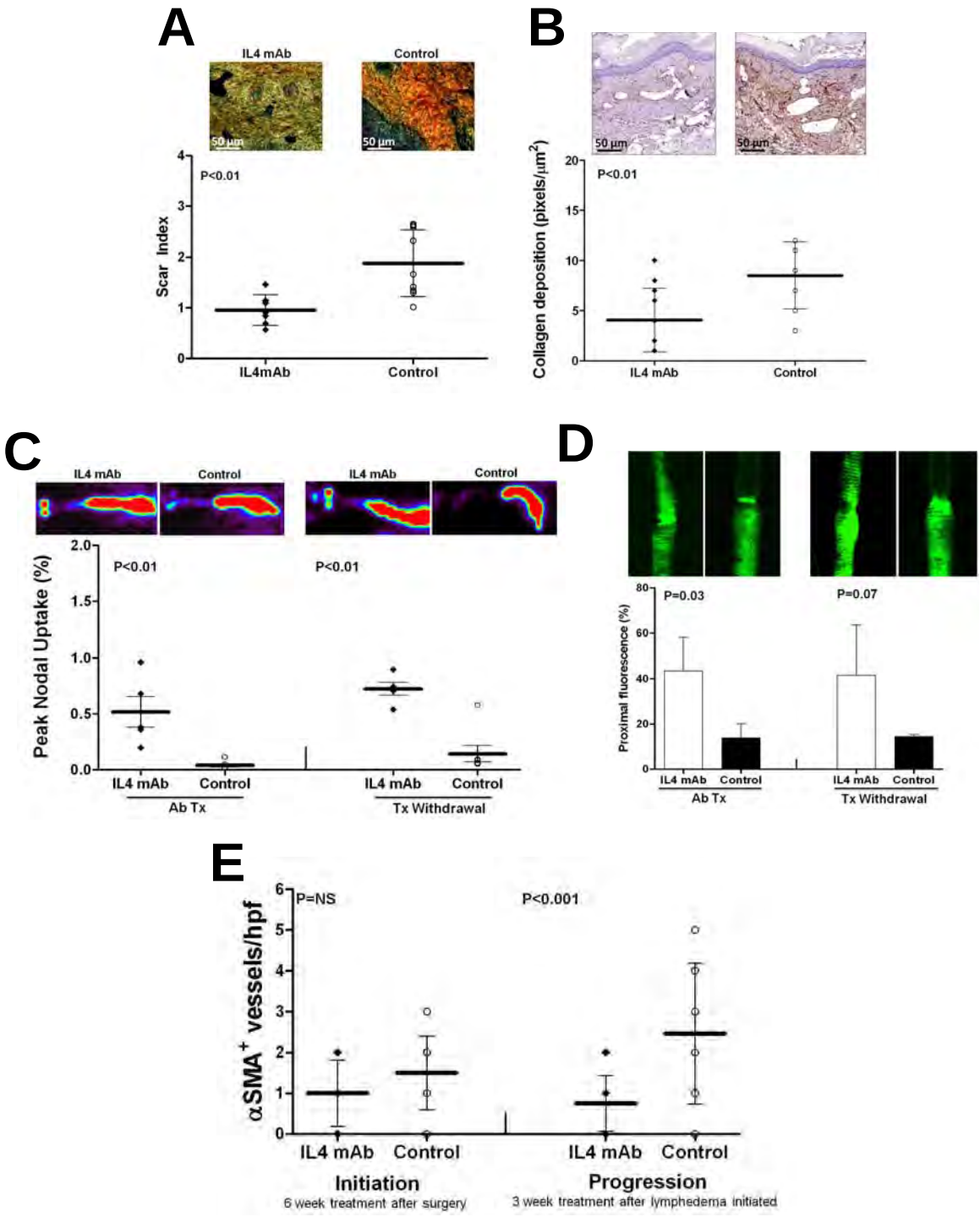


**Figure 6. Inhibition of Th2 differentiation decreases established fibrosis and improves lymphatic function.**

**A,B.** Scar index (**A;** representative 40x views) and collagen staining (**B;** representative 20x views) of distal tail tissues post-treatment with IL-4/control antibodies.

**C.** Representative heat maps (above) and peak nodal uptake of $^{99m}$Tc in sacral lymph nodes following distal tail injection post-treatment (Ab Tx) and following treatment withdrawal (Tx withdrawal).

**D.** Representative microlymphangiography and proximal tail fluorescence post-treatment (Ab Tx) and following treatment withdrawal (Tx withdrawal) with IL4/control antibodies.

**E.** Number of α-sma$^+$ capillary lymphatic vessels/hpf.

**Figure 6**

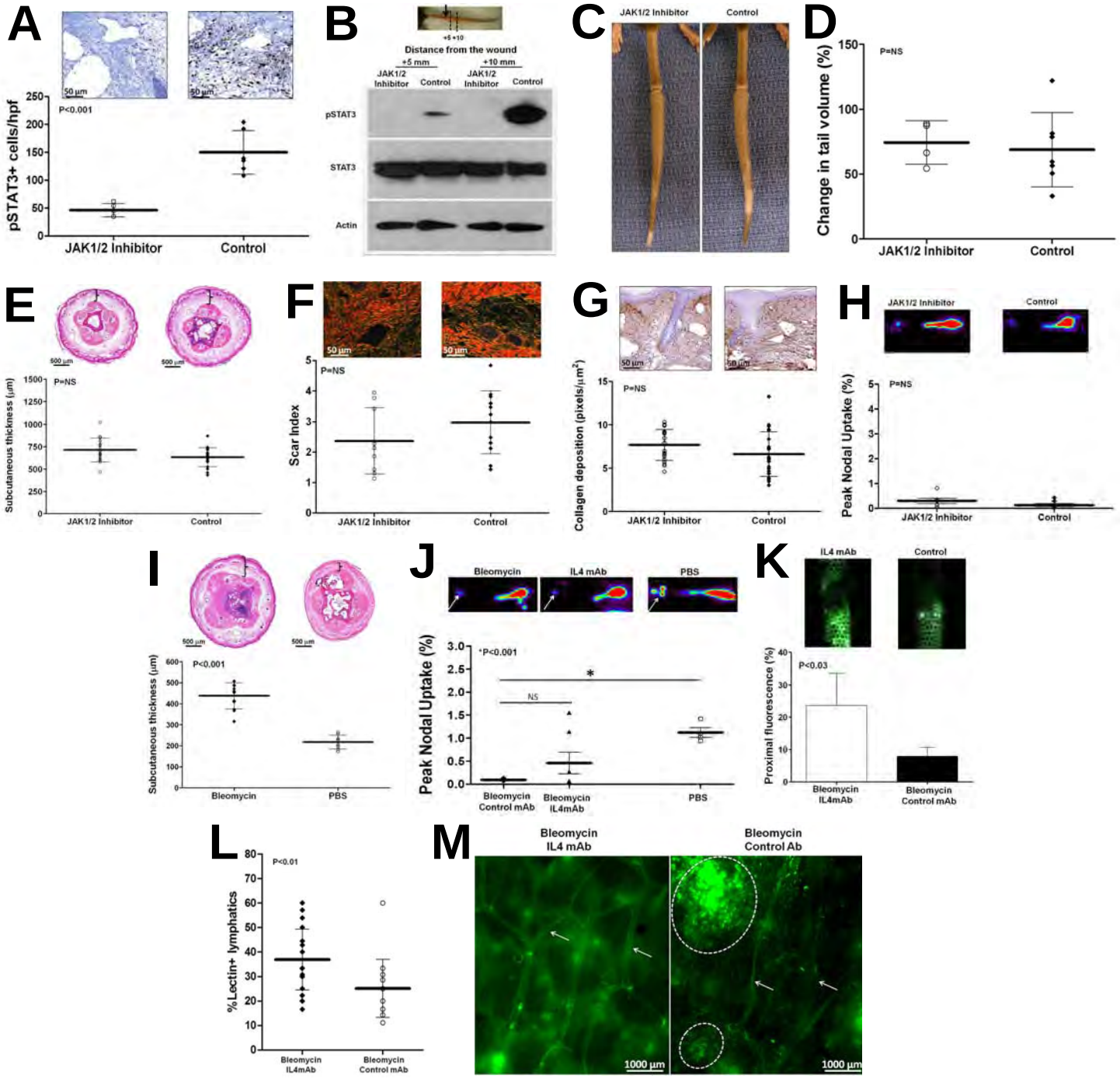


**Figure 7. Inhibition of JAK1/2 does not prevent fibrosis or preserve lymphatic function.**

**A,B.** pSTAT3 cell counts (**A**) and representative western blot of pSTAT3 and total STAT3 (**B**) in distal tail tissues of JAK1/2 inhibitor- or control-treated animals.

**C.** Representative photographs of JAK1/2 inhibitor or control-treated mouse tails 6 weeks post-operatively.

**D,E.** Change in tail volume (**D**) and subcutaneous tissue thickness (**E**) in JAK1/2 inhibitor or control treated mice 6 weeks postoperatively.

**F,G.** Scar index (**F;** representative 40X views) and collagen staining (**G;** representative 20X views) of distal tail tissues following treatment with JAK1/2 inhibitor or control 6 weeks post-operatively.

**H.** Peak nodal uptake of $^{99m}$Tc in JAK1/2 inhibitor or control-treated animals 6 weeks post-operatively.

**I.** Subcutaneous tissue thickness of animals treated with bleomycin or phosphate-buffered saline (PBS).

**J,K.** Peak nodal uptake of $^{99m}$Tc by sacral lymph nodes (**J**) and microlymphangiography/proximal fluorescence (**K**) in animals treated with bleomycin, bleomycin and IL-4mAb, or PBS control.

**L,M.** Quantification of lectin$^+$ capillary lymphatics (**L;** % of total lymphatics) and representative whole mount lectin stain (**M**) in bleomycin/IL4mAb and bleomycin/control antibody-treated animals. White arrows are capillary lymphatics; dotted circles represent pooled areas of lectin in interstitial space.

**Figure 7**

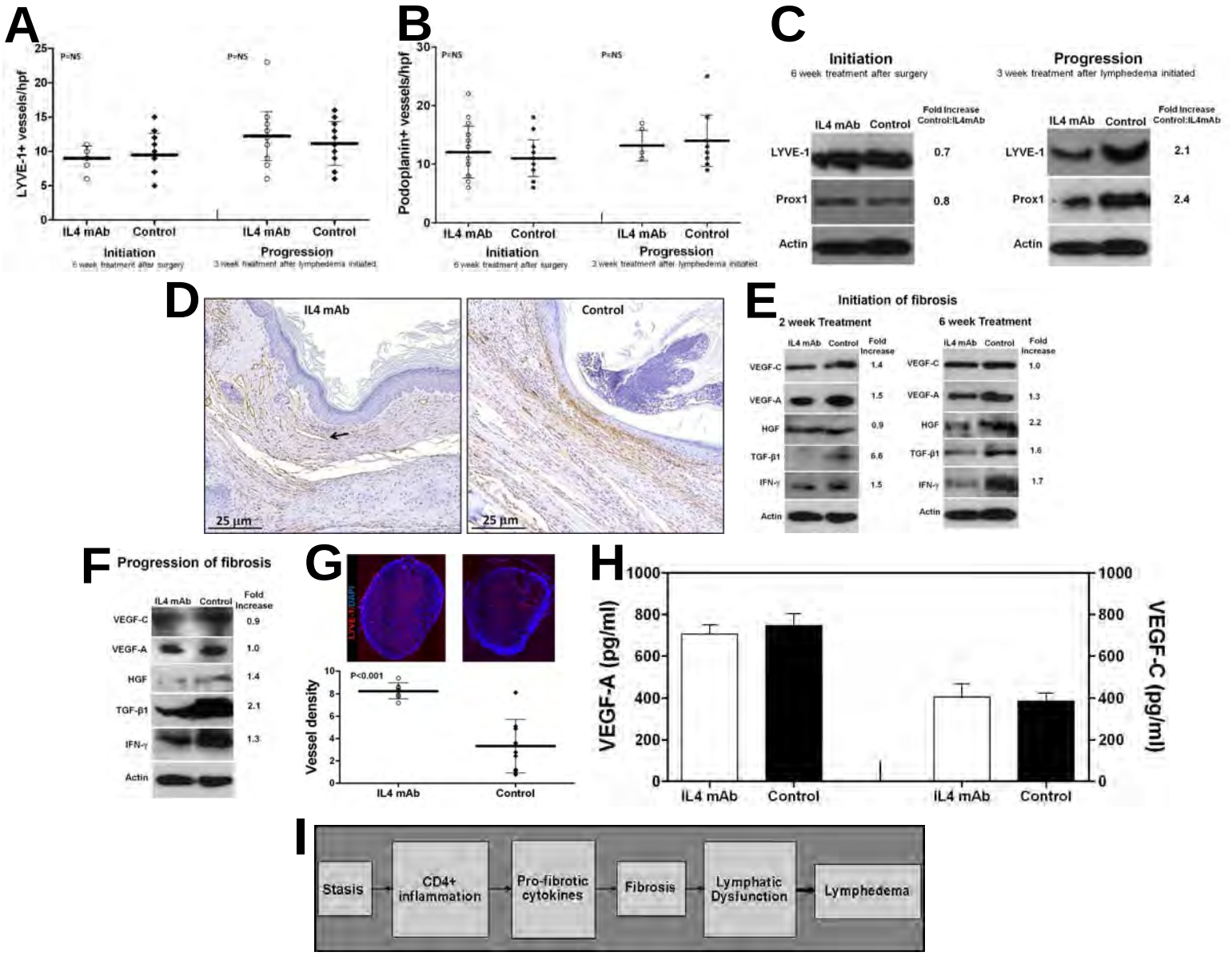


**Figure 8. IL4 blockade does not increase VEGF-A or VEGF-C expression.**

**A,B.** LYVE-1⁺ (**A**) and Podoplanin⁺ (**B**) vessel counts in IL4/control antibody-treated animals beginning immediately after surgery and continued for 6 weeks (initiation) or beginning 6 weeks after surgery and continued for 3 weeks (progression).

**C.** Representative western blots (of triplicate experiments) for LYVE-1 and PROX1 expression in distal tail protein of animals treated with IL4mAb/control antibody for 6 weeks beginning immediately after surgery (left) or after treatment with IL4mAb/control antibodies for 3 weeks beginning 6 weeks post-operatively (right). Normalized fold-increase in expression relative to controls is shown.

**D.** Representative 40x photomicrograph of wound area following treatment with IL4mAb/control antibody for 6 weeks beginning immediately after surgery. Arrow shows lymphatic vessel crossing the wound.

**E,F.** Representative western blots (of triplicate experiments) from distal tail protein isolated from animals treated with IL4mAb/control antibody for 2 or 6 weeks beginning immediately after surgery (**D;** Initiation of fibrosis) or after treatment with IL-4/control antibodies for 3 weeks beginning 6 weeks after surgery (**E;** Progression of fibrosis). Normalized fold-increase in expression relative to controls is shown.

**G.** LYVE-1⁺ lymphatic vessel density and representative photomicrographs of popliteal lymph nodes harvested from animals treated with IL4mAb/control antibodies 2 weeks post-CFA/OVA injection into hind paw.

**H.** Expression of VEGF-A/C (by ELISA) in popliteal lymph nodes harvested from animals treated with IL4mAb/control antibodies 2 weeks post-CFA/OVA injection into the hind paw.

**I.** Schema depicting proposed mechanism of lymphedema development in response to lymphatic fluid stasis.

**Figure 8**

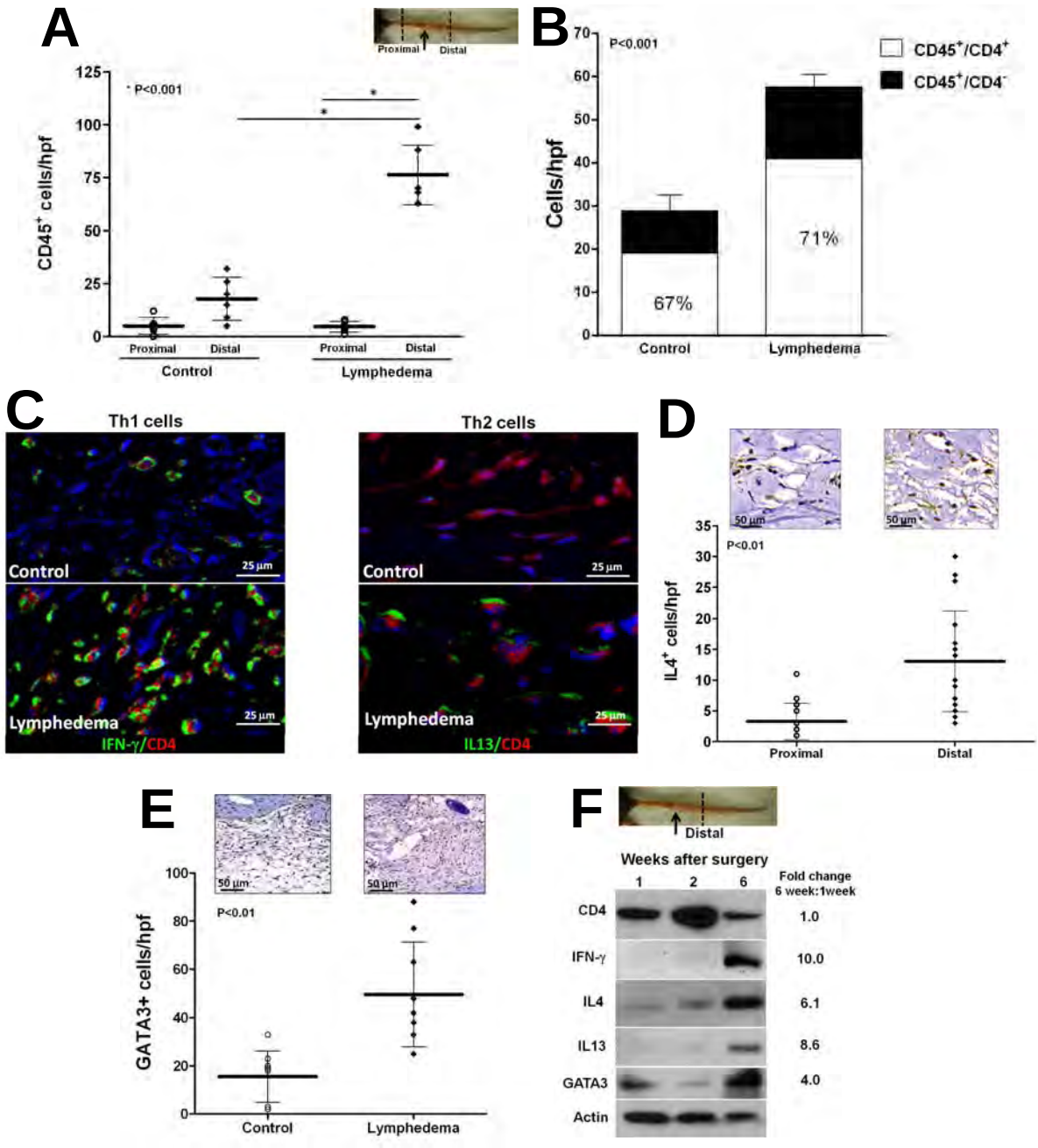


**Supplemental figure 1.**

- **A.** Number of CD45⁺ cells/hpf in proximal and distal tail tissues of control and lymphedema groups 6 weeks after surgery.
- **B.** Number of CD4⁺/CD45⁺ and CD4⁻/CD45⁺ cells and percentage of total number in distal tail tissues of control and lymphedema groups.
- **C.** Representative fluorescent photomicrographs of Th1 (CD4⁺/IFN-γ⁺) and Th2 (CD4⁺/IL13⁺) cells in distal tail tissues of control and lymphedema groups 6 weeks after surgery (60x magnification).
- **D.** Cell counts of IL4⁺ cells/hpf in proximal and distal tail sections of mice 6 weeks after tail skin and lymphatic excision. Representative 40x figures are shown above.
- **E.** Cell counts of GATA-3⁺ cells in distal tail tissues of control and lymphedema groups 6 weeks after surgery.
- **F.** Western blot analysis of temporal protein expression in the distal tail (protein harvested at the region of the dotted line in photograph). Fold-change represents ratio of expression between 1 and 6 weeks post-operatively.

## Supplemental figure 1

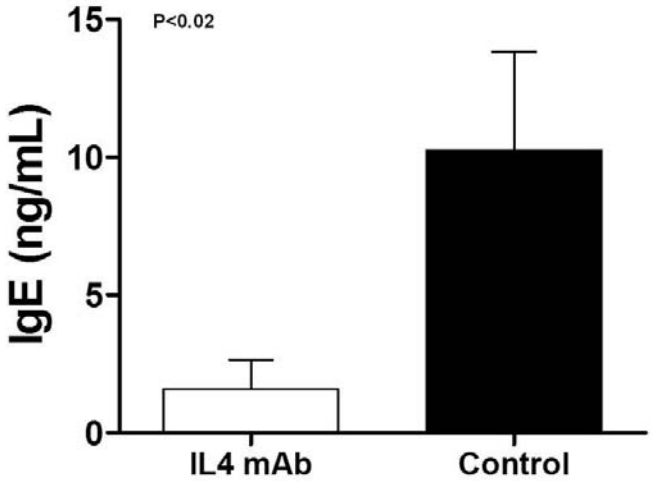


**Supplemental figure 2.** IgE concentration in the peripheral serum of animals treated with IL4mab or control antibody for 6 weeks beginning immediately after tail skin/lymphatic excision.

**Supplemental figure 2**

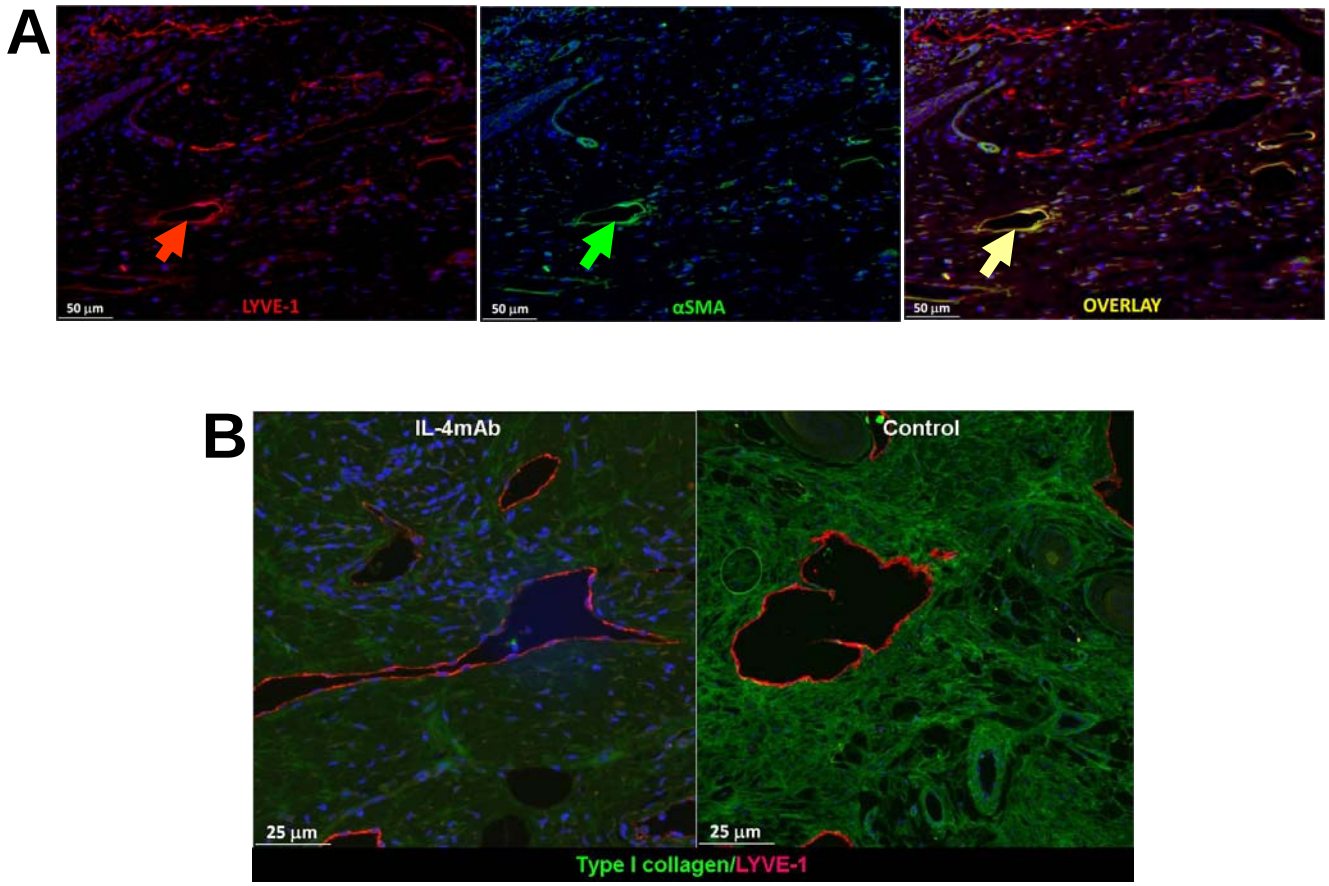


**Supplemental figure 3.**

**A.** Representative photomicrographs in tail tissues from animals treated with antibodies beginning either immediately after surgery (initiation) or for 3 weeks after lymphedema was established (progression).

**B.** Type I collagen staining (green) surrounding capillary lymphatics (red=LYVE-1) from tail tissues of animals treated with IL4/control antibodies for 3 weeks beginning 6 weeks after surgery.

## Supplemental figure 3

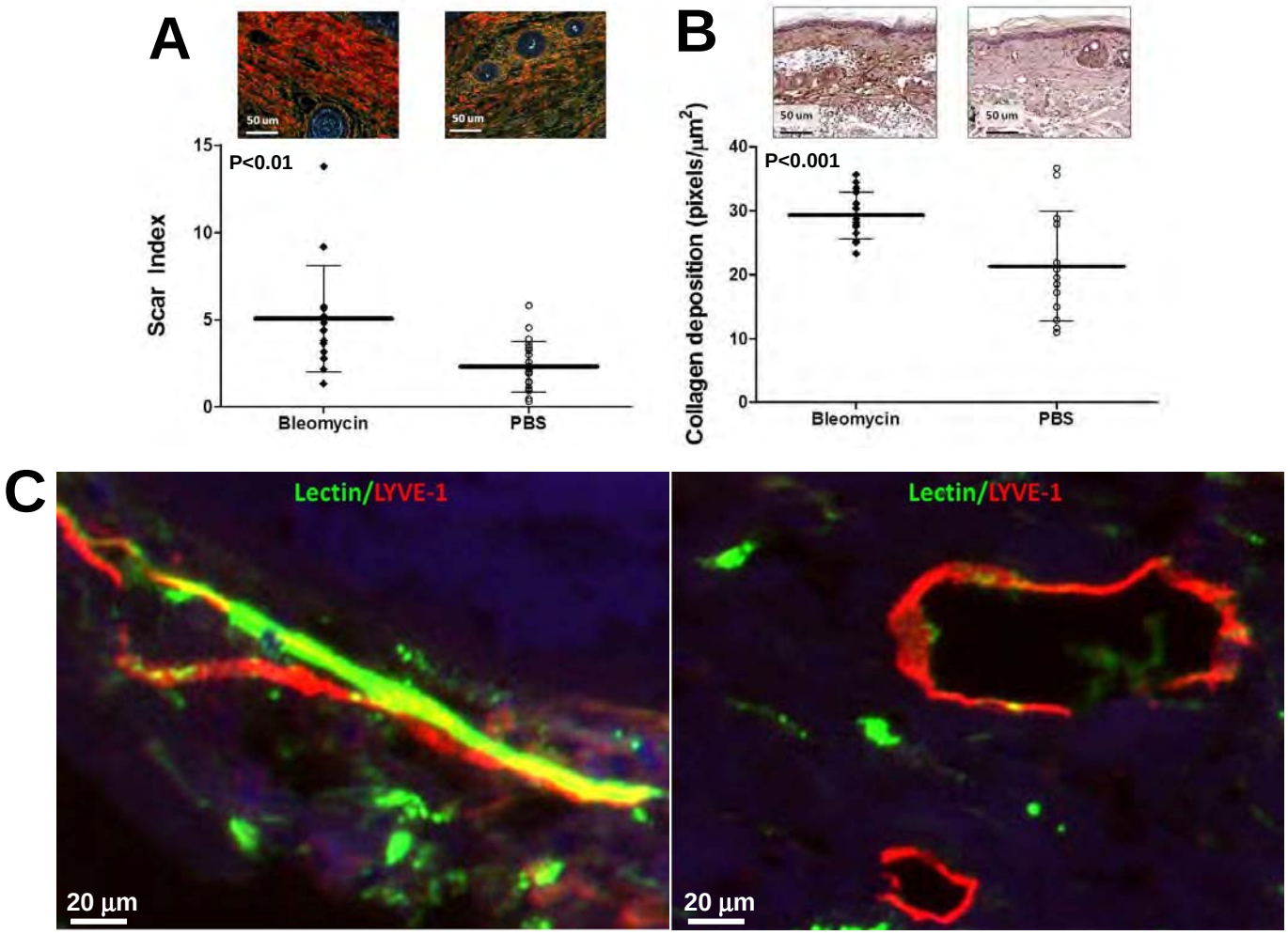


**Supplemental figure 4.**

**A,B.** Scar index (**A;** representative 40x views) and collagen staining (**B;** representative 20x views) of distal tail tissues in animals treated with Bleomycin or PBS for 3 weeks.

**C.** Representative figure (100x) demonstrating lectin$^{+}$ (functional) and lectin$^{-}$ (non-functional) lymphatic vessels in proximal tail tissues. Lectin is stained green; LYVE-1 is red.

**Supplemental figure 4**

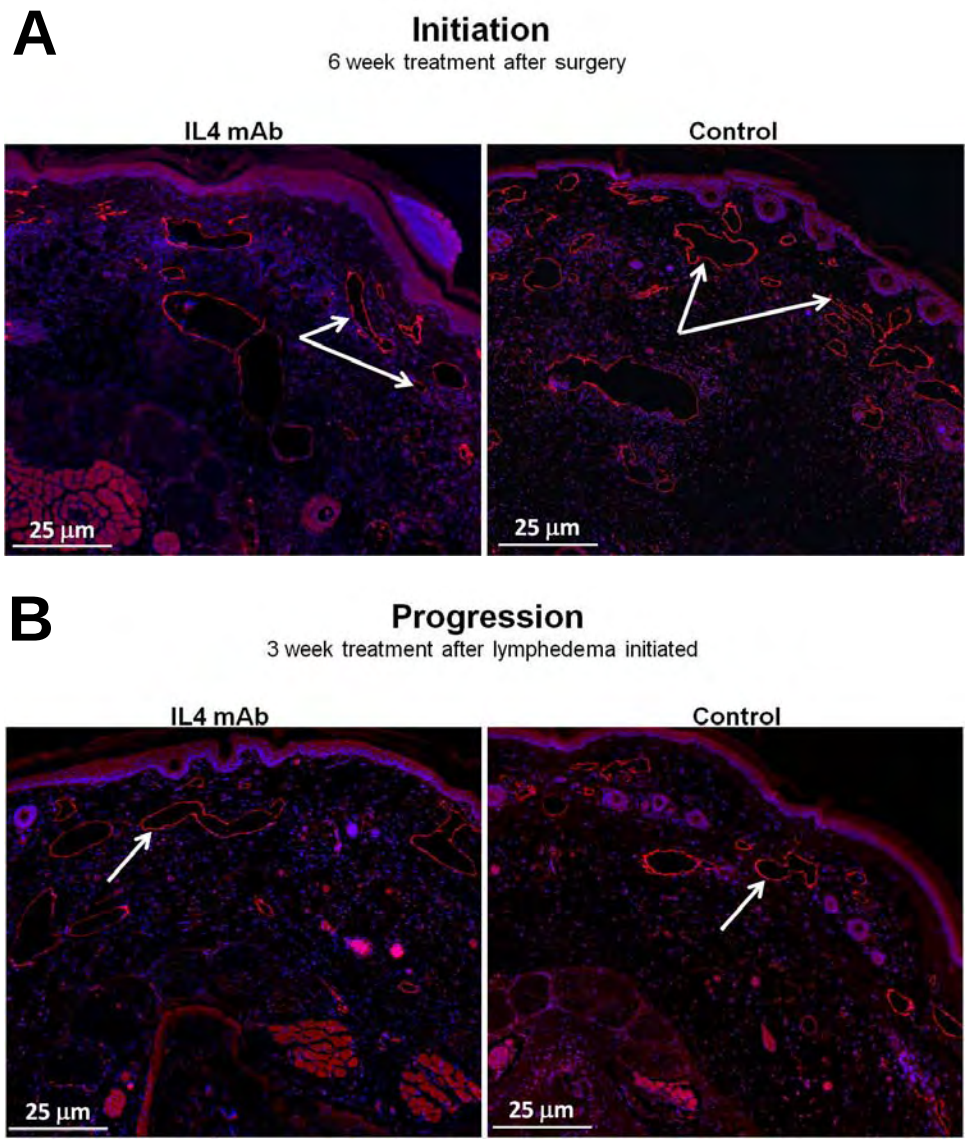


**Supplemental figure 5.**

**A,B.** Representative figure (40x views) demonstrating LYVE-1 staining in IL4mAb and control animals with treatment initiated immediately after surgery for 6 weeks (**A**, initiation) or beginning 6 weeks after surgery for 3 weeks (**B**, progression). Arrows show LYVE-1-positive capillary lymphatics.

**Supplemental figure 5**

# CD4+ cells regulate fibrosis and lymphangiogenesis in response to lymphatic fluid stasis

Key words: Lymphedema, fibrosis, CD4, inflammation, lymphangiogenesis
Running Head: Lymphedema and inflammation

**Jamie C. Zampell, MD[1], Alan Yan, MD[1], Sonia Elhadad, PhD, Tomer Avraham, MD, Evan Weitman, MD, and Babak J. Mehrara, MD**

**[1]These authors contributed equally to this manuscript**

From: The Division of Plastic and Reconstructive Surgery, Department of Surgery, Memorial Sloan-Kettering Cancer Center, New York, NY 10065

Correspondence:
Babak J. Mehrara, MD FACS
1275 York Avenue
Room MRI 1005
New York, NY 10065
mehrarab@mskcc.org
212-639-8639
212-717-3677 Fax

Disclosures

None of the authors have any commercial associations or financial relationships that would create a conflict of interest with the work presented in this article.

## Abstract

**Introduction:** Lymphedema is a chronic disorder that occurs commonly after lymph node removal for cancer treatment and is characterized by swelling, fibrosis, inflammation, and adipose deposition. Although previous histological studies have investigated inflammatory changes that occur in lymphedema, the precise cellular make up of the inflammatory infiltrate remains unknown. It is also unclear if this inflammatory response plays a causal role in the pathology of lymphedema. The purpose of this study was therefore to characterize the inflammatory response to lymphatic stasis and determine if these responses are necessary for the pathological changes that occur in lymphedema.

**Methods:** We used mouse-tail lymphedema and axillary lymph node dissection (ANLD) models in order to study tissue inflammatory changes. Single cell suspensions were created and analyzed using multi-color flow cytometry to identify individual cell types. We utilized antibody depletion techniques to analyze the causal role of CD4+, CD8+, and CD25+ cells in the regulation of inflammation, fibrosis, adipose deposition, and lymphangiogenesis.

**Results:** Lymphedema in the mouse-tail resulted in a mixed inflammatory cell response with significant increases in T-helper, T-regulatory, neutrophils, macrophages, and dendritic cell populations. Interestingly, we found that ALND resulted in significant increases in T-helper cells suggesting that these adaptive immune responses precede changes in macrophage and dendritic cell infiltration. In support of this we found that depletion of CD4+, but not CD8 or CD25+ cells, significantly decreased tail lymphedema, inflammation, fibrosis, and adipose deposition. In addition, depletion of CD4+ cells significantly increased lymphangiogenesis both in our tail model and also in an inflammatory lymphangiogenesis model.

**Conclusions:** Lymphedema and lymphatic stasis result in CD4+ cell inflammation and infiltration of mature T-helper cells. Loss of CD4+ but not CD8+ or CD25+ cell inflammation markedly decreases the pathological changes associated with lymphedema. In addition, CD4+ cells regulate lymphangiogenesis during wound repair and inflammatory lymphangiogenesis.

## Introduction

Lymphedema is a chronic disorder that is characterized by progressive tissue swelling and fat deposition secondary to congenital defects, infections, or injury to the lymphatic system. In its most advanced forms, lymphedema results in massive changes in the extremities referred commonly to as elephantiasis. Although the most common cause of lymphedema worldwide is parasitic infections with nematodes such as *Wuchereria bancrofti*, these infections are rarely seen in developed countries where lymphedema occurs most commonly after cancer surgery.[1] In these cases, patients develop lymphedema after direct injury to the lymphatic system resulting from lymph node dissection or secondarily from wide skin excision and radiation therapy. It is estimated that as many as 1 in 3 women treated with axillary lymph node dissection for breast cancer develop lymphedema.[2] Lymphedema is also common in other solid malignancies occurring in nearly 1 in 8 patients treated for a variety of tumors.[3]

The lack of a clear understanding of the pathology of lymphedema has served as a significant barrier to the development of effective, targeted treatments or preventative options for this disabling complication. Instead, current treatments are palliative in nature with a goal of preventing disease progression and decreasing symptoms rather than curing the underlying pathology. The fact that lymphedema in most cases develops 8-12 months after surgery (rather than immediately following lymph node dissection)[4] suggests that lymphatic injury is merely an initiating event that is necessary for activation of cellular and molecular changes that over time lead to chronic tissue edema, inflammation, fibrosis, and fat deposition. It remains unknown, however, if the key histological features of lymphedema such as inflammation and fibrosis play a causal role in this pathology or if these changes simply reflect worsening pathology. Similarly, although previous reports have demonstrated that patients with secondary lymphedema have high concentrations of lymphocytes in peripheral lymph, increased density of Langerhans cells and class II antigen expression in the skin, and increased granulocyte margination in lymphedematous tissues,[5,6,7,8] the precise cellular response to lymphatic fluid stasis and chronic lymphedema remain unknown. This is important since recent studies have shown critical roles for

inflammatory cells in the regulation of fibrosis, lymphangiogenesis, and adipose tissue deposition in other disorders.[9,10,11,12] Therefore, understanding how lymphatic fluid stasis regulates these responses acutely, and more importantly, how these responses are coordinated chronically is an important first step in developing targeted treatments that can block initiation or progression of the pathological consequences of lymphatic injury.

With these goals in mind, the purpose of this study was to determine how lymphatic stasis regulates tissue inflammatory changes. In addition, we sought to determine if these chronic inflammatory responses play a pathological role in lymphatic dysfunction, fibrosis, and adipose deposition in lymphedema. We show that specific T cell subpopulations are a critical component of the subacute and chronic inflammatory cell response to lymphatic fluid stasis. In addition, using antibody depletion studies, we show that T-helper cell inflammatory responses are necessary for fibrosis, lymphatic dysfunction, subcutaneous fat deposition, and chronic inflammation occurring in response to sustained lymphatic fluid stasis. Our findings are important because we show for the first time that lymphedema results in characteristic inflammatory responses. Further, we show that these responses play a role in the pathology of lymphedema rather than simply reflecting worsening pathology.

## Methods

### *Animal Models*

Adult female (10-12 week old) wild-type C57B6 or transgenic C57B6 mice deficient in CD4+ cells (CD4KO; Jackson Labs, Bar Harbor, ME) were used and all studies were performed according to IACUC standards and approved animal protocols at Memorial Sloan-Kettering Cancer Center. A total of 8-10 animals were used for each group/experiment.

In order to study the effects of sustained, severe lymphatic stasis on inflammatory responses, we used a well-described mouse tail model of lymphedema in which the superficial and deep lymphatic system of the tail are disrupted by excising a 3mm portion of the skin and microsurgically ligating the deep lymphatic channels that run along the lateral tail veins.[13,14,15,16] Our group, and others, have

previously shown that this model results in sustained lymphedema of the distal tail, severe impairment in lymphatic function, and histological features of clinical lymphedema (e.g. chronic inflammation, adipose deposition, fibrosis) for at least 10 weeks postoperatively.[13,14,15,16] Control animals underwent circumferential tail skin incision but did not undergo superficial or deep lymphatic system disruption. Lymphatic function, flow cytometry, and histological analysis were performed 6 weeks after surgery as described below.

We also used a mouse model of axillary lymph node dissection to study the consequences of lymphadenectomy and disruption of the deep lymphatic system. We have previously shown that similar to the clinical scenario, axillary lymph node dissection (ALND) in mice results in minor though significant increases in limb volume enabling us to study acute tissue changes that occur in response to lymphatic stasis.[17] Experimental mice underwent ALND dissection using a 1 cm axillary incision and all identifiable axillary lymph nodes were removed. Control animals underwent axillary skin incision without lymph node removal.

***Flow Cytometry***

A 1 cm portion of tissue was harvested 1 cm distal to the site of axillary lymph node dissection or 1.5 cm distal to the site of tail skin excision. Flow cytometry and analysis was performed using a modification of our previously reported methods.[18] Briefly, skin and subcutaneous tissues were stripped from the underlying tissues and digested at 37$^{o}$ C for 30 min in phosphate-buffered saline (PBS) solution of collagenase D (0.2 mg/ml), DNAse I (0.1 mg/ml), Dispase (0.1 mg/ml), and 2% fetal calf serum (all from Sigma Aldrich, St. Louis, MO). Tissue digests were then filtered and resuspended as a single cell suspension in PBS/2%FCS/Sodium azide solution for flow cytometry analysis. Splenocytes were isolated simultaneously by rupturing spleens, lysing red blood cells, and filtering to achieve single cell suspensions. Cells were blocked at 4$^{o}$ with Fc block (CD16/CD32, eBiosciences (San Diego, CA) to block endogenous Fc receptors. Single stains were performed on splenocytes for optimization of cytometer settings. Cell suspensions isolated from peripheral tissues were then stained using fluorophore-conjugated antibodies for the following cell surface markers: CD45, CD4, CD8, TCRB, CD25, F4/80,

CD11b, CD11c, Ly6c, Ly6g, B220 (all antibodies from Biolegend, San Diego, CA), and NK T cell-specific Tetramer (PBS57-CD1d tetramers were obtained from the US National Institutes of Health Tetramer Core Facility). Alternatively, cell suspensions were Fc-blocked followed by fixation, permeabilization overnight at $4^{o}$ C, and stained for the intracellular marker FoxP3 (eBiosciences ) and cell surface markers CD4 and CD25 (Biolegend).

Cell suspensions were analyzed using an LSR II flow cytometer (BD Biosciences, San Jose CA) with BD FACSDiva software and subsequent data analysis performed using FlowJo software (Tree Star, Ashland, OR). Cell populations were analyzed and defined using the cell surface markers listed in Table 1 using 5-7 animals/group/experiment with each experiment performed in triplicate.

***Depletion Experiments***

Depletion experiments were performed using the tail model of lymphedema as described above. Following tail skin and lymphatic vessel excision, animals were allowed to recover for 2 weeks and then randomized to experimental or control groups (n= 8-10/group). Experimental animals were depleted of CD4, CD8, or CD25 cells using intraperitoneal administration of monoclonal neutralizing antibodies (all from Bio-X-Cell, Lebanon, New Hampshire) every 5 days for a total of 4 weeks (i.e. 6 weeks postoperatively) as previously described. Control animals were treated with non-specific isotype control antibodies delivered at the same dose and timing. Adequacy of depletion was confirmed by flow cytometry analysis of splenic single cell suspensions comparing experimental and control animals at the time of sacrifice (6 weeks postoperatively).

***Tail volume, Lymphoscintigraphy, Microlymphangiography***

Tail lymphedema was monitored weekly using multiple digital caliper tail circumference measurements distal to the zone of lymphatic injury and calculation of tail volumes using the truncated cone formula as previously described.[15] Lymphoscintigraphy was performed as previously described to quantify lymphatic flow by injecting 50ml of filtered technetium ($Tc^{99m}$ ) sulfur colloid in the distal tail and analyzing decay adjusted uptake in the sacral lymph nodes using an X-SPECT camera (Gamma Medica, Northridge, CA) and region-of-interest analysis using ASIPro software (CTI Molecular Imaging,

Knoxville, TN).[15] To analyze lymphatic architecture and calculate interstitial fluid flow, we performed microlymphangiography using our previously published techniques.[14] Briefly, fluorescein isothiocyanate (FITC)-conjugated dextran (2,000 kDa, 10 mg/ml, Invitrogen, Carlsbad, CA) was injected under constant anatomic pressure in the distal tail and then visualized 15 minutes later at fixed 10mm intervals along the tail using the Lumar Stereoscope (Carl Zeiss Inc, Peabody, MA) and Metamorph imaging software (Molecular Devices, Sunnyvale CA). Exposure, gain, magnification, and body temperature were kept constant and the animal was anesthetized to prevent motion artifact. Uptake of FITC-dextran was expressed as a ratio of mean pixel intensity of regions proximal relative to those distal to the surgical site 15 minutes post-injection.

***Lymph node lymphangiogenesis***

Lymph node lymphangiogenesis was used as previously described to determine how CD4 cells regulate inflammatory lymphangiogenesis independent of wound healing. Briefly, a mixture of complete Freund's adjuvant (Sigma) and ovalbumin (1:1) was emulsified and injected in the hind paws of adult female wild-type C57B6 mice and popliteal lymph nodes were harvested 7 days later. Experimental animals (n=8) were depleted of CD4+ cells using monoclonal neutralizing antibodies beginning 3 days prior to CFA/OVA injection as outlined above while control animals (n=8) were treated with an equivalent dose of non-specific isotype control antibodies. To confirm our findings with CD4 depletion, we performed identical experiments in wild-type C57B6 mice (n=8) and compared them with transgenic C57B6 mice deficient in CD4 cells (CD4KO; n=8; Jackson labs).

***Immunohistochemistry and histological analysis***

Tail tissues were fixed in 4% paraformaldehyde and decalcified in Immunocal prior to paraffin embedding. Lymph nodes were embedded in OCT medium (Sigma-Aldrich, St. Louis, MO) and frozen at -80$^{o}$ C; 5 um sections were prepared from all tissues for analyses.

Immunohistochemical staining using horseradish-peroxidase based staining techniques were performed according to our established techniques[14]. Briefly, paraffin-embedded tissues were rehydrated, and antigen unmasking was performed using boiling sodium citrate (Sigma). Endogenous

peroxidase activity was quenched and non-specific binding was blocked with 2% BSA/20% animal serum. Tissues were incubated with primary antibody overnight and antibody staining was visualized using horseradish-peroxidase conjugated secondary antibodies and development with diaminobenzamine complex (DAB; Vector, Burlingame, CA). Primary antibodies used for immunohistochemical stains included collagen I, collagen III, podoplanin, CD4, F4/80, CD45 (all from Abcam, Cambridge, MA), and vascular endothelial growth factor-C (VEGF-C; Novus biological, Littleton, CO). All secondary antibodies were obtained from Vector Laboratories. Sections were analyzed using brightfield microscopy and regions of interest were scanned using a Mirax slide scanner (Zeiss, Munich, Germany). Cell counts were performed on high-powered sections from a minimum of 4-6 animals per group and 4-5 hpf/animal by 2 blinded reviewers.

Immunofluorescent stains were performed as described above, excluding peroxidase quenching steps. Primary antibody to LYVE-1 (R&D Systems, Minneapolis, MN) and TRITC-conjugated secondary antibody were utilized for staining. For frozen lymph node sections, slides were fixed briefly in acetone followed by blocking and staining techniques as described above. Lymphatic vessel density was determined using Metamorph Scanner and Metamorph Offline software (Molecular Devices, Sunnyvale CA) as previously described.[19]

Subcutaneous tissue thickness analysis was performed in histological cross-sections located 1.5 cm distal to the surgical site by blinded reviewers (n=6-8 per group). The distance from the basal layer of the epidermis to deep fascia was analyzed in 4 standardized regions per section. Lymphatic vessel area was measured as previously described.[14] Briefly, the widest radius of individual lymphatic vessels identified by podoplanin or LYVE-1 staining in histological cross sections was used to calculate lymphatic vessel area. Tissue fibrosis was assessed using our previously published methods for Sirius red quantification (scar index) as well as by immunohistochemical staining for type I and type III collagen.[14] Collagen deposition was quantified as a ratio of positively stained dermis and subcutaneous tissues within a fixed threshold to total tissue area using Metamorph Offline software.

***Protein analysis***

Tail tissues or lymph nodes were lysed (Thermofischer Scientific, Waltham, MA) and 20-30 mg of pooled protein (n=3-5 animals) was used for western blot analysis using our previously published methods.[14] We analyzed the expression of interferon-gamma (IFN-γ), interleukin-4 (IL-4; both from Abcam), FoxP3, Tbet, GATA3, (all from Santa Cruz Biotechnology, Santa Cruz, CA), type I collagen, type III collagen, alpha-smooth muscle actin (α-SMA), E-cadherin, phosphorylated SMAD-3 (pSMAD3; all from Abcam), TGFB-1 (Santa Cruz), VEGF-A (Abcam), and VEGF-C (Novus Biologic). Equal loading was ensured with actin (Abcam) and band density was determined using ImageJ analysis (http://rsbweb.nih.gov/ij/). Normalized expression was determined as a ratio relative to controls. For ELISA, 20-30 mg of protein from pooled samples (n=3-5 animals/group) was analyzed to quantify VEGF-A and VEGF-C according to the manufacturer's directions (eBioscience, San Diego, CA). All experiments were performed in triplicate.

***Statistical analysis***

Student's T-test was used to compare differences between 2 groups; paired T-tests were performed for all matched ALND and sham control samples. Multi-group comparisons were performed using 2-way analysis of variance (ANOVA) with Tukey-Kramer post-hoc test. Data are presented as mean ± standard deviation unless otherwise noted with $p<0.05$ considered significant.

## Results

**Chronic lymphedema results in a mixed inflammatory cell response**

We used a well-described mouse-tail model of lymphedema to determine how chronic lymphatic stasis regulates tissue inflammation. As expected, mice that underwent tail skin and lymphatic excision demonstrated markedly increased tail volumes, tail contracture and fibrosis, and hyperkeratosis 6 weeks after surgery (**Figure 1A, B**). In contrast, control animals that underwent tail skin incision only had no swelling or abnormal changes at this time. Analysis of tissue digests harvested 1.5 centimeter distal to the zone of lymphatic injury also confirmed our previous observations[14] and demonstrated markedly

increased numbers of $CD45^+$ cells consistent with tissue inflammation when compared with controls (2.3 fold; **Figure 1C**). Multicolor flow cytometry analysis of these tissue samples demonstrated that the percentage of mature T-helper ($CD45^+/CD4^+/TCR\beta^+$) was also dramatically increased in lymphedematous tissues (2.2 fold; **Figure 1D**). In contrast, we noted no significant differences in the percentage of mature cytotoxic T cells, NKT cells, or B Cells. Interestingly, and consistent with our previous reports,[17] we also noted significantly increased percentage of neutrophils (1.4 fold), macrophages (1.6 fold), and dendritic cells (1.9 fold) in lymphedematous tissues (**Figure 1E**).

**Axillary lymph node dissection results in T cell inflammation**

In order to determine the type of inflammatory responses that are initiated by lymphatic injury prior to the onset of chronic lymphedema, we analyzed tissue inflammation in the upper extremity of mice that had undergone axillary lymph node dissection (ALND) or axillary skin incision without lymphatic injury 3 or 6 weeks after surgery. This approach was based on our previous studies demonstrating that: **1).** ALND in this model (similar to the clinical scenario) results in mild but significant edema of the upper extremity at 3 weeks postop and resolves by 6 weeks; **2.)** Tissue inflammatory responses to ALND are histologically evident beginning primarily 3 weeks after surgery.[17,20]

At the 3-week time point, we noted a mild (1.3 fold) but insignificant increase in the percentage of CD45+ leukocytes in animals treated with ALND as compared to controls (**Figure 2A**). This difference became more pronounced (1.8 fold) and significant by 6 weeks post operatively. Interestingly, when we analyzed inflammatory cell subtypes 3 weeks after surgery, we noted significant increases in the percentages of T cell subtypes (1.8 fold increase T-helper cells, 2 fold increase in cytotoxic T cells, and 1.7 fold increase in NKTs) as well as neutrophils (2.1 fold). However, B cells, monocytes, macrophages, and dendritic cells were little changed (**Figure 2B**). The increased percentage of T helper cells (1.3 fold) and NKTs (1.4 fold) persisted at the 6 week time point, however, differences between cytotoxic T cells and neutrophils became insignificant (**Figure 2C)**. Similarly, we found no significant differences in the percentage of neutrophils, monocytes, macrophages, or dendritic cells at this time point.

**CD4 cell depletion reduces lymphedema**

Based on the finding that T cell inflammation is initiated by lymphatic injury (ALND) and persists in chronic lymphedema, we tested the hypothesis that these inflammatory reactions contribute to the pathology of lymphedema by performing antibody depletion studies. This hypothesis is supported by recent findings demonstrating that T cells can regulate lymphangiogenesis[11,21,22] and are known to play a role in fibrotic disorders and may therefore contribute to the pathologic fibrosis that is associated with chronic lymphedema.

As expected, depletion of CD4 or CD8 cells with neutralizing antibodies was highly effective resulting in near complete absence of these cells in the spleen (**Figure 3A**). We chose to begin T cell depletion 2 weeks after tail skin and lymphatic excision based on our previous studies demonstrating that inflammatory reactions in this model first become manifest at this time point.[15] Interestingly, we found that depletion of CD4 cells resulted in marked decreases in tail lymphedema and reduced fibrotic tail curvature distal to the site of lymphatic disruption when compared to controls or animals treated with CD8 neutralizing antibodies (**Figure 3B**). These changes were reflected in significantly decreased tail volumes (1.9 fold) and subcutaneous tissue thickness of histological sections (1.5 fold) in CD4 depleted mice (**Figure 3C, D**). Histological sections demonstrated markedly decreased inflammation and subcutaneous edema and fat deposition in CD4 depleted animals (**Figure 3C**). In contrast, CD8 depletion had little effect. Changes in tail volume, subcutaneous adipose tissue deposition, and inflammation in CD4 depleted mice correlated with decreased podoplanin positive lymphatic vessel diameter (**Figure 3E**) suggesting that these animals have decreased lymphatic stasis because their capillary and collecting lymphatics are collapsed.[16] In contrast, control and CD8 depleted animals had large, dilated, ecstatic lymphatic vessels consistent with persistent lymphatic dysfunction. Taken together, these findings suggest that lymphatic stasis causes T cell inflammation and that CD4+ cells may contribute to the pathologic changes that ensue.

**$CD4^+$ cell depletion reduces lymphedema induced chronic inflammation**

Since CD4 depletion after lymphatic injury resulted in decreased lymphedema, we hypothesized that CD4 cells may be responsible for regulating inflammatory changes in tissues exposed to lymphatic fluid stasis. To test this hypothesis, we analyzed inflammatory cell populations in the tissues located distal to the zone of lymphatic injury using immunohistochemistry in animals treated with CD4 or CD8 neutralizing antibodies. This analysis demonstrated that animals treated with CD4 neutralizing antibodies had significantly decreased numbers of infiltrating $CD45^+$ leukocytes (2.5-fold), $CD4^+$ cells (16.7-fold), and $F4/80^+$ macrophages (2-fold; **Figures 4 A-C**).

Western blot analysis of whole tissue protein demonstrated marked decreases in expression of Th1 and Th2 markers in CD4 but not CD8 depleted animals as compared with controls (**Figure 4D**). For example, expression of Th1 markers IFN-γ and T-bet were decreased by 9 and 2.7 folds, respectively. Similarly, expression of the Th2 marker Gata-3 was decreased by 4.8 fold. The expression of FoxP3, a marker of T regulatory cell differentiation was also slightly decreased (1.3 fold) in CD4 depleted animals. Together, these findings suggest that CD4 but not CD8 depletion after lymphatic injury decreases inflammatory responses to lymphatic stasis resulting in decreased overall inflammation, decreased numbers of T cells and macrophages, and decreased expression of both Th1 and Th2 cytokines.

**$CD4^+$ cell depletion inhibits fibrosis and improves lymphatic function**

T cell inflammatory reactions have been shown to play critical roles in the regulation of fibrosis in a variety of fibroproliferative disorders both clinically and experimentally.[22] Our group has previously shown that fibrosis is a critical regulator of lymphatic function and lymphatic regeneration[14,15,23,24] and fibrosis is a clinical histopathologic hallmark of lymphedema.[25] Therefore, in these experiments we sought to determine if CD4 or CD8 cell inflammation contributes to fibrosis and lymphatic dysfunction in the mouse tail model of lymphedema.

Interestingly, we found that depletion of CD4+ cells resulted in a marked decrease in dermal fibrosis as reflected by collagen deposition and organization (scar index; **Figure 5A, B**). CD4 depleted

animals demonstrated 6.8 fold decrease in dermal scar index as compared with controls. In contrast, CD8 depleted animals demonstrated non-significant decreases in scar index as compared with controls. These findings were confirmed by type I collagen immunohistochemistry demonstrating a 2.8 fold decrease in type I collagen deposition in the dermis of CD4 depleted animals (**Figure 5B**). Furthermore, the ratio of type I:III collagen was significantly reduced (2.3 fold) in CD4-depleted animals, a finding consistent with decreased extracellular matrix deposition and fibrosis **(Figure 5C**).

Western blot analysis of whole tissue lysates from control, CD4 or CD8 depleted animals similarly revealed reductions in extracellular matrix markers consistent with decreased fibrosis (**Figure 5D**). For example, the expression of α-sma, E-cadherin, and type III collagen was decreased by 2-3 fold in CD4 depleted animals as compared with controls (**Figure 5D**). Similarly, the expression of phosphorylated SMAD-3 (14-fold) and TGF-β1 (1.4 fold) were also markedly decreased in CD4 depleted animals. This is important since we have previously shown that activation of TGF-β signaling plays an important role in tissue fibrosis in lymphedema both clinically and in our mouse-tail model.[14,15,24]

To determine if decreased fibrosis in CD4 depleted animals corresponds to improved lymphatic function, we analyzed lymphatic fluid transport grossly using microlymphangiography and by analyzing radioactive tracer uptake of $Tc^{99}$ by draining tail lymph nodes. Analysis of microlymphangiography demonstrated flow of interstitial fluid across the tail scar only in CD4 depleted animals (**Figure 5E**). In addition, quantification of florescent tracer in the proximal portion of the tail demonstrated markedly increased transport of interstitial fluid in CD4 (8.8 fold) but not CD8 depleted animals as compared with controls. These findings were confirmed with lymphoscintigraphy of the sacral lymph nodes after distal tail injection with $Tc^{99}$ demonstrating both an increased slope (i.e. more rapid lymphatic transport) and increased decay adjusted total uptake (23-fold) in the draining lymph nodes of CD4 depleted animals (**Figure 5F**).

**$CD25^+$ cell depletion does not improve lymphedema or augment lymphatic function**

Because immune dysregulation and immunosuppression are a major pathological hallmark of lymphedema[6,26] and since T regulatory (T-reg) cells are an important component of the CD4+ cell

population, we next sought to determine if improvements in tail lymphedema noted in CD4 depleted animals were due to alterations in T-reg cell inflammation. In support of this hypothesis, we found that the percentage of T-reg cells (CD4+/CD25+/Foxp3+) in the upper extremity soft tissues of animals treated with axillary lymph node dissection (ALND) was significantly increased as compared with sham controls both in the early (3 week; 5.5 fold) and late (6 week; 6 fold) time points (**Figure 6A**). Similarly, we found that the percentage of T-reg cells was significantly increased (7.7 fold) in mice with tail lymphedema as compared to controls (**Figure 6B**).

In order to more specifically study the role of T-reg cells, we treated mice with CD25+ neutralizing antibodies as this treatment has been previously shown to significantly deplete T-reg cell populations and used to study T-reg responses.[27,28] In support of this, we found that treatment with CD25 neutralizing antibodies significantly decreased the percentage of T-reg cells as compared with controls in splenic homogenates (16.8 fold; **Figure 6C**). More importantly, this treatment did not alter the percentage of CD4+/CD25- cells in these animals (**Figure 6D**).

However, despite significant T-reg cell depletion, we did not note significant differences in the gross morphology of the tail or tail volumes in animals treated with CD25 neutralizing antibodies as compared to controls **(Figure 7A-C)**. Similarly, there were no significant differences in tissue edema/subcutaneous adipose deposition, inflammatory responses, or expression of Th1/Th2 markers after CD25 depletion (**Figure 7D**). Most importantly, we found that depletion of CD25 cells did not alter fibrosis, type I/type III collagen deposition, or collagen I/III ratios (**Figure 7E-H**) and there were also no differences in the expression of fibrotic markers such as α-sma, E-cadherin, TGF-B1, p-SMAD3 (**Figure 7I**). Depletion of CD25 also failed to improve lymphatic transport across the wound or lymph node uptake of $Tc^{99}$ (**Figure 7E**). Taken together, these findings indicate that although T-reg cell populations are increased in response to lymphatic stasis and in chronic lymphedema, the loss of these cell populations does not significantly alter the pathological manifestations (inflammation, fibrosis, lymphatic dysfunction) of this disorder.

**Loss of $CD4^+$ but not $CD8^+$ or $CD25^+$ cells increases lymphangiogenesis**

To explore the mechanisms regulating improved lymphatic function in CD4 depleted animals, we determined the effect of CD4 depletion on lymphangiogenesis and lymphangiogenic cytokine expression. When we analyzed tail tissues located distal to the zone of lymphatic disruption 6 weeks after surgery, we noted a significant increase (2.3 fold increase in LYVE-1+ vessels; 2.2 fold increase in podoplanin+ vessels) in the number lymphatic capillaries (LYVE-1+ or podoplanin+) in CD4 depleted animals as compared with controls (**Figure 8A, B**). In contrast, CD8 or CD25 depletion had little effect on this outcome. Interestingly, we did not note significant changes in the number of collecting lymphatics in any group (not shown). Western blot analysis of tail tissue lysates from these animals demonstrated little change in the expression of VEGF-A in any experimental group (**Figure 8C**). However, expression of VEGF-C was markedly increased in CD4 depleted animals (4 fold) and decreased in CD8 depleted mice (3.3 fold). Despite these changes in VEGF-A and VEGF-C protein expression in CD4 or CD8 depleted animals, we did not find significant differences in the number of VEGF-A or VEGF-C positive cells localized by immunohistochemistry suggesting that changes in total protein expression may reflect regulation of these proteins at the cellular level (**Figure 8D)**.

We used an inflammatory lymph node model in order to further explore the effects of CD4 cell depletion on inflammatory lymphangiogenesis since this model avoids changes that may be secondary to wound healing effects. In confirmation of our tail model observations, we found that depletion of CD4+ cells markedly increased LYVE-1+ vessel density 5-7 days after hind limb CFA/OVA injection as compared with controls (**Figure 9A)**. We found similar results when we repeated these experiments in transgenic mice deficient in CD4+ cells (CD4KO). In addition, we found modest though significant increases in the expression of both VEGF-A (1.3 fold) and VEGF-C (1.6 fold) protein in the lymph nodes of CD4 depleted animals as compared with controls (**Figure 9B, C**).

## Discussion

In the current study, consistent with previous reports, we found that chronic lymphedema results in tissue inflammation. Using multi-color flow cytometry to characterize the cellular populations in tissue digests, we found that lymphedema in the mouse-tail model results in significant alterations in the populations of inflammatory cells that are present. More specifically, unlike previously published studies, the use of multiple cell surface antigens enabled us to identify specific cell populations and demonstrated that the percentage of mature T-helper cells, T-regulatory cells, neutrophils, macrophages, and dendritic cells were all significantly elevated in lymphedematous tissues as compared with surgical controls. Our findings are supported by those reported by Galkowska and Olszewsk using Giemsa staining of cell smears on lymphatic fluid collected from dogs with chronic lymphedema or sham controls demonstrating significantly increased numbers of lymphocytes and veiled cells (dendritic cells) in animals with chronic lymphedema.[7] In a later study on patients with lymphedema, these same authors used histological stains and single antigen immunohistochemistry to characterize inflammatory cells populations in patients with long standing lymphedema versus normal skin and found that lymphedema patients had qualitatively more lymphocytes than controls.[5] The findings of our study are also supported by microarray studies in the mouse-tail model demonstrating acute increases in gene families regulating acute inflammation and immune responses.[16] Taken together, our findings and these previous studies support the hypothesis that lymphedema results in a mixed inflammatory response including a prominent lymphocyte component.

In order to determine how acute, low-grade lymphatic stasis resulting from lymph node resection regulates inflammatory responses, we analyzed single cell suspensions from the upper arm area of mice treated with axillary lymphadenectomy (ALND) versus axillary incision without lymph node removal 3 or 6 weeks after surgery. Interestingly, we found that ALND, similar to tail lymphedema, resulted in a persistent and significant increase in tissue inflammation even as long as 6 weeks after surgery. More importantly, we found that similar to tail lymphedema, inflammatory responses to ALND included a prominent increase in the percentage of a variety of T lymphocytes (T-helper, T-cytotoxic, Treg, NKT).

However, in contrast to the inflammatory changes in the tail model, we found that ALND had only modest, and largely insignificant effects on macrophages, monocytes, and dendritic cells suggesting that T cell inflammatory responses precede and possibly contribute to the pathology of lymphedema.

We next explored the hypothesis that inflammatory responses contribute to the pathology of lymphedema and regulate, either directly or indirectly, tissue edema, adipose deposition, fibrosis, and lymphatic dysfunction. We found that depletion of CD4+ but not CD8+ or CD25+ cells resulted in marked improvements in lymphedema and decreased tail swelling, adipose tissue deposition, and fibrosis. In addition, only depletion of CD4+ cells significantly decreased tissue inflammation (CD45+ cell infiltration) and expression of Th1 and Th2 markers including IFN-γ, T-Bet, and GATA-3. The hypothesis that CD4+ cell inflammation contributes to the pathology of lymphedema is supported by our previous studies demonstrating that blockade of TGF-β1 activation in the mouse tail model significantly improves lymphedema and is associated with markedly decreased tissue inflammation, CD4+ cell infiltration, and expression of Th1/Th2 markers.[14] Similarly, our hypothesis is supported by our previous studies demonstrating that mice deficient in all T cells (nude mice) have significantly decreased tail lymphedema, fibrosis, and lymphatic dysfunction as compared with wild-type littermates.[21] The hypothesis that inflammation contributes to the pathology of lymphedema is also supported by previous studies by Rockson and colleagues demonstrating that inhibition of generalized inflammatory responses using ketoprofen, a non-steroidal anti-inflammatory medication, markedly improves lymphatic function and decreases lymphedema in the mouse tail model.[29] Finally, the hypothesis that CD4+ cells either directly or indirectly contribute to the initiation and progression of lymphedema is supported by the fact that these responses have been implicated in the pathology of obesity including metabolic dysfunction and adipose deposition.[10,30] These latter effects are important since a defining feature of end stage lymphedema is adipose deposition.

In order to determine how CD4+ cell inflammation contributes to pathology of lymphedema, we analyzed tissue fibrosis and regulators of extracellular matrix deposition. Interestingly, and consistent with our previous observations,[14] we found that depletion of CD4+ cells markedly inhibited tissue

fibrosis in the regions of the tail exposed to chronic lymphatic stasis as compared with control animals or mice depleted of CD8+ or CD25+ cells. CD4+ depleted mice had significantly decreased scar index (a measure of type I collagen deposition and organization), decreased type I collagen staining by immunohistochemistry, and a decreased ratio of type I/IIII collagen deposition. These findings are important as we have previously shown that fibrosis is a significant regulator of lymphatic function. For example, we have previously shown that inhibition of radiation-induced fibrosis markedly improves lymphatic function.[24] Similarly, we have previously shown that clinical lymphedema specimens have increased expression of the profibrotic regulator TGF-β1 and that inhibition of TGF-β signaling either locally or systemically decreases tissue fibrosis and markedly improves lymphatic function in the mouse tail model.[14] Our current studies, also suggest that regulation of fibrosis by T cell inflammatory reactions interact with TGF-β signaling since we found that depletion of CD4+ cells markedly decreased the expression of TGF-β1 and its downstream mediator pSMAD-3.This finding is consistent with our previous study demonstrating that inhibition of TGF-β1 markedly decreases T cell inflammation and that depletion of CD3+ cells (all T cell subsets) decreased TGF-β1 expression.[14] Taken together, these findings suggest that CD4+ cells regulate lymphatic function in chronic lymphedema at least in part by regulating tissue fibrosis.

Recent studies by our lab and others have also shown that T cells are independent and important regulators of lymphangiogenesis. For example, we have previously shown that nude mice (lacking all T cells) have significantly improved lymphatic function and markedly decreased expression of anti-lymphangiogenic cytokines such as TGF-β1, IFN-γ, and endostatin.[21] Similarly, Koh and colleagues have shown in recent elegant studies that T cells regulate lymph node lymphangiogenesis at least in part by expressing IFN-γ.[11] Finally, we have previously shown that CD4+ cell inflammation is necessary for hypoxia inducible factor-1 alpha (HIF-1α) stabilization and regulation of VEGF-A/C expression in chronic lymphedema and in inflammatory lymphangiogenesis.[19] The findings of our current study are consistent with these results as we found that depletion of CD4+ but not CD8+ or CD25+ cells markedly increased lymphangiogenesis in the lymphedematous regions of the tail. Similarly, we found that

depletion of CD4+ cells or inflammation in transgenic mice lacking CD4+ cells markedly increased lymphatic vessels density in draining lymph nodes and was associated with increased expression of VEGF-A and VEGF-C. Our findings complement and add to the work of Koh and colleagues since unlike the former study we show that CD4+ cells (rather than T cells in general) are important regulators of lymphangiogenesis during wound repair and that these effects likely involve regulation of both pro- and anti-lymphangiogenic pathways. Future studies will be required to determine precisely how the balance between pro- and anti-lymphangiogenic pathways regulates lymphatic repair and regeneration during wound healing and in physiologic inflammation.

An interesting finding of our study was the massive increase in the number of T-reg cells in response to lymphatic stasis both after ALND or in response to tail lymphedema. We did not observe significant changes in pathological findings of lymphedema after depletion of CD25+ cells (i.e. fibrosis, lymphatic function, adipose tissue deposition, tail volumes) suggesting that T-regulatory cells may play additional or distinct roles in lymphatic stasis. Indeed, increased numbers of T-reg cells may simply represent a homeostatic response to the chronic inflammation induced by lymphatic stasis. This response may be responsible for immune disturbances in patients with lymphedema such as increased risk of infections (lymphangitis and cellulitis) and inability to mount immune responses or acquire immunity to vaccines when administered in the lymphedematous limb. Similarly, our findings provide a rationale for previous reports demonstrating improved allograft skin graft survival after ligation of afferent lymphatics and delayed rejection of allograft tumors in animal models.[7,31] Additional studies are clearly required and will be performed in future reports to determine the role of T-reg cells in the pathology of lymphedema.

In conclusion, in the current study we have characterized the cellular immune response to lymphatic fluid stasis resulting from lymph node dissection and chronic lymphedema using mouse models. In addition, we have shown that depletion of CD4+ cells, but not CD8+ or CD25+ cells markedly decreases that pathological findings of lymphedema including swelling, fibrosis, adipose deposition, and lymphatic dysfunction. In addition, we have shown that CD4+ cells play an important

role in the regulation of lymphangiogenesis in lymphedema and inflammatory lymphangiogenesis. Finally, we have shown that lymphatic stasis promotes a significant T-regulatory cell inflammatory response and that this response is not necessary for pathologic responses to sustained lymphatic fluid stasis.

## References


1. Rockson SG, Rivera KK (2008) Estimating the population burden of lymphedema. Ann N Y Acad Sci 1131: 147-154.

2. Petrek JA, Heelan MC (1998) Incidence of breast carcinoma-related lymphedema. Cancer 83: 2776-2781.

3. Cormier JN, Askew RL, Mungovan KS, Xing Y, Ross MI, et al. (2010) Lymphedema beyond breast cancer: a systematic review and meta-analysis of cancer-related secondary lymphedema. Cancer 116: 5138-5149.

4. Hayes SC, Janda M, Cornish B, Battistutta D, Newman B (2008) Lymphedema after breast cancer: incidence, risk factors, and effect on upper body function. J Clin Oncol 26: 3536-3542.

5. Olszewski WL, Jamal S, Lukomska B, Manokaran G, Grzelak I (1992) Immune proteins in peripheral tissue fluid-lymph in patients with filarial lymphedema of the lower limbs. Lymphology 25: 166-171.

6. Olszewski WL, Engeset A, Romaniuk A, Grzelak I, Ziolkowska A (1990) Immune cells in peripheral lymph and skin of patients with obstructive lymphedema. Lymphology 23: 23-33.

7. Galkowska H, Olszewski WL (1986) Cellular composition of lymph in experimental lymphedema. Lymphology 19: 139-145.

8. Olszewski WL, Loe K, Engeset A (1978) Immune proteins and other biochemical constituents of peripheral lymph in patients with malignancy and postirradiation lymphedema. Lymphology 11: 174-180.

9. Wynn TA (2008) Cellular and molecular mechanisms of fibrosis. J Pathol 214: 199-210.

10. Winer S, Winer DA (2012) The adaptive immune system as a fundamental regulator of adipose tissue inflammation and insulin resistance. Immunol Cell Biol.

11. Kataru RP, Kim H, Jang C, Choi DK, Koh BI, et al. (2011) T lymphocytes negatively regulate lymph node lymphatic vessel formation. Immunity 34: 96-107.

12. Kim KE, Koh YJ, Jeon BH, Jang C, Han J, et al. (2009) Role of CD11b+ macrophages in intraperitoneal lipopolysaccharide-induced aberrant lymphangiogenesis and lymphatic function in the diaphragm. Am J Pathol 175: 1733-1745.

13. Rutkowski JM, Moya M, Johannes J, Goldman J, Swartz MA (2006) Secondary lymphedema in the mouse tail: Lymphatic hyperplasia, VEGF-C upregulation, and the protective role of MMP-9. Microvasc Res 72: 161-171.

14. Avraham T, Daluvoy S, Zampell J, Yan A, Haviv YS, et al. (2010) Blockade of Transforming Growth Factor-{beta}1 Accelerates Lymphatic Regeneration during Wound Repair. Am J Pathol 177: 3202-3214.

15. Clavin NW, Avraham T, Fernandez J, Daluvoy SV, Soares MA, et al. (2008) TGF-beta1 is a negative regulator of lymphatic regeneration during wound repair. Am J Physiol Heart Circ Physiol 295: H2113-2127.

16. Tabibiazar R, Cheung L, Han J, Swanson J, Beilhack A, et al. (2006) Inflammatory manifestations of experimental lymphatic insufficiency. PLoS Med 3: e254.

17. Zampell JC, Yan A, Avraham T, Andrade V, Malliaris S, et al. (2011) Temporal and spatial patterns of endogenous danger signal expression after wound healing and in response to lymphedema. Am J Physiol Cell Physiol 300: C1107-1121.

18. Mehrara BJ, Avraham T, Soares M, Fernandez JG, Yan A, et al. (2010) p21cip/WAF is a key regulator of long-term radiation damage in mesenchyme-derived tissues. FASEB J 24: 4877-4888.

19. Zampell JC, Yan A, Avraham T, Daluvoy S, Weitman ES, et al. (2011) HIF-1alpha coordinates lymphangiogenesis during wound healing and in response to inflammation. FASEB J.

20. Zampell J, Aschen S, Weitman E, Elhadad S, De Brot Andrade M, et al. (2012) Regulation of Adipogenesis by Lymphatic fluid Stasis: Part I Adipogenesis, fibrosis, and inflammation. Plast Reconstr Surg 129; 825-34.

21. Zampell JC, Avraham T, Yoder N, Fort N, Yan A, et al. (2012) Lymphatic function is regulated by a coordinated expression of lymphangiogenic and anti-lymphangiogenic cytokines. Am J Physiol Cell Physiol 302: C392-404.

22. Wynn T (2008) Cellular and molecular mechanisms of fibrosis. J Pathol 214: 199-210.

23. Avraham T, Clavin NW, Daluvoy SV, Fernandez J, Soares MA, et al. (2009) Fibrosis is a key inhibitor of lymphatic regeneration. Plast Reconstr Surg 124: 438-450.

24. Avraham T, Yan A, Zampell JC, Daluvoy SV, Haimovitz-Friedman A, et al. (2010) Radiation therapy causes loss of dermal lymphatic vessels and interferes with lymphatic function by TGF-beta1-mediated tissue fibrosis. Am J Physiol Cell Physiol 299: C589-605.

25. Olszewski WL, Jamal S, Manokaran G, Lukomska B, Kubicka U (1993) Skin changes in filarial and non-filarial lymphoedema of the lower extremities. Trop Med Parasitol 44: 40-44.

26. Olszewski WL (2003) Pathophysiological aspects of lymphedema of human limbs: I. Lymph protein composition. Lymphat Res Biol 1: 235-243.

27. Liu F, Liu J, Weng D, Chen Y, Song L, et al. (2010) CD4+CD25+Foxp3+ regulatory T cells depletion may attenuate the development of silica-induced lung fibrosis in mice. PLoS One 5: e15404.

28. Morgan ME, Sutmuller RP, Witteveen HJ, van Duivenvoorde LM, Zanelli E, et al. (2003) CD25+ cell depletion hastens the onset of severe disease in collagen-induced arthritis. Arthritis Rheum 48: 1452-1460.

29. Nakamura K, Radhakrishnan K, Wong YM, Rockson SG (2009) Anti-inflammatory pharmacotherapy with ketoprofen ameliorates experimental lymphatic vascular insufficiency in mice. PLoS One 4: e8380.

30. Winer S, Chan Y, Paltser G, Truong D, Tsui H, et al. (2009) Normalization of obesity-associated insulin resistance through immunotherapy. Nat Med 15: 921-929.

31. Stark RB, Deforest M, Poliakoff C, Schuh F (1965) The Lymph Node and Homoplasty. Am J Surg 110: 394-397.

## Figure Legends

**Figure 1. Chronic lymphedema results in a mixed inflammatory cell response.**

**A.** Photograph of mouse-tails 6 weeks after skin/lymphatic excision (lymphedema; left) or skin incision (control; right).

**B.** Representative cross sectional histology of mouse tails comparing lymphedema (left) and control (right) mice 6 weeks after surgery. Cross sections were obtained 2 centimeters distal to the tail wound (arrow in figure A). Note fat deposition (brackets), dilated lymphatics, and inflammation in lymphedema section.

**C.** Flow cytometry analysis for CD45+ cells in single cell suspensions prepared from tail tissue 2 cm distal to the wound of lymphedema or control mice (n=5-7/group) 6 weeks after surgery. The percentage of CD45+ cells as a function of total cell population is shown. A representative histogram is shown to the right.

**D., E.** Flow cytometry analysis of T-helper, T-cytotoxic, natural killer T cells (NKT), B cell (Figure D) and neutrophils, monocytes, macrophage, and dendritic cells (Figure E) in single cell suspensions of lymphedematous or control mice (n=5-7/group) 6 weeks after surgery. Representative dot plots are shown to the right.

**Figure 2. Axillary lymph node dissection results in a T cell inflammatory reaction.**

**A.** Flow cytometry analysis for CD45+ cells in single cell suspensions prepared from upper extremity soft tissues 1.5 cm distal to the axillary wound in animals treated with axillary lymph node dissection (ALND) or axillary incision without lymphadenectomy (sham; n=5-7/group) 3 or 6 weeks after surgery. A representative histogram is shown to the right.

**B**. Flow cytometry analysis of T-helper, T-cytotoxic, natural killer T cells (NKT), B cell (top panel) and neutrophils, monocytes, macrophage, and dendritic cells in single cell suspensions of upper extremity soft tissues harvested **3 weeks** after ALND or sham incision (n=5-7/group). Representative dot plots are shown below.

**C**. Flow cytometry analysis of T-helper, T-cytotoxic, natural killer T cells (NKT), B cell (top panel) and neutrophils, monocytes, macrophage, and dendritic cells in single cell suspensions of upper extremity soft tissues harvested **6 weeks** after ALND or sham incision (n=5-7/group). Representative dot plots are shown below.

**Figure 3. CD4 cell depletion reduces lymphedema.**

**A.** Flow cytometry analysis of splenic single cell suspensions from mice treated with isotype control antibodies or depleted of CD4+ cells (upper panel) or CD8+ cells (lower panel) using neutralizing antibodies (n=5-7/group). Representative dot plots are shown to the right.

**B.** Representative photograph of control, CD8+ cell depleted, or CD4+ cell depleted mice 6 weeks after tail superficial and deep lymphatic excision. Note near complete resolution of edema in CD4+ treated animals and loss of fixed tail contracture ("J" shape seen in control or CD8+ treated animals).

**C.** Representative cross sectional histology and quantification of subcutaneous tissue thickness (brackets) in control, CD8+, and CD4+ depleted animals.

**D.** Tail volumes in control, CD8+, or CD4+ depleted animals over the course of the experiment. CD4+ or CD8+ cell depletion was begun 2 weeks after surgery (arrow).

**E.** Analysis of lymphatic vessel diameter (podoplanin+ vessels) in control, CD8+, or CD4+ depleted animals (left) and representative photomicrographs (right). Lymphatic vessel diameter is shown in brackets.

**Figure 4. $CD4^+$ cell depletion reduces lymphedema induced chronic inflammation.**

**A, B, C.** Representative photomicrographs of CD45 (figure A), F4/80 (figure B), and CD4 (figure C) immunohistochemical staining in tail tissues of control, CD8+, or CD4+ cell depleted animals 6 weeks after tail superficial and deep lymphatic excision. Quantification of cell numbers per high-powered field (hpf) are shown below for each cell type.

**D.** Representative (of triplicate experiments) western blots from tail tissues for Th1 (IFN-γ, Tbet), T-reg (FoxP3), and Th2 (Gata-3) markers in control, CD8+, and CD4+ depleted animals 6 weeks after tail superficial and deep lymphatic excision. Quantification of band density relative to controls (arbitrarily set at 1 and represented by dotted line) is shown to the right.

**Figure 5. CD4+ cell depletion decreases fibrosis and improves lymphatic function.**

**A.** Scar index analysis (below) and representative photomicrographs of polarized light microscopic views (above) in control, CD8+, and CD4+ depleted animals (n=5-7 per group) 6 weeks after surgery.

**B.** Representative photomicrographs of type I collagen immunohistochemistry (above) and calculation of type I collagen staining in the dermis (positive pixels/$mm^2$; below) in control, CD8+, and CD4+ depleted animals 6 weeks after surgery.

**C.** Calculation of type I:type III collagen staining ratio in tail tissue sections from control, CD8+, and CD4+ depleted mice 6 weeks after surgery.

**D.** Representative (of triplicate experiments) western blot analysis of α-sma, E-cadherin, type III collagen, pSMAD, and TGF-β1 in protein lysates obtained from tail tissues of control, CD8+, and CD4+ cell depleted animals 6 weeks after surgery. Quantification of band density relative to controls (arbitrarily set at 1 and represented by dotted line) is shown to the right.

**E.** Representative microlymphangiography (upper) and quantification of tissue florescence proximal to the tail wound (ratio of proximal to distal florescence) in control, CD8+, and CD4+ depleted mice 6 weeks after surgery. Note crossing of the tail wound by florescent marker only in CD4+ depleted mice.

**F.** Lymphoscintigraphy and sacral lymph node uptake in control, CD8+, and CD4+ depleted mice 6 weeks after surgery. Representative heat map is shown to the right (white arrow = injection site; red circle = sacral lymph nodes).

**Figure 6. T-regulatory cell inflammation is potently increased by lymphatic fluid stasis and lymphedema.**

**A.** Flow cytometry analysis for T-regulatory (T-reg) cells in single cell suspensions prepared from upper extremity soft tissues 1.5 cm distal to the axillary wound in animals treated with axillary lymph node dissection (ALND) or axillary incision without lymphadenectomy (sham; n=5-7/group) 3 or 6 weeks after surgery.

**B.** Flow cytometry analysis for T-regulatory (T-reg) cells in single cell suspensions prepared from tail tissue 2 cm distal to the wound of lymphedema or control mice (n=5-7/group) 6 weeks after surgery.

**C.** Flow cytometry of splenic single cell suspensions for CD4+/CD25- cells after treatment with control or CD25 neutralizing antibodies. Note no significant decrease in the overall number of CD4+ cells. Representative dot plot is shown to the right.

**D.** Flow cytometry of splenic single cell suspensions for CD4+/CD25+/Foxp3+ (T-regs) cells after treatment with control or CD25 neutralizing antibodies. Note no significant decrease in the overall number of CD4+ cells. Representative dot plot is shown to the right.

**Figure 7. $CD25^+$ cell depletion does not improve lymphedema, decrease fibrosis, or augment lymphatic function.**

**A.** Representative photograph of control or CD25+ depleted mice 6 weeks after tail superficial and deep lymphatic excision.

**B.** Representative cross sectional histology and quantification of subcutaneous tissue thickness (brackets) in control and CD25+ cell depleted animals.

**C.** Tail volumes in control and CD25+ cell depleted animals over the course of the experiment. CD25+ cell depletion was begun 2 weeks after surgery (arrow).

**D.** Representative (of triplicate experiments) western blots from tail tissues for Th1 (IFN-γ, Tbet), and Th2 (Gata-3, IL4) markers in control and CD25+ cell depleted animals 6 weeks after tail superficial and deep lymphatic excision. Quantification of band density relative to controls (fold change) is shown to the right.

**E.** Lymphoscintigraphy and sacral lymph node uptake in control and CD25+ cell depleted mice 6 weeks after surgery. Representative heat map is shown to the right (white arrow = injection site; red circle = sacral lymph nodes).

**F.** Scar index analysis (below) and representative photomicrographs of polarized light microscopic views (above) in control and CD25+ cell depleted animals (n=5-7 per group) 6 weeks after surgery.

**G.** Representative photomicrographs of type I collagen immunohistochemistry (above) and calculation of type I collagen staining in the dermis (positive pixels/$mm^2$; below) in control and CD25+ cell depleted animals 6 weeks after surgery.

**H.** Calculation of type I:type III collagen staining ratio in tail tissue sections from control and CD25+ cell depleted mice 6 weeks after surgery.

**I.** Representative (of triplicate experiments) western blot analysis of α-sma, E-cadherin, type III collagen, pSMAD, and TGF-β1 in protein lysates obtained from tail tissues of control and

CD25+ cell depleted animals 6 weeks after surgery. Quantification of band density relative to controls (fold change) is shown to the right.

**Figure 8. Loss of $CD4^+$ but not $CD8^+$ or $CD25^+$ cells increases lymphangiogenesis.**

**A.** LYVE-1+ vessel counts (left) and representative figures (right) of tail sections from control, CD8+, CD4+, or CD25+ cell depleted mice 6 weeks after surgery.

**B.** Podoplanin+ vessel counts (left) and representative figures (right) of tail sections from control, CD8+, CD4+, or CD25+ cell depleted mice 6 weeks after surgery.

**C.** VEGF-C+ cells/high powered field (hpf) counts (left) and representative figures of VEGF-C immunohistochemistry in tail tissues from control, CD8+, CD4+, or CD25+ cell depleted animals (right) 6 weeks after surgery.

**D.** Representative (of triplicate experiments) western blot analysis of VEGF-A, and VEGF-C expression in protein lysates obtained from tail tissues from control, CD8+, CD4+, or CD25+ cell depleted animals 6 weeks after surgery. Quantification of band density relative to controls (arbitrarily set at 1 and represented by dotted line) is shown to the right.

**Figure 9. CD4+ cells regulate inflammatory lymphangiogenesis.**

**A.** LYVE-1+ vessel density in popliteal lymph nodes 7 days after CFA/OVA induced lymph node lymphangiogenesis in control, CD4+ cell depleted, or CD4 knockout (CD4KO) mice. Representative cross sectional histology of the lymph node (blue DAPI stain, red LYVE-1 stain) are shown to the right.

**B., C.** Expression of VEGF-A (A) and VEGF-C (B) protein by ELISA in popliteal lymph nodes harvested 7 days after CFA/OVA induced lymph node lymphangiogenesis in control or CD4 depleted mice.

**Table 1.** Cell surface markers for identification of leukocyte cell types.

| Cell Type | Surface marker |
|---|---|
| Leukocytes | $CD45^+$ |
| Mature T-helper cells | $CD45^+/CD4^+/TCR\beta^+$ |
| Mature T-cytotoxic cells | $CD45^+/CD8^+/TCRb^+$ |
| T-regulatory cells | $CD4^+/D25^+/Foxp3^+$ |
| Natural killer T cell | NKT; $CD4^+/TCR\beta^+/Tetramer^+$ |
| Macrophage | $CD45^+/CD11b^+/F4/80^+$ |
| Dendritic cell | $CD45^+/CD11c^+/MHC\ II^{hi}$ |
| Neutrophil | $CD45^+/CD11b^+/Ly6g^{hi}$ |
| Monocyte | $CD45^+/CD11b^+/Ly6c^{hi}$ |
| B cell | $CD45^+/B220^+$ |

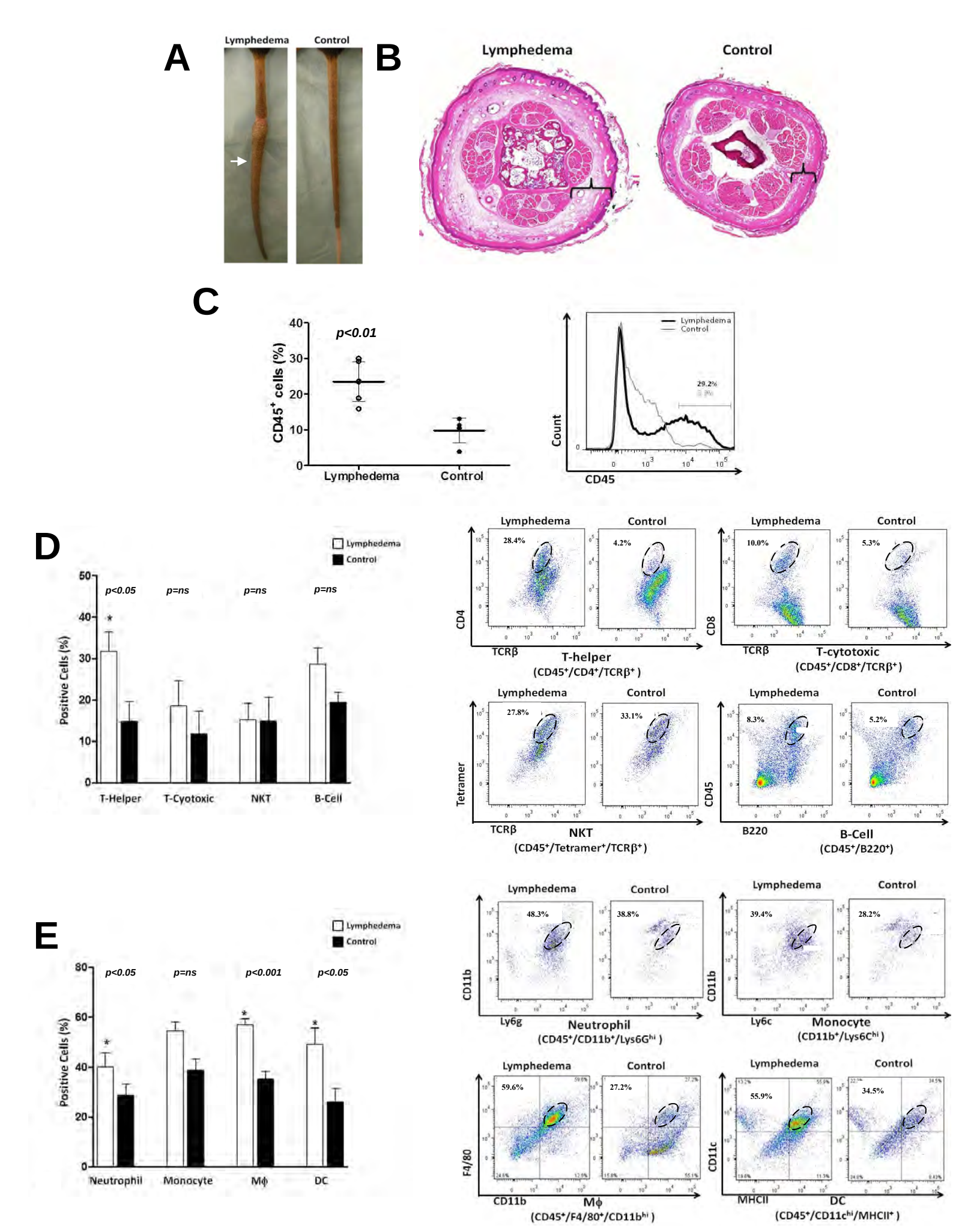
A
Lymphedema
Control
B
Lymphedema
Control
C
p<0.01
CD45+ cells (%)
Lymphedema
Control
Count
CD45
29.2%
D
Lymphedema
Control
p<0.05
p=ns
p=ns
p=ns
Positive Cells (%)
T-Helper
T-Cyotoxic
NKT
B-Cell
28.4%
4.2%
10.0%
5.3%
CD4
TCRβ
T-helper
(CD45+/CD4+/TCRβ+)
CD8
T-cytotoxic
(CD45+/CD8+/TCRβ+)
27.8%
33.1%
8.3%
5.2%
Tetramer
NKT
(CD45+/Tetramer+/TCRβ+)
CD45
B220
B-Cell
(CD45+/B220+)
E
Lymphedema
Control
p<0.05
p=ns
p<0.001
p<0.05
Positive Cells (%)
Neutrophil
Monocyte
Mϕ
DC
48.3%
38.8%
39.4%
28.2%
CD11b
Ly6g
Neutrophil
(CD45+/CD11b+/Lys6Ghi)
Ly6c
Monocyte
(CD11b+/Lys6Chi)
59.6%
27.2%
55.9%
34.5%
F4/80
Mϕ
(CD45+/F4/80+/CD11bhi)
CD11c
MHCII
DC
(CD45+/CD11chi/MHCII+)

Figure 1

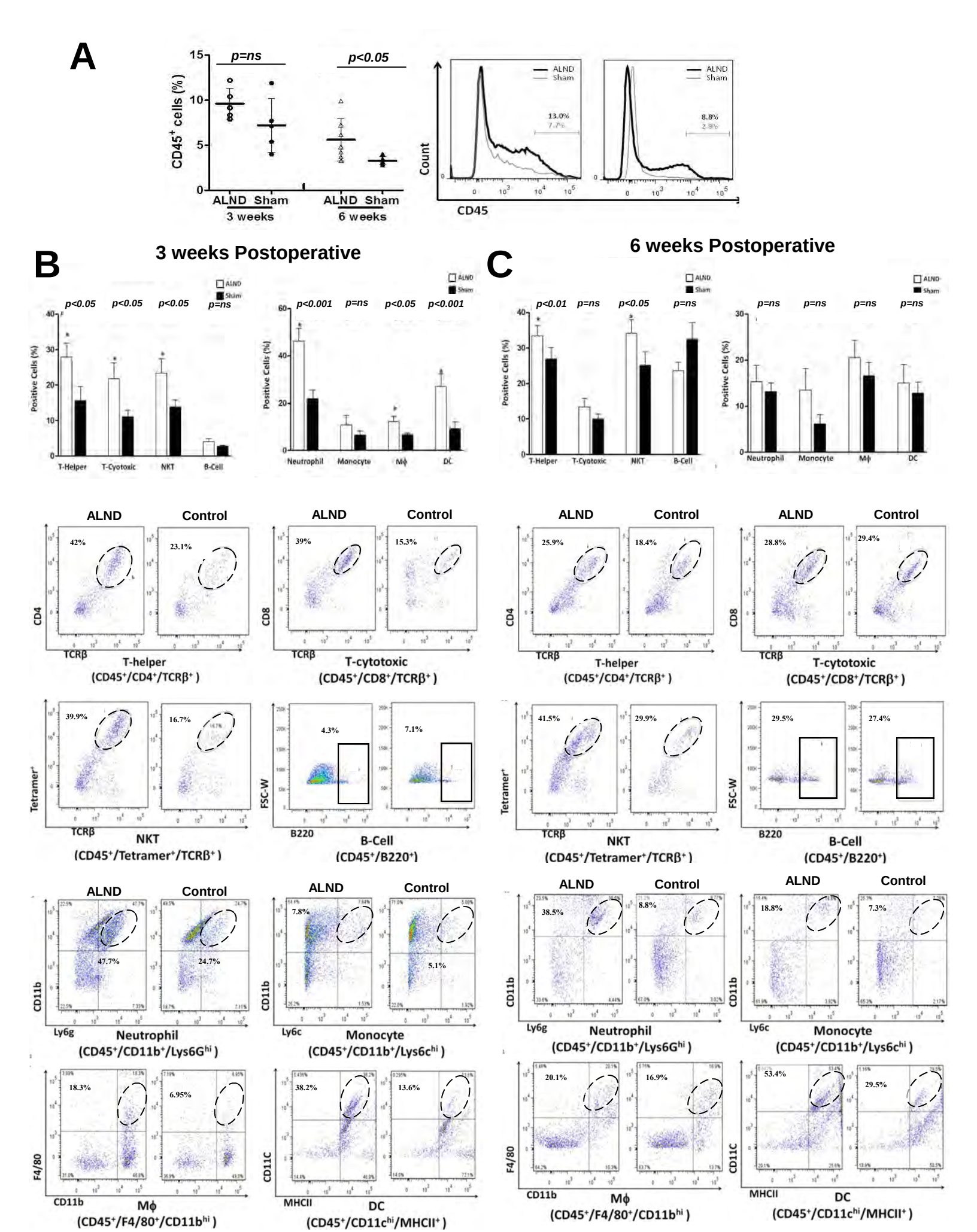
A
p=ns
p<0.05
CD45+ cells (%)
ALND Sham
3 weeks
6 weeks
ALND
Sham
13.0%
7.7%
8.8%
2.8%
Count
CD45
B
3 weeks Postoperative
C
6 weeks Postoperative
p<0.05 p<0.05 p<0.05 p=ns
p<0.001 p=ns p<0.05 p<0.001
p<0.01 p=ns p<0.05 p=ns
p=ns p=ns p=ns p=ns
Positive Cells (%)
T-Helper
T-Cytotoxic
NKT
B-Cell
Neutrophil
Monocyte
Mϕ
DC
ALND
Control
42%
23.1%
39%
15.3%
25.9%
18.4%
28.8%
29.4%
CD4
CD8
TCRβ
T-helper
(CD45+/CD4+/TCRβ+)
T-cytotoxic
(CD45+/CD8+/TCRβ+)
39.9%
16.7%
4.3%
7.1%
41.5%
29.9%
29.5%
27.4%
Tetramer+
FSC-W
B220
NKT
(CD45+/Tetramer+/TCRβ+)
B-Cell
(CD45+/B220+)
7.8%
47.7%
24.7%
5.1%
38.5%
8.8%
18.8%
7.3%
CD11b
Ly6g
Ly6c
Neutrophil
(CD45+/CD11b+/Lys6Ghi)
Monocyte
(CD45+/CD11b+/Lys6chi)
18.3%
6.95%
38.2%
13.6%
20.1%
16.9%
53.4%
29.5%
F4/80
CD11C
MHCII
Mϕ
(CD45+/F4/80+/CD11bhi)
DC
(CD45+/CD11chi/MHCII+)

Figure 2

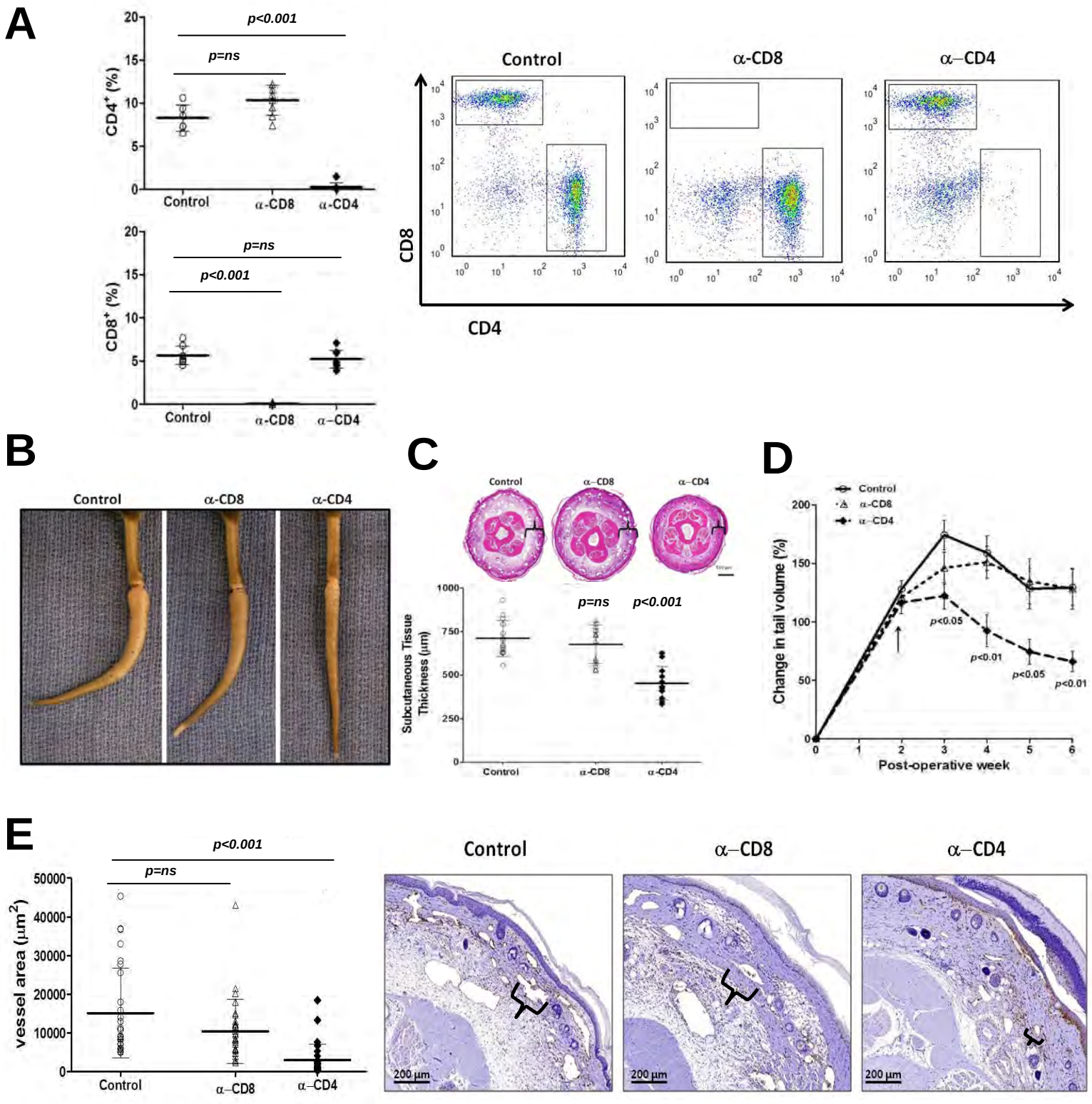
A
p<0.001
p=ns
CD4+ (%)
Control
α-CD8
α-CD4
p=ns
p<0.001
CD8+ (%)
Control
α-CD8
α-CD4
Control
α-CD8
α-CD4
CD8
CD4
B
Control
α-CD8
α-CD4
C
Control
α-CD8
α-CD4
p=ns
p<0.001
Subcutaneous Tissue Thickness (μm)
Control
α-CD8
α-CD4
D
Control
α-CD8
α-CD4
Change in tail volume (%)
p<0.05
p<0.01
p<0.05
p<0.01
Post-operative week
E
p<0.001
p=ns
vessel area (μm2)
Control
α-CD8
α-CD4
Control
α-CD8
α-CD4
200 μm
200 μm
200 μm

Figure 3

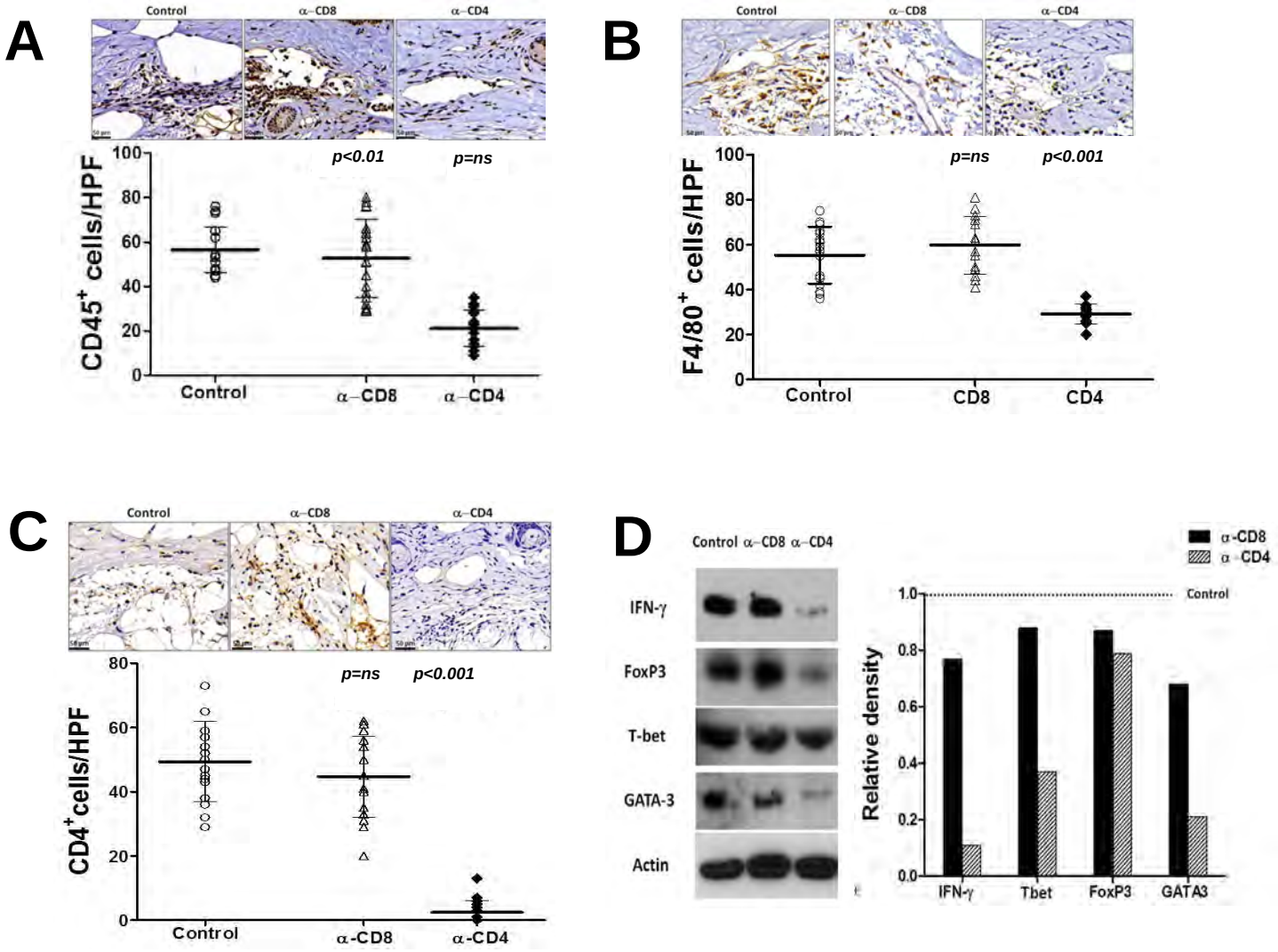
A
Control
α–CD8
α–CD4
p<0.01
p=ns
CD45+ cells/HPF
Control
α–CD8
α–CD4
B
Control
α–CD8
α–CD4
p=ns
p<0.001
F4/80+ cells/HPF
Control
CD8
CD4
C
Control
α–CD8
α–CD4
p=ns
p<0.001
CD4+cells/HPF
Control
α-CD8
α-CD4
D
Control α–CD8 α–CD4
IFN-γ
FoxP3
T-bet
GATA-3
Actin
α-CD8
α-CD4
Control
Relative density
IFN-γ
Tbet
FoxP3
GATA3

Figure 4

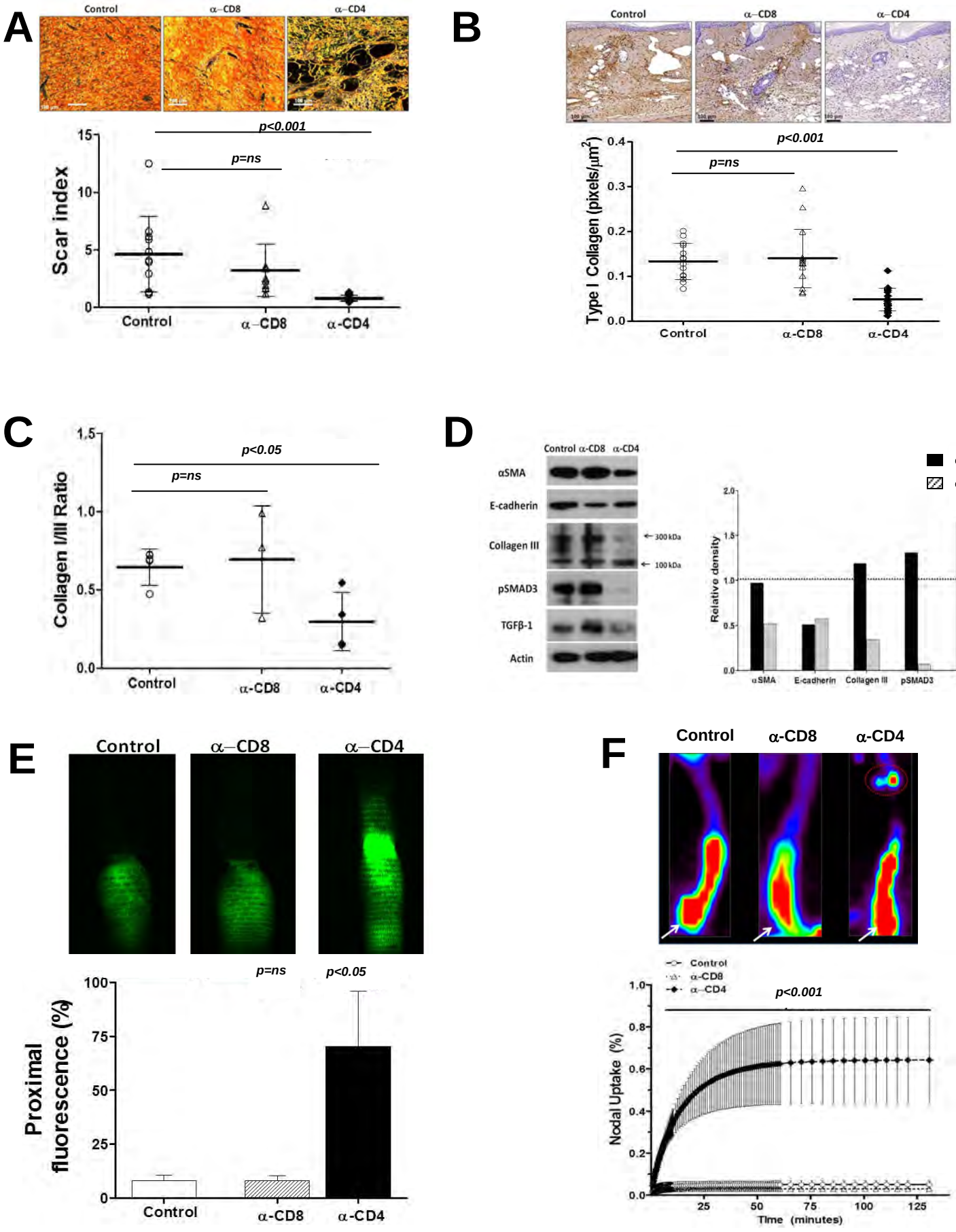
A
Control
α–CD8
α–CD4
p<0.001
p=ns
Scar index
15
10
5
0
Control
α–CD8
α-CD4
B
Control
α–CD8
α–CD4
p<0.001
p=ns
Type I Collagen (pixels/μm²)
0.4
0.3
0.2
0.1
0.0
Control
α-CD8
α-CD4
C
p<0.05
p=ns
Collagen I/III Ratio
1.5
1.0
0.5
0.0
Control
α-CD8
α-CD4
D
Control α-CD8 α-CD4
αSMA
E-cadherin
Collagen III
300 kDa
100 kDa
pSMAD3
TGFβ-1
Actin
α-CD8
α-CD4
Relative density
2.0
1.5
1.0
0.5
0.0
Control
αSMA
E-cadherin
Collagen III
pSMAD3
TGFβ-1
E
Control
α–CD8
α–CD4
p=ns
p<0.05
Proximal fluorescence (%)
100
75
50
25
0
Control
α-CD8
α–CD4
F
Control
α-CD8
α-CD4
Control
α-CD8
α–CD4
p<0.001
Nodal Uptake (%)
1.0
0.8
0.6
0.4
0.2
0.0
25
50
75
100
125
Time (minutes)

Figure 5

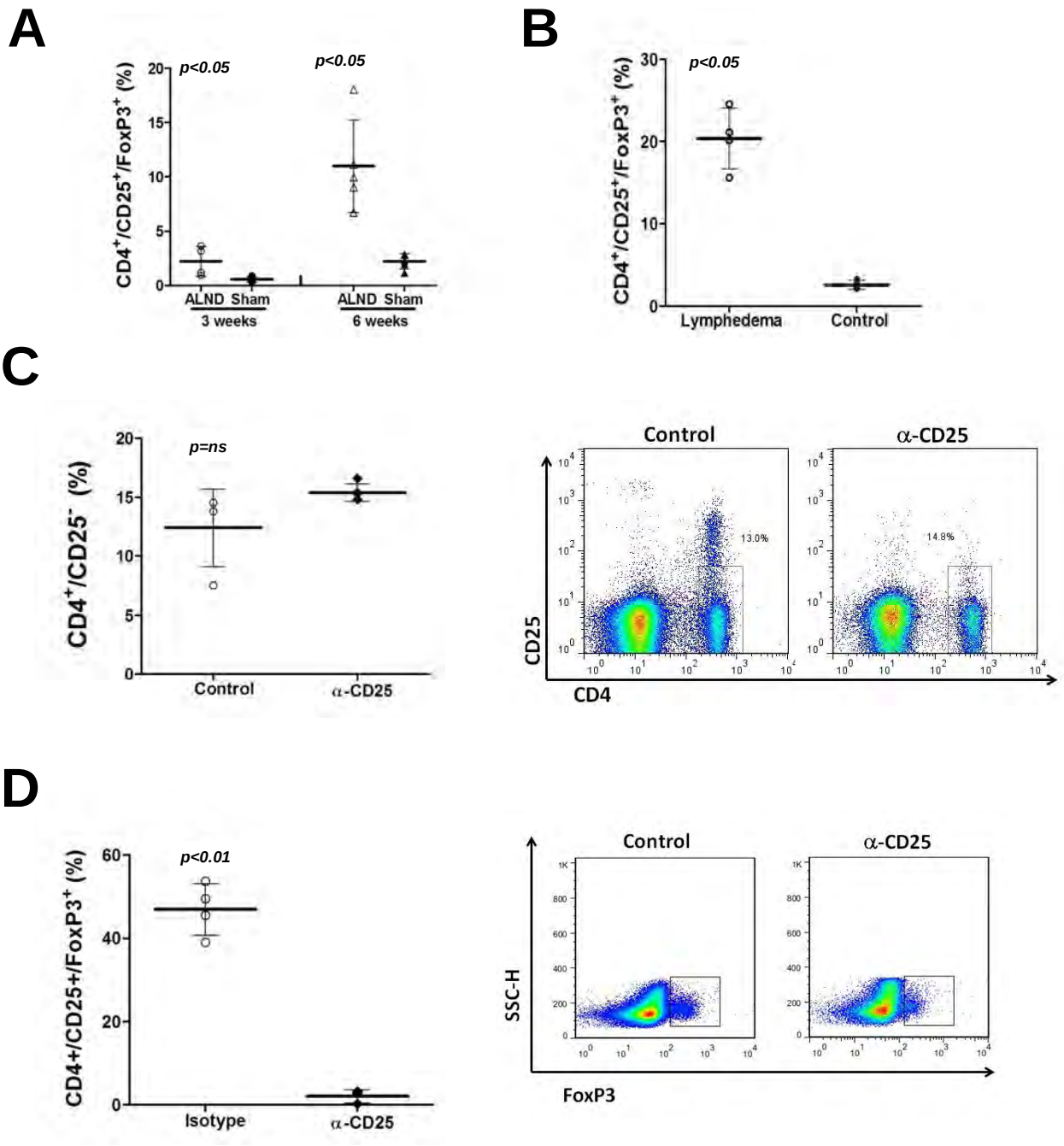
A
p<0.05
p<0.05
CD4+/CD25+/FoxP3+ (%)
ALND Sham
3 weeks
ALND Sham
6 weeks
B
p<0.05
CD4+/CD25+/FoxP3+ (%)
Lymphedema
Control
C
p=ns
CD4+/CD25- (%)
Control
α-CD25
Control
α-CD25
13.0%
14.8%
CD25
CD4
D
p<0.01
CD4+/CD25+/FoxP3+ (%)
Isotype
α-CD25
Control
α-CD25
SSC-H
FoxP3

Figure 6

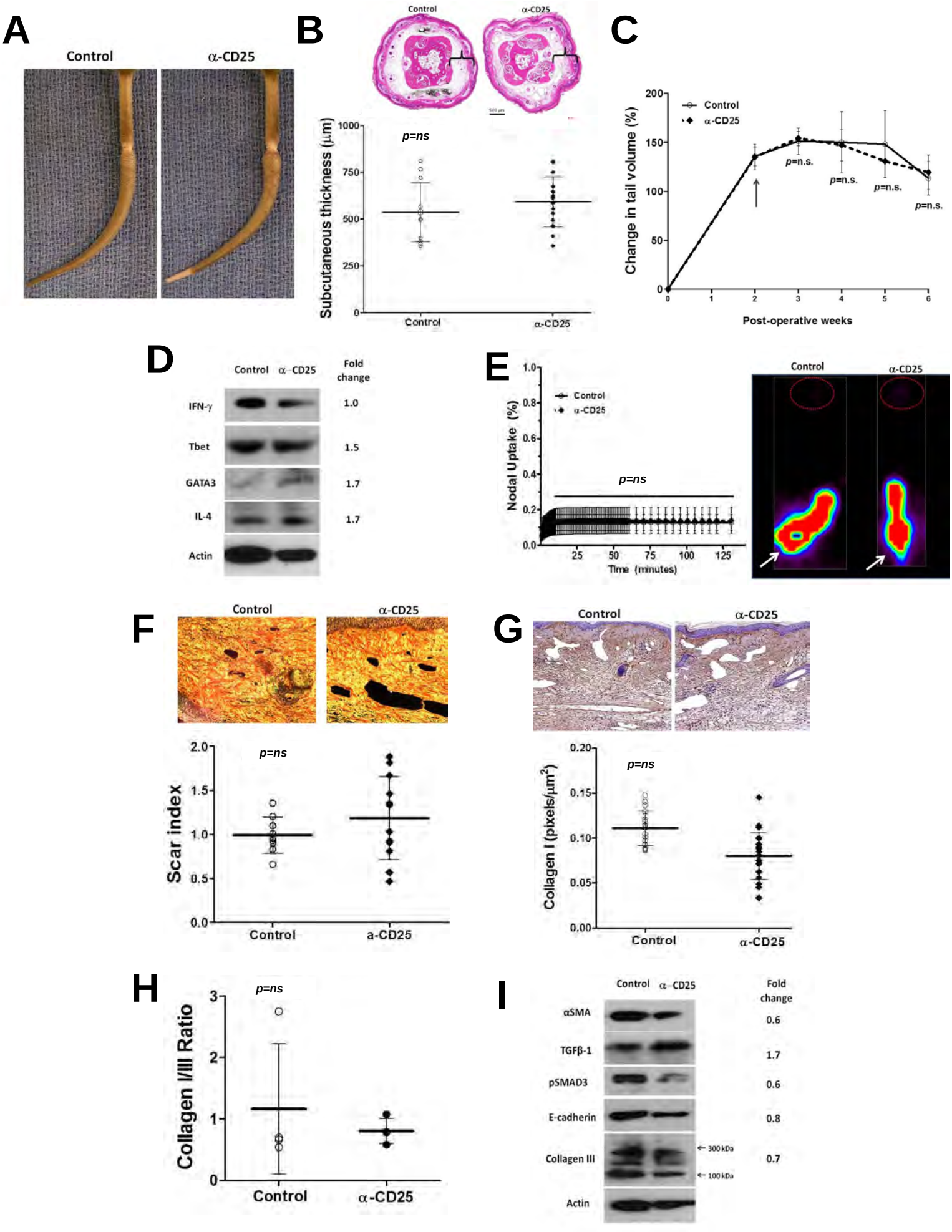
A
Control
α-CD25
B
Control
α-CD25
p=ns
Subcutaneous thickness (μm)
1000
750
500
250
0
Control
α-CD25
C
Control
α-CD25
Change in tail volume (%)
200
150
100
50
0
p=n.s.
p=n.s.
p=n.s.
p=n.s.
0
1
2
3
4
5
6
Post-operative weeks
D
Control
α-CD25
Fold change
IFN-γ
1.0
Tbet
1.5
GATA3
1.7
IL-4
1.7
Actin
E
Control
α-CD25
Nodal Uptake (%)
1.0
0.8
0.6
0.4
0.2
0.0
p=ns
25
50
75
100
125
Time (minutes)
Control
α-CD25
F
Control
α-CD25
Scar index
2.0
1.5
1.0
0.5
0.0
p=ns
Control
a-CD25
G
Control
α-CD25
Collagen I (pixels/μm²)
0.20
0.15
0.10
0.05
0.00
p=ns
Control
α-CD25
H
Collagen I/III Ratio
3
2
1
0
p=ns
Control
α-CD25
I
Control
α-CD25
Fold change
αSMA
0.6
TGFβ-1
1.7
pSMAD3
0.6
E-cadherin
0.8
Collagen III
← 300 kDa
← 100 kDa
0.7
Actin

Figure 7

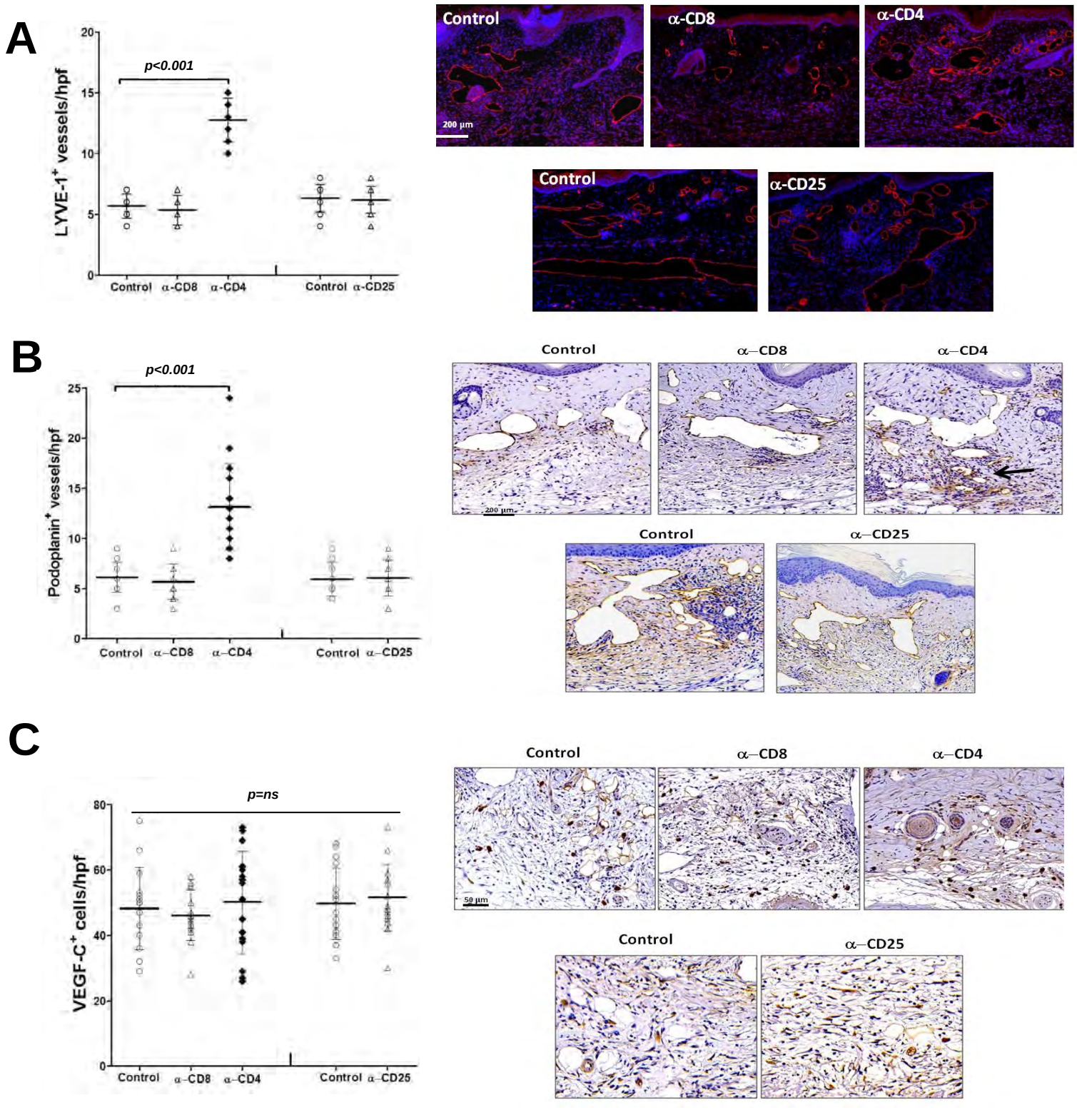
A
p<0.001
LYVE-1+ vessels/hpf
Control
α-CD8
α-CD4
α-CD25
200 μm
B
p<0.001
Podoplanin+ vessels/hpf
C
p=ns
VEGF-C+ cells/hpf
50 μm
D
Control α–CD8 α–CD4 Control α–CD25
VEGF-A
VEGF-C
Actin
Relative density

Figure 8

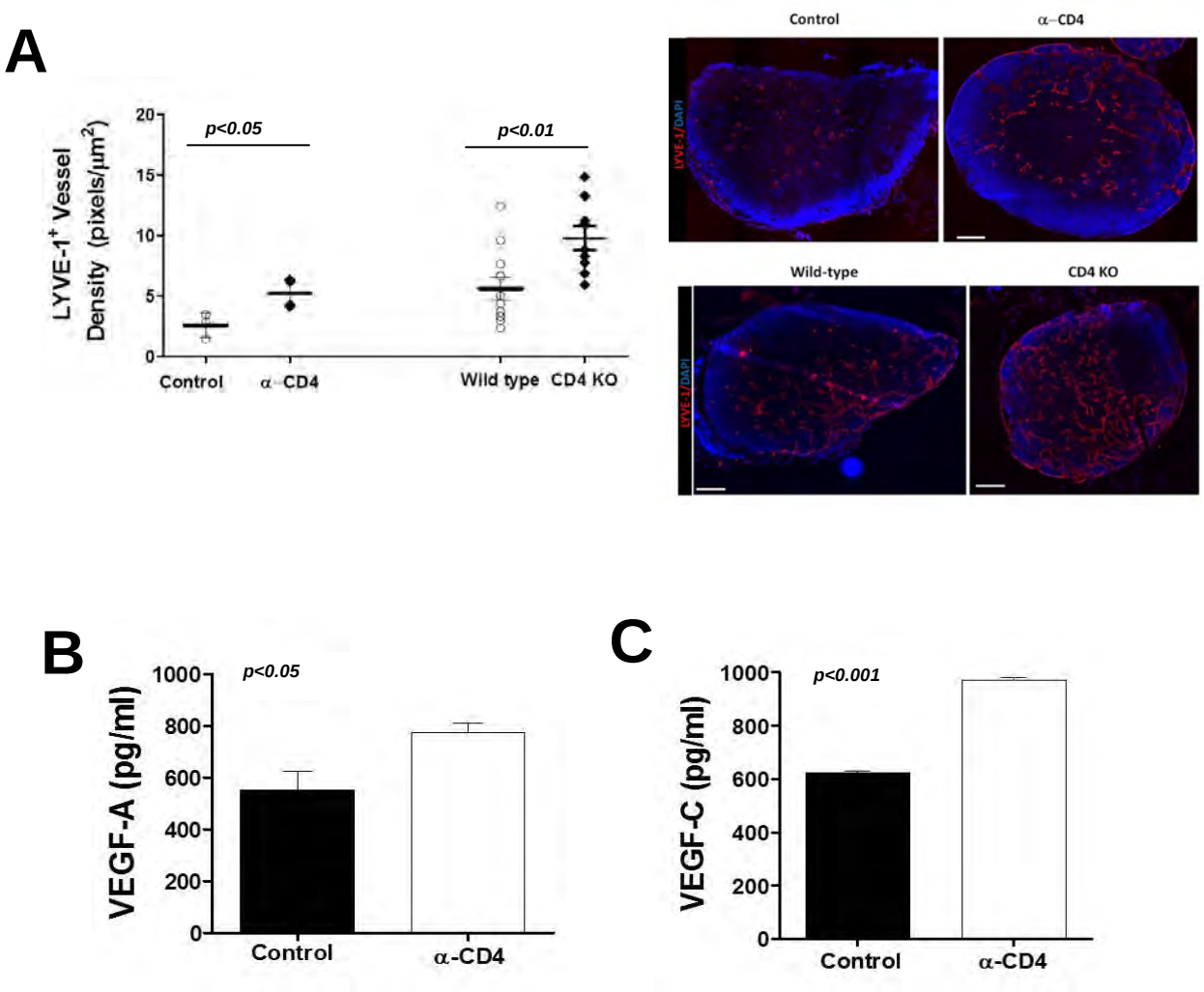
A
LYVE-1+ Vessel Density (pixels/μm2)
p<0.05
p<0.01
Control
α-CD4
Wild type
CD4 KO
Control
α-CD4
Wild-type
CD4 KO
LYVE-1/DAPI


B
VEGF-A (pg/ml)
p<0.05
Control
α-CD4


C
VEGF-C (pg/ml)
p<0.001
Control
α-CD4

Figure 9